École Polytechnique Fédérale de Lausanne

Solar Energy and Building Physics Laboratory

Master thesis

An "Energy hub" on the EPFL campus: heat demand and supply

Author:
Emmanuel Walter
Master in Energy management and Sustainability

Supervisor:
Pr François Maréchal, IPESE
Dr Jérôme Kaempf, kaemco SARL

Assistant:
Ms Silvia Coccolo, LESO-PB
M Jakob Rager, IPESE

June 20, 2014

Submitted on the :

Signature

Acknowledgements

First, I express my greatest thanks to Dr Jérome Kaempf for allowing me to work with him again. Also all my gratitude for his constant help and his unflinching cheerfulness all along my master thesis.

My thanks also to Prof. François Maréchal for his supervision.

For their precious help in my work, at all times and despite their personal constraints, my gratitude to Ms Silvia Coccolo of the LESO-PB and Mr Jakob Rager of the IPESE.

My gratitude to the team of the LESO-PB and in particular to Pr Jean-Louis Scartezzini for his warm welcome.

My thanks to the team of the Infrastructure and housing deparment of EPFL (DII) and in particular to Mr Christophe Roberts, Mr Pierre Antille Mr Jean-Marc Schwab and Mr Florent Deseneux for providing me the whole data I needed on the EPFL campus.

For his punctual but very helpful and valuable help in programming, special thanks to Mr Frédéric Calatayud.

To my friends and family, in Switzerland, France or abroad whose support was decisive to the success of my studies at EPFL.

My thanks goes to Dr David Berardan, Dr Sebastien Sorgues and Mr Matthieu Lebois of University Paris-South XI whose recommendation letters allowed me to enter EPFL.

Finally, I would like to acknowledge the thousands of individuals who have coded on LaTeXprojects for free!

Abstract

Urban settlements became a major consumer of energy resources and are still expected to grow. It is therefore crucial to plan, design and adapt urban settlements in order to minimize their energy consumption.

With this in mind, the Integration of Decentralized Energy Adaptive Systems project (IDEAS4cities) was created. The concept of this project is that the integration of renewable energy in urban context requires the creation of energy hubs able to self-regulate energy fluxes within their borders. This smart regulation would allow reaching zero energy and if possible zero power. In the project IDEAS4cities, the EPFL is a fundamental case study.

The creation of an "energy hub" on the EPFL campus requires the ability to simulate its energy fluxes. The focus of this work is on heat demand and supply. The main simulation tool is CitySim, a large-scale building energy simulation tool developed at the Solar Energy and Building Physics Laboratory(LESO-PB).

The work is divided into three main parts.

The first task is to verify the consistency of CitySim outputs using the BESTEST procedure. Citysim is found to generate consistent results for heating and cooling. Some discrepancies appear and they are explained by (i) a rather weak influence of the building thermal mass in regulating the inside air temperature due to the thermal model implemented in Citysim and (ii) the dynamic computation of surface coefficients.

Then, this program is used to simulate the heating profile of EPFL buildings. Results are validated by the monitoring of EPFL heating consumption in 2013. Building heating profile is shown to vary significantly depending on solar gains and ventilation. A few energy saving scenarios are also simulated. Mainly, the effect of windows replacement and walls insulation is

contrasted. The impact of the two are similar on the annual load but diverge for the impact on the peak demand.

Finally, Citysim is linked to another program, Python Energy Integration (PEI). This program determines the optimal sizing of the energy conversion system based on a given heating profile. The communication methodology consists is reducing the year to a set of k typical days using the k-medoids clustering method. The analysis of the chosen typical days reveals that the peak heating is not taken into account and that the limitations on the heating period have a strong influence in the shape of the load duration curve.

Contents

List of Figures **vii**

List of Tables **ix**

Introduction **xi**

1 CitySim BESTEST certification **1**

1.1 Introduction . . . 1

1.2 General description . . . 2

1.3 Justification of BESTEST application on CitySim . . . 6

1.4 IEA BESTEST Methodology . . . 7

1.4.1 Specific input information . . . 7

1.4.2 Final Results presentation . . . 7

1.4.2.1 Solar irradiation . . . 8

1.4.2.2 Heating and cooling demand . . . 8

1.4.2.3 Inside temperature variations . . . 8

1.4.3 The IEA BESTEST procedure . . . 9

1.5 Specific input information . . . 14

1.5.1 Weather . . . 14

1.5.2 Building geometry . . . 16

1.5.3 Scenarios definition . . . 16

1.5.3.1 Set point . . . 18

1.5.3.2 Building mass . . . 19

1.5.3.3 Internal Heat Gains . . . 19

1.5.3.4 Infiltration . . . 20

1.5.3.5 Convective heat transfer coefficients . . . 20

1.5.3.6 Radiative heat transfer coefficient 20
1.5.3.7 Windows 21
1.5.3.8 Shadings 22
1.5.3.9 Case 960 : Sunspace 22
1.5.3.10 Case 990 22
1.6 Final results Presentation 23
1.6.1 Solar Irradiation results 23
1.6.1.1 Annual Results 23
1.6.1.2 Daily results 25
1.6.2 Heating and cooling demand 28
1.6.2.1 Annual heating and cooling load 28
1.6.2.2 Annual peak heating and cooling demand 28
1.6.2.3 Daily results 30
1.6.3 Temperature Variations 33
1.7 The BESTEST Method 37
1.7.1 Annual heating load 37
1.7.2 Annual cooling load 40
1.7.3 Annual peak heating demand 42
1.7.4 Annual peak cooling demand 42
1.8 Discussion 45
1.9 Conclusion 47
1.10 Future work 48

2 Simulation of EPFL heating demand with CitySim 49

2.1 Introduction 49
2.2 Methodology 50
2.2.1 CitySim model development 50
2.2.2 Simulation results analysis 51
2.3 CitySim model development 52
2.3.1 Climate 52
2.3.2 Geometry 53
2.3.3 Air Change per Hour 56
2.3.4 Heating system 57

2.3.5 Envelope definition 57
2.3.6 Occupants and equipments 59
2.4 Simulation results 62
2.4.1 Model calibration with monitored energy consumption 62
2.4.2 Annual load and peak demand 64
2.4.3 Building specific consumption 68
2.4.4 Energy saving scenarios 72
2.5 Discussion 75
2.6 Conclusion 76
2.7 Future work 78

3 Programs intercommunication: CitySim and Python Energy Integration 79

3.1 Introduction 79
3.2 Methodology 80
3.2.1 CitySim outputs pre-treatment 80
3.2.2 CitySim outputs clustering 81
3.2.3 Energy Integration 85
3.3 Results 86
3.3.1 Clustering results 86
3.4 Discussion 91
3.5 Conclusion 92
3.6 Future work 93

General conclusion 95

References 1

A Appendix on part 1 5

A.1 Definition the envelope typology in the BESTEST 5
A.2 Definition of the shadings 7
A.3 Illustration of Citysim thermal model 7

B Appendix on part 2 **9**

B.1 Simulation data . . . 9

B.2 Treated floor area - comparison between the model and DII publications 11

B.3 Glazing ratio determination . . . 14

B.4 Print-screen of source wall types . . . 15

B.5 Results for the energy saving scenarios . . . 21

C Appendix on part 3 **23**

C.1 Hourly profile of typical days . . . 23

List of Figures

1.1 BESTEST validation procedure principles 2

1.2 BESTEST - Low and high-mass qualification flow diagram 11

1.3 BESTEST - Low-mass diagnostics flow diagram test 12

1.4 BESTEST - High-mass diagnostic flow diagram 13

1.5 Incident solar irradiation for North (N), East (E), South (S), West (W) and horizontal façades 24

1.6 Unshaded and shaded transmitted solar irradiation for W and S façades 24

1.7 Transmissivity coefficient and shading coefficient for W and S façades . 25

1.8 Hourly incident solar irradiance on the S (top) and W (bottom) façades for a cloudy day (March 5) 26

1.9 Hourly incident solar irradiance on the S (top) and W (bottom) façade for a clear day (July 27) 27

1.10 Results dispersion for annual heating load (top left), annual cooling load (top right), peak heating demand (bottom left) and peak cooling demand (bottom right) - Cases 600 and 900 encircled 29

1.11 Hourly heating (+) and cooling (-) for the low-weight (top) and heavy-weight (bottom) cases on the 4^{th} of January 32

1.12 Annual maximum (left), minimum (middle) and average (right) temperature for the light-weight (600FF), heavy-weight (900FF) free float cases and the sun-zone case (960) 34

1.13 Annual occurence of hourly temperature in bins of 1 $^\circ$C for the high-mass free-floating case (900FF) 34

1.14 Hourly temperature for the low-weight (top) and heavy-weight (bottom) cases on the 4^{th} of January 35

2.1 Evolution of the temperature during the year for Ecublens 52
2.2 CitySim output for the irradiance received by the south surface of building AI on the 13^{th} of December at 13:00 53
2.3 Top view of the EPFL on Rhinoceros with added building names 55
2.4 Combined Schedules for offices and restaurants 60
2.5 Dispersion graph of monitored energy consumption and simulation results, bisector (dark line) and linear regression of the cloud (blue line) . 63
2.6 Situation of BSP (right) and CE (left) buildings 64
2.7 Simulation results for annual (left) and hourly peak (Right) heating demand 65
2.8 Peak heating demand to annual heating load ratio $(-)$ 67
2.9 Specific consumption per building $(\frac{kWh}{m^2})$ 69
2.10 Situation of BCH and BSP (top), BC (bottom left) and AA buildings (bottom right) 71
2.11 Evolution of the annual load (left) and peak demand (right) with building insulation of various thickness 73
2.12 Evolution of the annual load (left) and peak demand (right) with glazing of various performances 74

3.1 Variation of the annual error, the silhouette and the number of times the optimal solution is found in function of k 87
3.2 Original and clustered heating load duration curves 89
3.3 Original and clustered yearly heating profile 90

A.1 Positioning of the shadings is cases 1.0MHV (left) and 1.0MH (right) . . 7
A.2 Schema of Citysim (top) and ideal thermal model 7

B.1 Absolute consumption of EPFL buildings (2007) $\frac{kWh}{an}$ 12
B.2 Specific consumption of EPFL buildings (2007) $\frac{kWh}{m^2.an}$ 12
B.3 Plan (left) and picture (right) of the environmental sciences building north façade, assumed to be the representative of the 1^{st} period of construction, GR=36% 14
B.4 Plan (left) and picture (right) of the microtechnology building, GR = 47% 14
B.5 Roof typology for the first period of construction 15

B.6 Wall typology for the first period of construction 16
B.7 Floor typology for the first period of construction 17
B.8 Roof typology for the first period of construction 17
B.9 Wall typology for the first period of construction 19

C.1 Original and clustered heating profile of consumption on the 26^{th} of september 23
C.2 Original and clustered solar profile of consumption on the 26^{th} of september 24

List of Tables

1.1 Overview of published BESTEST suites 3
1.2 CitySim weather file required entries 15
1.3 Weather summaries comparison between used and theoretical data . . . 15
1.4 IEA BESTEST basecase dimensions 16
1.5 List of cases in the BESTEST 17
1.6 U-value of the envelope for lightweight and heavyweight cases 19
1.7 Schedule Style 19
1.8 IEA BESTEST windows properties 21
1.9 Characteristics of the common wall 22
1.10 BESTEST results color code example 37
1.11 BESTEST sequence applied on results for the annual heating load . . . 39
1.12 BESTEST sequence applied on results for the annual cooling load . . . 41
1.13 BESTEST sequence applied on results for the annual peak heating demand 43
1.14 BESTEST sequence applied on results for the annual peak cooling demand 44

2.1 CitySim weather file required entries 50
2.2 Summary of used climate for the site of Ecublens 52
2.3 Description of highly ventilated buildings 56
2.4 Summary of the U-values of the two construction period 57
2.5 Evolution of the U-value depending on the insulation thickness 58
2.6 Occupants and equipments density for restaurants and offices (SIA, 2006) 59
2.7 Value of the yearly schedule coefficient depending on the period of the year 60
2.8 Comparison between buildings CE and BSP 64
2.9 Value of ACH and specific consumption for highly ventilated buildings . 68

2.10 Global savings obtained with the different energy saving scenarios . . . 77

3.1 Distribution of typical days with associated weight depending on the value of k 87

A.1 Lightweight walls definition 5
A.2 Heavyweight walls definition 6

B.1 Data input 10
B.2 Comparison results for real and modelized treated surface 13
B.3 Envelope definition for the 1^{st} construction period - Aluminium facades 18
B.4 Envelope definition for the 2^{nd} construction period - Clay facades 20
B.5 New definition of the wall after the renovation of the first construction period 21
B.6 Summary of the results of the energy saving scenarios 22

Introduction

Today, urban settlements represent more than half of the world population and are expected to absorb the 2.3 billions world population increase by 2050 UN (2011). Cities residents consume more coal, gas and electricity than the global average. Urban complexes account for two-thirds of the world energy consumption and 70% of the global CO2 emissions IEA (2008). In view of the growth of cities, it is therefore crucial to plan, design and adapt urban settlements in order to minimize their energy consumption.

In this purpose, CitySim was developed at the Solar Energy and Building Physics Laboratory (LESO-PB). This program is a large scale building energy simulation tool conceived to support sustainability in urban development. In its current version, CitySim focuses on energy flows but the simulation of wastes, water or embodied energy are also to considered in further developments.

This master thesis focuses on the use of this software. The objectives are to (i) test its consistency and trustability, (ii) to simulate the heating demand of the EPFL campus and (iii) to link CitySim with a complementary program called Python Energy Integration (PEI). The present work is divided into three parts according to those objectives.

These goals are all contributing to the creation process of an energy hub on the EPFL campus according to the definition (IDEAS4cities). The concept of this project is that the integration of renewable energy in urban context requires the creation of energy hubs able to self-regulate energy fluxes within the borders of a district. This smart regulation would allow reaching zero energy and if possible zero power. In the project IDEAS4cities, the EPFL is a fundamental case study.

Part 1

CitySim BESTEST certification

1.1 Introduction

Today, there is a proliferation of building energy simulation programs, many of which may actually contain errors or inaccuracies. Using a deficient program for the design of a building can result in a negative impact building operation.

For instance, if the program predicts too low heating loads, this means that the energy conversion system designed on the basis of this program is undersized and doesn't have a sufficient capacity to heat the building during coldest periods of the year. By contrast, if predictions are too high, the heating is oversized and operates below its optimal performances.

This is why an internationally accepted procedure to certify the outputs of building energy simulation programs was set up.

The Building Energy Simulation Test (BESTEST) is a systematic procedure developed by the U.S. National Renewable Energy Laboratory (NREL) and the International Energy Agency (IEA). The general goal of the BESTEST is to validate the use of a program for a specific range of buildings and climate type. This program is nowadays actively followed and improved by organisations in Australia, Belgium, Canada, Denmark, France, Germany, Ireland, Japan, the Netherlands, Sweden, Switzerland, the United Kingdom, and the United States (Source: ECBCS).

1.2 General description

The BESTEST procedure is based on three guiding principles that are illustrated in Figure 1.1.

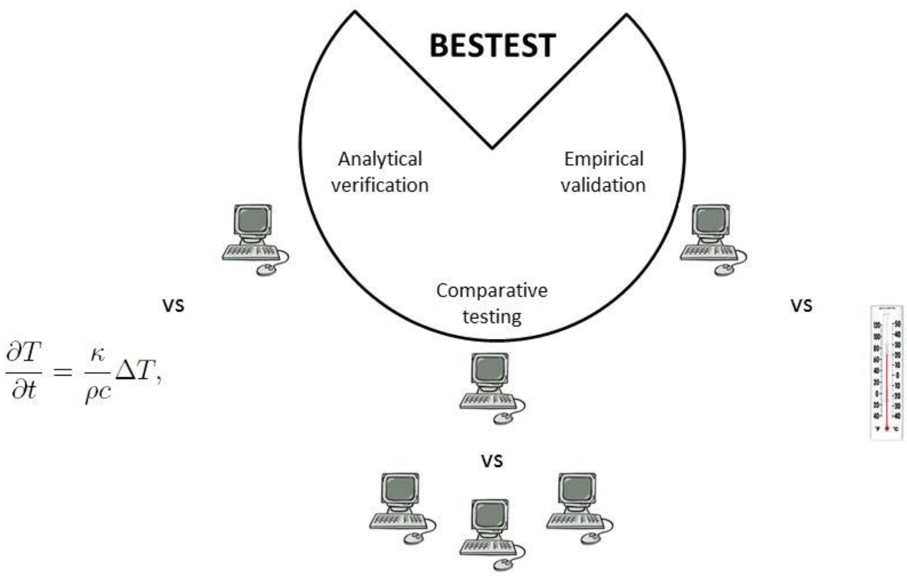

Figure 1.1: BESTEST validation procedure principles - own illustration

Analytical verification The outputs of the candidate program are compared to a known and generally accepted mathematical solution. This type of verification is inexpensive and there is no input uncertainty. However, the inherent complexity of building physics limits drastically the number of cases where such an analytical solution can be derived.

Empirical validation The outputs of the candidate program are compared to the monitored energy use of a real structure, a test cell or a laboratory experiment. It is in principle the ultimate test. However, obtaining reliable information on energy consumption is very costly. In addition this kind of test may not be the most revealing due to the limited number of cases for which monitored values are available (cf (Judkoff & Neymark, 1998)).

Comparative testing The candidate program is compared to itself and to a set of reference programs that reflect the state-of-the-art of building energy simulation through a set of simple and meticulously described tests. Although there is no truth standard regarding building energy simulation software, this type of test presents the crucial advantage of being quick and inexpensive, for any level of complexity and with no input uncertainty.

Table 1.1: Overview of published BESTEST suites

BESTEST suite name	**Study object**	**Year**	**Reference**
IEA	Building Envelope	1995	(Judkoff & Neymark, 1995c)
HERS	Building Envelope	1995	(Judkoff & Neymark, 1995a) (Judkoff & Neymark, 1995b)
Florida-HERS	Building Envelope	1997	(Judkoff & Neymark, 1997b) (Judkoff & Neymark, 1997a)
HVAC	Heating, Ventilation and Air Conditioning devices	2002 2004	(Judkoff & Neymark, 2002) (Judkoff & Neymark, 2004)
EX	Existing houses	2010	(Judkoff *et al.*, 2010a) (Judkoff *et al.*, 2010b)

A short description of each suite can be found in the following paragraphs.

IEA BESTEST The International Energy Agency (IEA) BESTEST is the very first BESTEST suite. It is a comparative testing and diagnostic procedure for building envelope simulation programs. It consists in the simulation of 40 test cases performed on a very simple building in a hot summer and cold winter climate. The candidate program should provide hourly outputs on heating, cooling, solar irradiation and inside temperature. The state-of-the-art is represented by the following programs: ESP (UK), BLAST 3.0 Level 215 (USA), DOE2.1E-W54 (USA), SERIRES/SUNCODE (USA), SERIRES-1.2 (USA), S3PAS (Spain), TRNSYS (USA) and TASE (Finland). The outputs of those programs define a validity range. To pass the test, the outputs of the tested program must be within that range.

HERS BESTEST Home Energy Rating Systems (HERS) BESTEST was developed a few months after IEA BESTEST. These two suites are very different although the methodology is similar and the focus is on building envelope in both cases. As opposed to the IEA version, the study object is here a simplified house that represents "typical" constructions with "typical" thermal and physical properties. Furthermore, the simulations are performed in two different climates, one hot (cooling only) and one cold (heating only). The level of detail in the outputs is also much smaller. Only annual and monthly loads are required. Finally, the number of reference programs is limited to three: BLAST 3.0 (USA), DOE2.1E (USA) and SERIES/SUNCODE 5.7(USA). For these reasons, HERS is far less academically rigorous than the IEA version. It was developed for a class of much simpler simulation tools. However, it is recommended that the two suites should be used in parallel.

Florida-HERS BESTEST This suite was developed at the demand of the Florida Solar Energy Center (FSEC). The reason was that Florida's energy analysis software is based on a climate specific correlation methodology, which means that it is only working in Florida-like climates. Moreover, the effort necessary to generate new HERS BESTEST reference results for Florida climate was much easier and less expensive than the development of new correlation coefficients. Finally, developing test specifications for the hot, humid climate of Florida is necessary for future test suites.

HVAC BESTEST The first suites of the BESTEST were strictly focusing of the simulation of the building envelope. The HVAC BESTEST is an extension for the test of mechanical systems. The first cases E100 to E200 (Judkoff & Neymark,

2002) describe unitary space cooling equipments. The simulations are performed over steady-state conditions with a highly simplified near-adiabatic envelope. In a second volume (Judkoff & Neymark, 2004), cases E300 to E545, the HVAC systems are described in an hourly dynamic context over an expanded range of performance conditions. It is highly recommended that envelope-load tests be performed in addition to the HVAC simulations.

ESTEST-EX This BESTEST suite was developed to test the reliability of building energy retrofit software used to predict retrofit energy savings. It is based on the HERS BESTEST procedure. Input uncertainty is introduced for inputs that have both high uncertainty (range to be defined) and great effect on the outputs. These inputs are chosen randomly in the reference programs and kept secret. The reference programs are producing synthetic utility bill and reference energy saving results. A non-calibrated base-case model is then developed on the tested program. This model is calibrated using synthetic utility bills and reference energy saving results.

Suites testing ground coupled heat transfer (Judkoff & Wijsman, 2009) and in-depth multi-zone non-airflow cases (Judkoff *et al.*, 2008) were also developed.

1.3 Justification of BESTEST application on CitySim

During its development, CitySim was confronted to analytical (Kämpf, 2009) and to empirical tests (Walter, 2013) with satisfying results.

In this work, CitySim is confronted with the IEA BESTEST suite. This choice of this particular suite is driven by its focus. Indeed, the energy consumption of buildings varies mainly depending on the characteristics of the building envelope, which is the focus of the IEA BESTEST suite. Therefore, applying this particular suite to CitySim allows to verify that the heating profiles generated are correct.

One may question the reasons for applying a purely software-to-software test suite in order to ensure reliable real energy consumptions. It is true that failing the BESTEST does not necessarily imply that the program is deficient and does not correspond to the reality. However, it was demonstrated that the BESTEST is a very effective procedure for trapping bugs and faulty algorithms in all tested programs and that it is often more revealing than empirical validation methods (Judkoff & Neymark, 1998). In addition, IEA experts unanimously recommend that all programs should be "BESTESTed" before use. Moreover, well-know programs like EnergyPlus (Web Source) or ESP-r (Strachan *et al.*, 2008) were submitted to the BESTEST during their development. Finally, the reference programs benefit from several decades of development and were already tested in a significant number of real cases.

One may question on the current validity of a near 20 year old suite. According to (Judkoff & Neymark, 2013), no substantive revisions were made to the founding test suite although the present state-of-the-art of building simulation largely evolved since 1995. A significant evolution of the BESTEST is required. For example, the weather data format TMY is obsolete and a new one should be chosen based on industry consensus. Similarly, the management of interior and exterior surface heat transfer coefficients and weather-driven infiltration would require updating. However, the intent would be to integrate these changes while maintaining the original kernel of fundamental diagnostic capabilities. In other words, the BESTEST is backward compatible. It is then meaningful to apply the IEA BESTEST suite to CitySim.

1.4 IEA BESTEST Methodology

1.4.1 Specific input information

In this section, the different inputs that were implemented in CitySim to simulate the different cases of the IEA BESTEST are described. These inputs include the weather data, the building geometry and the following parameters:

1. Set point [$^\circ$ C)]
2. Building mass
3. Internal heat gains [W]
4. Air Change per hour [h^{-1}]
5. Exterior long-wave emissivity [-]
6. Interior long-wave emissivity [-]
7. Exterior shortwave absorbance [-]
8. Interior shortwave absorbance [-]
9. Windows area [m^2]
10. Windows orientation
11. Fixed shading devices

The name of each case is a specific number from 195 to 960.

Among these parameters, #6 and #8 cannot be implemented. CitySim considers that the interior space behaves like a perfect black cavity. This means that entering irradiance is entirely absorbed as heat. Cases that vary only according to the interior radiative coefficients are therefore neglected.

1.4.2 Final Results presentation

In this section, the final results obtained with CitySim to validate the BESTEST procedure are presented. The results were split into three categories.

1.4.2.1 Solar irradiation

1. Annual incident unshaded total solar irradiation (diffuse and direct) on north east, west, south and horizontal surfaces ($\frac{kWh}{m^2 \cdot y}$) for case 600 or 900.
2. Unshaded annual transmitted solar irradiation (diffuse and direct) through west and south windows ($\frac{kWh}{m^2 \cdot y}$)
3. Annual transmitted solar irradiation through the shaded south window with a horizontal overhang for case 610 or 910, and through the shaded west window, as in case 630 or 930 ($\frac{kWh}{m^2 \cdot y}$).
4. Hourly unshaded incident solar irradiation on south and west surfaces on the 27th of July for case 600 or 900
5. Hourly unshaded incident solar irradiation on south and west surfaces on the 5th of March for case 600 or 900

1.4.2.2 Heating and cooling demand

6. Annual heating and cooling loads for all nonfree-float cases ($MWh/year$)
7. Annual hourly peak heating and cooling loads (kW) with the date and hour for all non-free float cases
8. Hourly heating (+) and cooling (-) (kWh) on the 4th of January for cases 600 and 900

1.4.2.3 Inside temperature variations

9. Annual hourly maximum, minimum temperature ($^\circ$C) with date and hour and annual average temperature for all free-float (FF) cases and for the sun zone case ($\frac{W}{m \cdot K}$).
10. Annual hourly 1°C temperature bin frequencies from -20°C to +70°C for the high weight free-float case (900FF).
11. Hourly free-float temperature on the 4th of January for cases 600FF and 900FF
12. Hourly free-float temperature on the 27th of July for cases 650FF and 950FF

Among those outputs, #12 is not obtainable as cases 650 and 950 are defined with a setpoint strategy that cannot be implemented in CitySim.

Due to the limited time dedicated to this certification procedure, some annual results are not extracted with date and hour of occurence. Only the value is considered. Others have already used the BESTEST in a similar way (Delsante, 2004).

1.4.3 The IEA BESTEST procedure

In part 1.4.2, the results are presented as a whole. This is useful to detect major discrepancies between the reference programs and CitySim and allow to identify tendencies in CitySim outputs.

Cases defined in the IEA BESTEST can be classified in two main sections that are qualification cases (600 to 630 and 900 to 960) and diagnostic cases (195 to 430 and 800). The former are used to validate the program according to the BESTEST procedure. The latter help finding the origin of a potential problem in the program code.

The BESTEST procedure is applied as follows:

1. Qualification cases are executed one after the other in a particular sequence defined in Figure 1.2. Simulation results are then compared with outputs of reference programs. The process is interrupted in case of discrepancies. If none are encountered, the candidate program is validated.

2. In case of discrepancy, the BESTEST procedure returns an indication on the source of the error and the series of diagnostic tests to be applied to analyse more precisely the error location in the program code.

3. The low-mass diagnostic cases (Figure 1.3) and high-mass diagnostic cases (1.4) unroll in a similar sequence and provide more explicit descriptions of the possible error location in the program code.

This test series is only applied to results #6 and #7, respectively the annual heating and cooling load and annual peak heating and cooling demand. Other categories of results are used to support final conclusions.

For instance, if tests 600, 610 and (610-600) are correct but 620 returns a wrong value. This means that there is probably an issue with the solar incidence and transmittance on the east and west façade. The location of the error is confirmed if test A13 (300-270) also fails. Otherwise, the problem is located elsewhere and tests A1 to A11 or B1 to B10 are applied to identify its location.

Figures 1.2, 1.3 and 1.4 differ from the originals in (Judkoff & Neymark, 1995c) p.1-28 to 1-31. Here, all tests specific to cases that cannot be implemented in CitySim are removed, i.e. the cases that involve changes in the interior IR emmissivity, setback setpoint or forced ventilation.

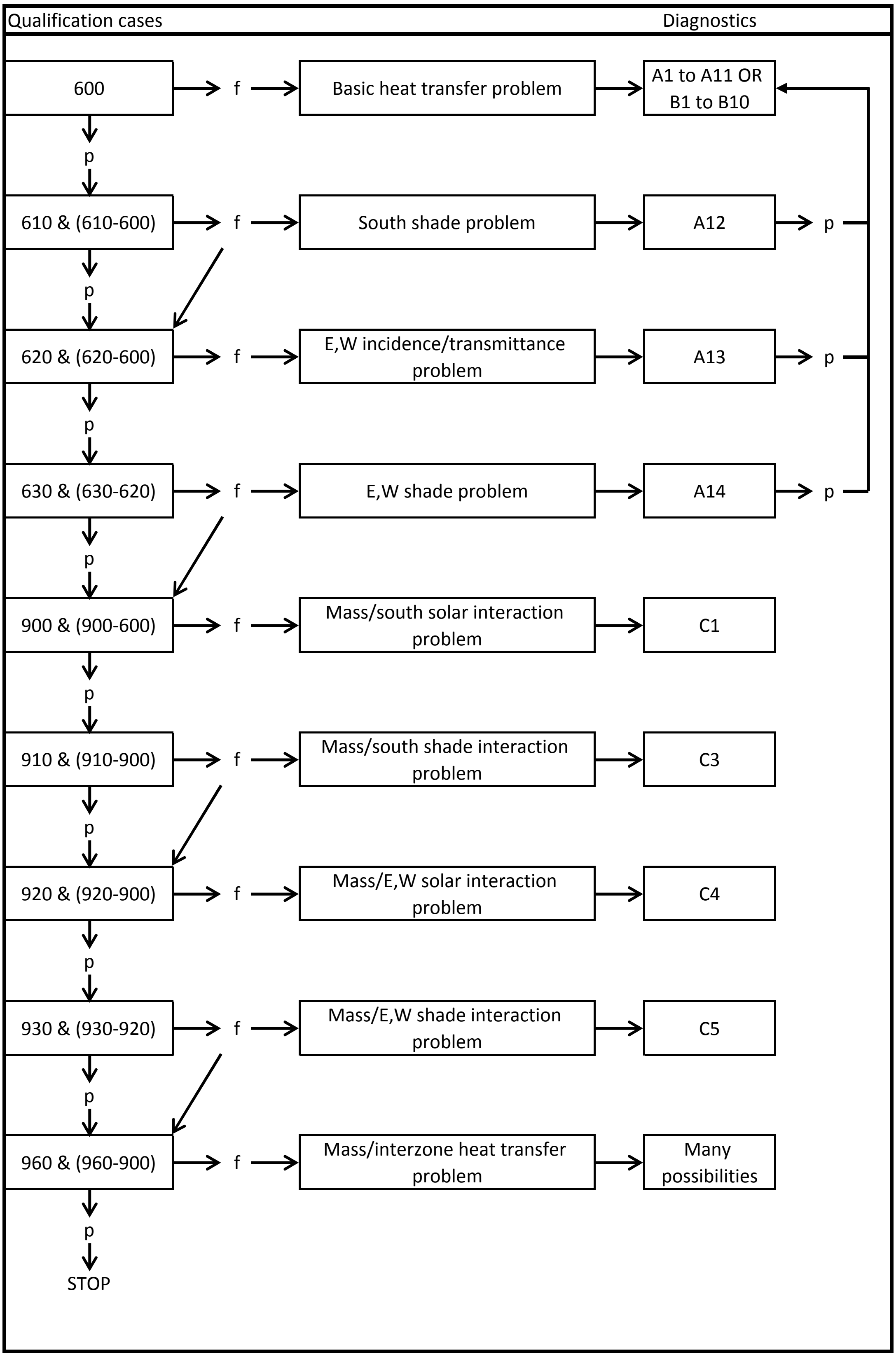

Figure 1.2: BESTEST - Low and high-mass qualification flow diagram - Adapted from (Judkoff & Neymark, 1995c)

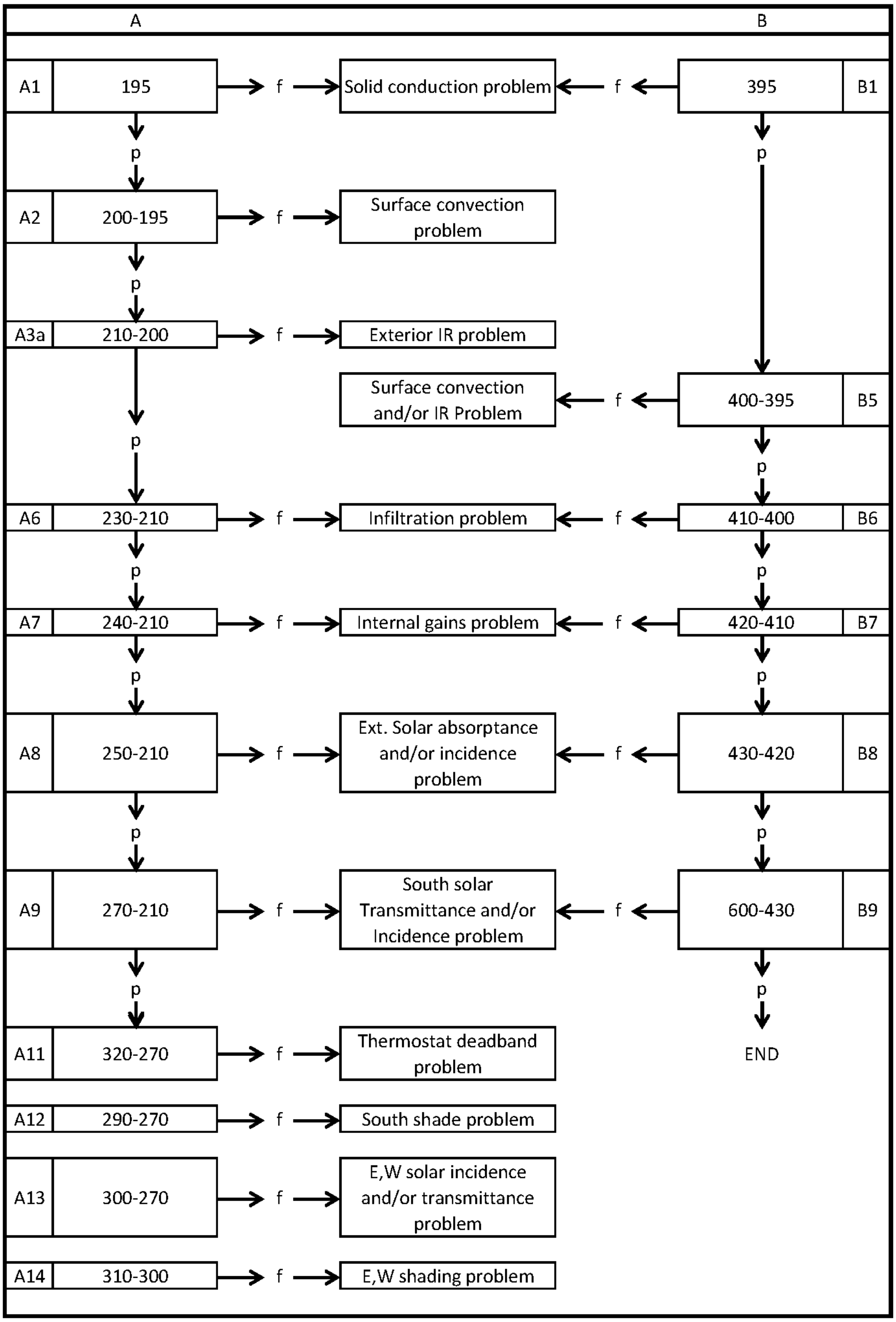

Figure 1.3: BESTEST - Low-mass diagnostics flow diagram test - Adapted from (Judkoff & Neymark, 1995c)

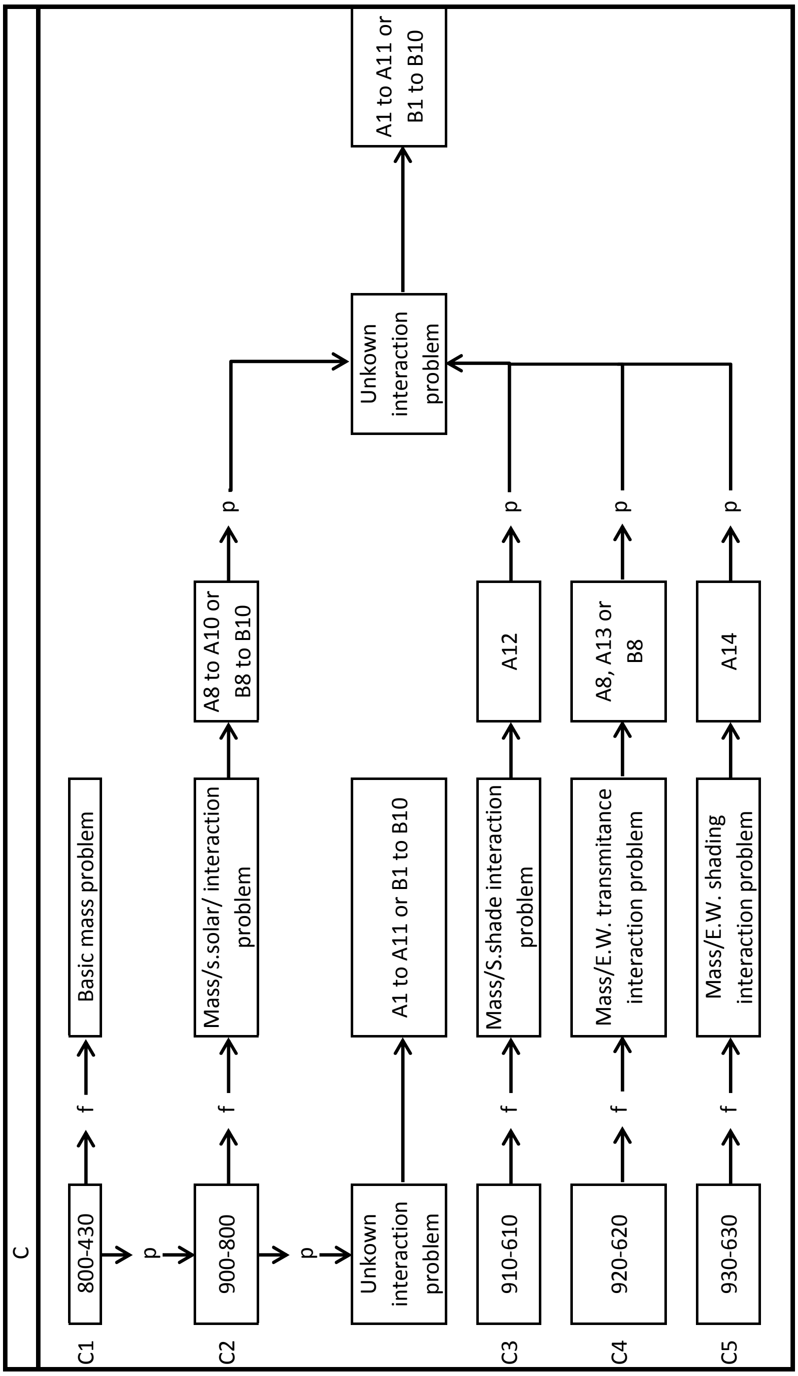

Figure 1.4: BESTEST - High-mass diagnostic flow diagram - Adapted from (Judkoff & Neymark, 1995c)

1.5 Specific input information

The software CitySim is tested according to the IEA BESTEST procedure. The test specification for these tests can be found in (Judkoff & Neymark, 1995c) but are reproduced below to explain how they were implemented in CitySim.

1.5.1 Weather

The IEA BESTEST is conducted using the weather of Denver, Colorado, United States. This site is located at latitude 39.8 ° north and longitude 104.9 ° west. The altitude is 1609 m and the time zone is -7. The weather data associated to this location is attached in (Judkoff & Neymark, 1995c) in TMY format (Typical Meteorological Year).

CitySim weather data input format is CLI and must contain the hourly weather information presented in Table 1.2.

The majority of these data are available in (Judkoff & Neymark, 1995c). However, some other data could not be found. For instance, the diffuse horizontal irradiation is not available and is recalculated with Eq. 1.1.

$$G_{Dh} = G_{Gh} - G_{Bn} \cdot cos(\frac{\pi}{2} - \theta_S) \tag{1.1}$$

Where G_{Dh} $[\frac{W}{m^2}]$ is the diffuse horizontal irradiation
G_{Gh} $[\frac{W}{m^2}]$ is the global horizontal irradiation (available in TMY)
G_{Bn} $[\frac{W}{m^2}]$ is the beam normal irradiation (available in TMY)
θ_S $[rad]$ is the solar altitude (given by CitySim).

The relative humidity and the precipitations are not available and cannot be computed with values given in the TMY. Further investigations should be undertaken to verify the results' sensibility to these particular parameters. In the present work, these data were extracted from Meteonorm.

There are no obstacles around the simulated building in IEA BESTEST. To implement this condition in CitySim, the far field obstruction is set to 0 all around the building.

In Table 1.3, theoretical values given in (Judkoff & Neymark, 1995c) for the original TMY weather file are compared with calculated values from the generated CLI file. The goal is to confirm the validity of the used weather data.

The comparison reveals a reasonable match between the two climates files. However, this method only consists in comparing a limited number of values and is therefore not comprehensive. In further investigations, the whole weather data should be obtained from NREL and integrated in CitySim.

Table 1.2: CitySim weather file required entries

Element	**Symbol**	**Unit**
Diffuse horizontal irradiance	G_{Dh}	$\frac{W}{m^2}$
Beam normal irradiance	G_{Bn}	$\frac{W}{m^2}$
Air temperature	T_a	$^\circ$C
Ground temperature	T_g	$^\circ$C
Wind speed	FF	$\frac{m}{s}$
Wind direction	DD	$^\circ$
Relative humidity	RH	-
Precipitations	RR	mm
Cloud cover fraction	N	Octas

Table 1.3: Weather summaries comparison between used and theoretical data

Element	CitySim	BESTEST	unit
Weather format	CLI	TWY	-
Mean annual wind speed	4	4.02	$\frac{m}{s}$
Ground temperature	10	10	$^\circ$C
Mean annual ambient air temperature	9.71	9.71	$^\circ$C
Minimum annual temperature	-24.4	-24.39	$^\circ$C
Maximum annual temperature	35	35	$^\circ$C
Maximal annual wind speed	14.9	14.89	$\frac{m}{s}$
Mean annual relative humidity	0.0051	0.0047	-
Global horizontal solar irradiation annual total	1831.95	1831.82	$\frac{kWh}{m^2.y}$
Direct normal solar irradiation annual total	2353.58	2353.58	$\frac{kWh}{m^2.y}$
Direct horizontal solar irradiation	1349.18	1339.48	$\frac{kWh}{m^2.y}$
Diffuse horizontal solar irradiation	482.77	492.34	$\frac{kWh}{m^2.y}$

1.5.2 Building geometry

The 3D definition of building geometry becomes crucial in the context of a neighborhood or a city. Indeed, the proximity of several buildings in the same location is likely to cause interactions between them like shadings or reflections. These interactions modify the solar gains received by each building and so their heating and cooling loads.

In CitySim, a building is defined as a set of surfaces in an orthogonal system where the X-axis is pointing to the east, the Y-axis to the north and the Z-axis to the top. Each surface owns three or more coordinates whose order defines the surface orientation.

The geometry of all cases in the IEA BESTEST is the same (except cases 960 and 990). It is a simple shoebox whose dimensions are summarized in Table 1.4.

Table 1.4: IEA BESTEST basecase dimensions

Element	Value
Building dimensions	8, 6, 2.7 m
South and North walls	21.6 m^2
East and West walls	16.2 m^2
Roof surface	48 m^2
Treated floor area	48 m^2
Interior air volume	129.6 m^3

1.5.3 Scenarios definition

There are 40 cases defined in IEA BESTEST. The geometry and weather conditions are identical for all of them (except cases 960 and 990). The varying parameters are described below. Table 1.5 summerises the simulated scenarios.

Table 1.5: List of cases in the BESTEST - adapted from (Judkoff & Neymark, 1995c) p. 1-16,1-17

Case #	Set Points (°C)	Mass	Internal gains (W)	Infiltration (h^{-1})	Int IR Emissivity	Ext IR Emissivity	Int SW Absorption	Ext SW Absorption	Glass (m2)	Windows Orientation	Shadings
195	20	L	0	0	0.1	0.1	NA	0.1	NO	NA	NO
200	20	L	0	0	0.1	0.1	NA	0.1	0	S	NO
210	20	L	0	0	0.1	0.9	NA	0.1	0	S	NO
230	20	L	0	1	0.9	0.9	NA	0.1	0	S	NO
240	20	L	200	0	0.9	0.9	NA	0.1	0	S	NO
250	20	L	0	0	0.9	0.9	NA	0.9	0	S	NO
270	20	L	0	0	0.9	0.9	0.9	0.1	12	S	NO
290	20	L	0	0	0.9	0.9	0.9	0.1	12	S	1.0mH
300	20	L	0	0	0.9	0.9	0.9	0.1	6,6	E,W	NO
310	20	L	0	0	0.9	0.9	0.9	0.1	6,6	E,W	1.0mHV
320	20-27	L	0	0	0.9	0.9	0.9	0.1	12	S	NO
395	20-27	L	0	0	0.9	0.9	NA	0.1	NO	NA	NO
400	20-27	L	0	0	0.9	0.9	NA	0.1	0	S	NO
410	20-27	L	0	0.5	0.9	0.9	NA	0.1	0	S	NO
420	20-27	L	200	0.5	0.9	0.9	NA	0.1	0	S	NO
430	20-27	L	200	0.5	0.9	0.9	NA	0.6	0	S	NO
600	20-27	L	200	0.5	0.9	0.9	0.6	0.6	12	S	NO
600FF	NONE	L	200	0.5	0.9	0.9	0.6	0.6	12	S	NO
610	20-27	L	200	0.5	0.9	0.9	0.6	0.6	12	S	1.0mH
620	20-27	L	200	0.5	0.9	0.9	0.6	0.6	6,6	E,W	NO
630	20-27	L	200	0.5	0.9	0.9	0.6	0.6	6,6	E,W	1.0mHV
800	20-27	H	200	0.5	0.9	0.9	0.6	0.6	0	S	NO
900	20-27	H	200	0.5	0.9	0.9	0.1	0.6	12	S	NO
900FF	NONE	H	200	0.5	0.9	0.9	0.1	0.6	12	S	NO
910	20-27	H	200	0.5	0.9	0.9	0.6	0.6	12	S	1.0mH
920	20-27	H	200	0.5	0.9	0.9	0.6	0.6	6,6	E,W	NO
930	20-27	H	200	0.5	0.9	0.9	0.6	0.6	6,6	E,W	1.0mHV
960	2ZONE SS	H									

1.5.3.1 Set point

The set-point defines the thermostat control strategy and determines when and how heating and cooling equipments operate. This parameter is important as it sets the objective of the HVAC equipment to insure the comfort of inhabitants.

In IEA BESTEST, the focus is on the building envelope, HVAC equipments are thus assumed to be 100% efficient, of infinite capacity and purely sensible (no latent load calculations).

In CitySim, the setpoint is defined with a minimum and maximum temperature (T_{min} and T_{max}). The gap between these two temperatures defines a comfort zone where the HVAC equipments are not operating.

The following Setpoint control strategies are encountered in the IEA BESTEST.

20 In this case, the heating(cooling) is on if the temperature is below(above) 20 °C.

20-27 This set-point strategy defines a comfort zone between 20 °C and 27 °C. The HVAC equipments only operate when the inside air temperature is outside this range.

SETBACK In this case, the required minimal inside air temperature is 20 °C during the day (from 07:00 to 23:00) and 10 °C during the night. The maximal inside temperature is still 27 °C. This strategy can not be implemented in CitySim, related scenarios (640 and 940) are not performed.

27,V This scenario differs greatly from the three others. There is no heating and fans are ventilating the building during the night (from 18:00 to 07:00). Cooling is off during the night and operates during the day to maintain the building below 27 °C. This strategy cannot be implemented in CitySim, related scenarios (650, 650FF, 950 and 950FF) are not performed.

2ZONE SS and GROUND COUPLED These set-point strategies differ drastically from the others. They are defined in paragraphs 1.5.3.9 and 1.5.3.10.

NONE In this case, the building is allowed to free-float, which means that the heating and cooling equipments never operate. To allow the free-float conditions in CitySim, HVAC equipments can be removed or the comfort zone can be defined as infinite (for instance, T_{min}=-50 °C and T_{max}=100 °C).

1.5.3.2 Building mass

The building envelope is composed of different layers with specific thicknesses, thermal conductivities (λ), density (ρ) and specific heat (Cp). The definition of the building envelope determines the thermal conductance and the heat storage capacity of the building.

There are two different types of envelopes in the IEA BESTEST, the lightweight (L) and the heavyweight (H). The U-value of these two configuration can be found in Table 1.6. Their composition is decribed from outside to inside in Tables A.1 and A.2 respectively.

Table 1.6: U-value of the envelope for lightweight and heavyweight cases

	Lightweight	Heavyweight
Wall	0.51	0.51
Roof	0.32	0.32
Floor	0.039	0.039

1.5.3.3 Internal Heat Gains

The Internal Heat Gains (IHG) represent the heat that is generated from sources like people or lighting that are not part of HVAC systems.

In CitySim, each inhabitant accounts for a constant value of 90W. The regulation of the IHG is done by defining a schedule (α_h) and a maximal number of occupants (P_{max}).

Table 1.7: Schedule Style

Hour of the day	Presence	Power
1	α_1	$P_{max} \cdot \alpha_1$
...	...	...
24	α_{24}	$P_{max} \cdot \alpha_{24}$

Where α_h is the fraction of P_{max} that is generated in the building during hour h.

In the IEA BESTEST, the IHG is constant during the year and accounts for either 0 or 200 W depending on the scenario. The corresponding number of inhabitants to be defined to meet these requirements in CitySim is then either 0 or 2.222. As this value is constant, all α_i are equal to 1.

1.5.3.4 Infiltration

The infiltration rate is defined as the Air Changed per Hour (ACH) and represents the part of the inside air volume that is replaced by fresh air every hour.

This air exchange is necessary to insure a comfortable and healthy environment inside the building by removing pollutants like CO2, smells, bacteria and water vapour.

At the altitude of the site, the density of air is approximately 20% smaller than at sea level. The ACH is then corrected from 0, 0.5 and 1 to 0, 0.41 and 0.822 depending on the scenario.

1.5.3.5 Convective heat transfer coefficients

The heat is transmitted through the wall by conduction and then to the air by convection. The rate of the latter is defined by a convective heat transfer coefficient that represents the thermal resistance of the thin air layer that surrounds the building. This coefficient varies depending on the wind speed and direction and the surface roughness.

In CitySim, the exterior and interior convective exchange coefficients are calculated for every hour of the year using the wind speed and direction. By contrast, these coefficient are fixed in the BESTEST. However, the BESTEST states that every program should be used in its maximum level of complexity when confronted to the BESTEST (cf (Judkoff & Neymark, 1995c) p. 1-2).

1.5.3.6 Radiative heat transfer coefficient

The building exchanges heat with its environment through radiation depending on radiative heat transfer coefficients. Here, the distinction is made between long-wave (IR) and short-wave (visible and UV) radiations.

According to the theory of the black body, a material spontaneously generates radiation depending on its temperature. The temperature range for a building is low, only IR are generated. This generation rate is calculated using the surface temperature and long-wave emissivity specific to the surface.

The shortwave radiation is coming from the sun. Part is absorbed by the envelope in the form of heat and transmitted by conduction. The rest is reflected. The amount of energy absorbed depends on the shortwave reflectance on the surface of incidence.

These two coefficients are defined in CitySim. In the BESTEST, other cases are considered that involve interior radiative coefficients. These cases are not considered as they cannot be implemented in CitySim. However, scenarios that differ only by interior long-wave or shortwave coefficients from other scenarios are assumed equivalent. Thus, case 215 is equivalent to 200, 220 to 210, 280 to 270, 440 to 600 and 810 to 900. The interest is to verify that CitySim validates the BESTEST even without varying the inside radiative coefficients.

1.5.3.7 Windows

Windows are often the weakest point of a building envelope. The high U-value of the glazing causes high losses through conduction. Moreover, depending on the frame, it is also a privileged point for air infiltration. In hot climates, the irradiation that penetrates through windows drastically increases the cooling needs.

There is a single type of glazing considered in all the different scenarios. Among the various information provided in IEA BESTEST to define the windows, CitySim requires the U-value and the g-value of the glazing. These properties are summarized in Table 1.8.

Table 1.8: IEA BESTEST windows properties

U-value	3.0 W/m2.K
SC	0.916
Glazing gvalue	0.787
gvalue	0.721

1.5.3.8 Shadings

The shading devices considered in the BESTEST are fixed.

In CitySim, they are defined as a new category of surfaces. These surfaces are not participating in the direct conductive thermal exchange but are impacting the solar gains and IR exchanges. The position of those shadings in the different cases can be found in Figure A.1.

1.5.3.9 Case 960 : Sunspace

In this particular scenario, the geometry is different. The dimension changed and the building is now separated into two different zones:

- the back-zone is strictly identical to Case 600 at the exception that the south wall is replaced by common wall and windows are removed.
- the sun-zone is built using the heavyweight envelope at the exception of the north wall, linked to the back-zone that is replaced by common wall. The ACH is set to 0.5 (0.41) h^{-1}, IHG are removed and the zone is allowed to free-float.

The characteristics of the common wall are presented in Table 1.9.

Table 1.9: Characteristics of the common wall

Thickness (m)	λ ($\frac{W}{m \cdot K}$)	ρ ($\frac{kg}{m^3}$)	Cp ($\frac{J}{kg \cdot K}$)
0.2	0.51	1400	1000

-

1.5.3.10 Case 990

The temperature of the soil varies depending on many parameters such as weather, soil properties and the heat exchange between the building and the ground. In precedent cases, the soil temperature was imposed in the weather file. In Case 990, it is allowed to vary.

The justification for this case is that the thermal relation between a building and the ground roughly takes a year to reach stability after construction.

However, for CitySim, the implementation of this case is not possible.

1.6 Final results Presentation

1.6.1 Solar Irradiation results

1.6.1.1 Annual Results

In this part, the objective is to determine if the solar irradiance model of CitySim is consistent. The comparison is done on a yearly and hourly scale.

In Figure 1.5, the results for annual incident solar irradiation are presented for façades of various orientations. The results given by CitySim are indicated in Orange. Blue, green and red represent respectively the minimum, mean and maximum values given by the reference programs. CitySim results show excellent agreement with reference results and are within the validity range for all cases.

Figure 1.6 presents results for the annual transmitted solar irradiation per meter square of glazing area for two orientations (W and S), with and without the shadings. The color code is the same as before. CitySim results are close, above the mean and within the validity range in all cases.

Figure 1.7 is derived from the above graphs. The transmissivity coefficient is equal to $\frac{Unshaded_i}{Incident_i}$ where i is the orientation. Similarly, the overhang and fins shading coefficient is obtained by $1 - \frac{Shaded_i}{Unshaded_i}$. CitySim results are globally below the mean value and within the validity range, which means that in CitySim, the glazing transmits less irradiation and the shadings have less influence than the average of reference results.

Figures 1.5, 1.6 and 1.7 demonstrate the validity of CitySim for the simulation of solar irradiation.

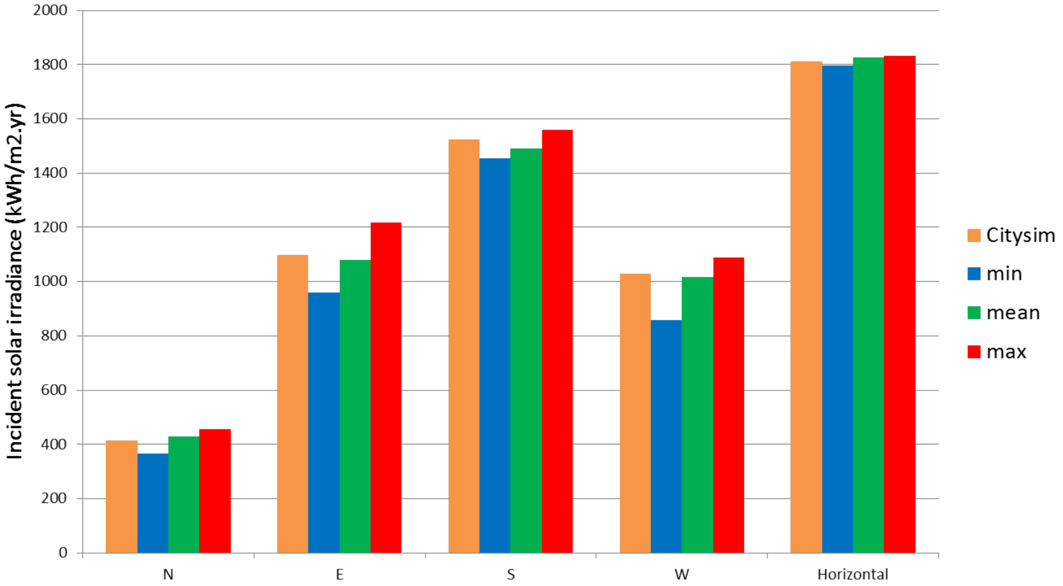

Figure 1.5: Incident solar irradiation for North (N), East (E), South (S), West (W) and horizontal façades - own illustration

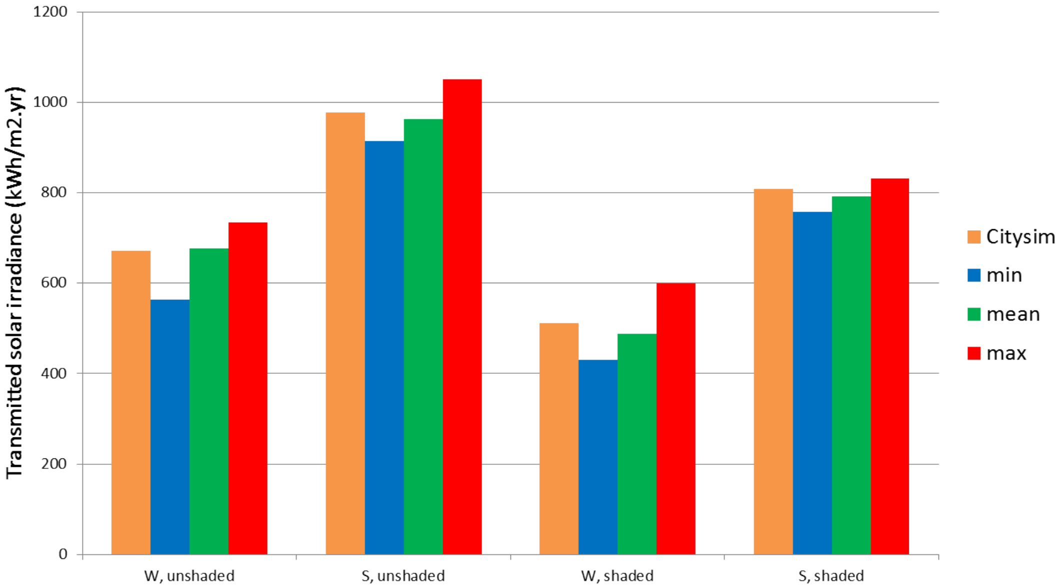

Figure 1.6: Unshaded and shaded transmitted solar irradiation for W and S façades - own illustration

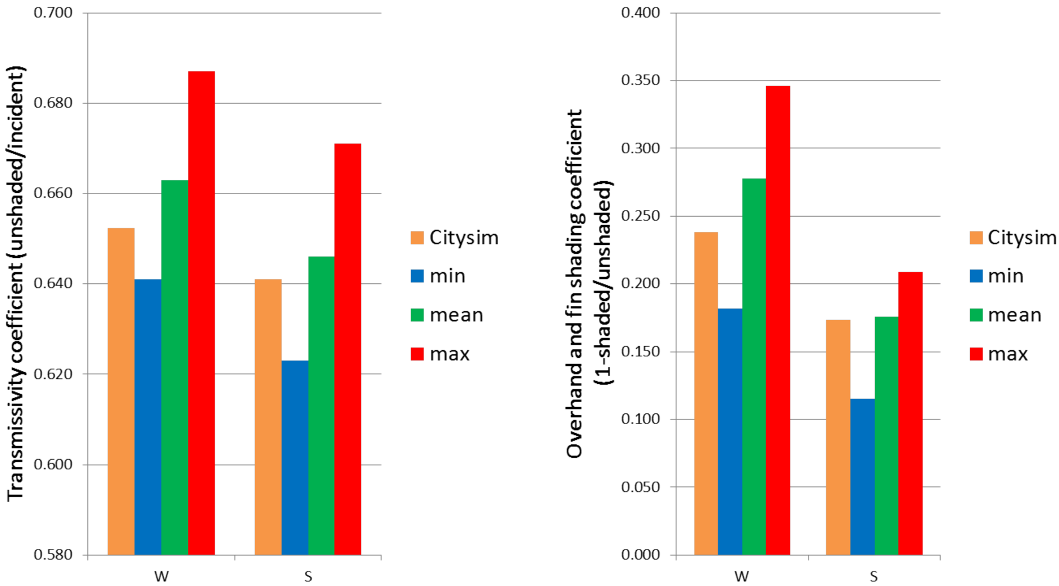

Figure 1.7: Transmissivity coefficient and shading coefficient for W and S façades - own illustration

1.6.1.2 Daily results

Values for annual solar irradiation are now validated. However, dynamic simulations are done on a hourly scale. The consistency of hourly irradiation values is therefore crucial.

Figures 1.8 and 1.9 summarise the results for hourly irradiance for south and west façades on a cloudy day (5^{th} of March) and on a clear day (27^{th} of July). CitySim results are highlighted in a squared marked red line on the four figures.

In all cases, CitySim has been shown to provide consistent results with the reference programs. Mostly, CitySim is located on a mean position between the hourly maximum and minimum of the validity range.

CitySim hourly results for solar irradiance can therefore be considered as validated.

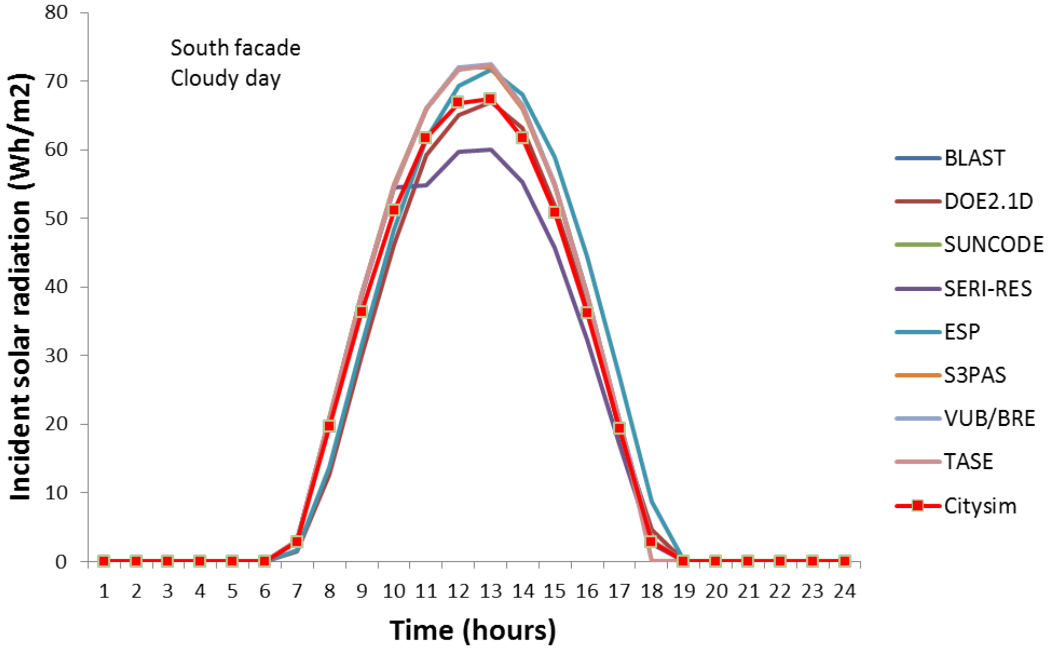

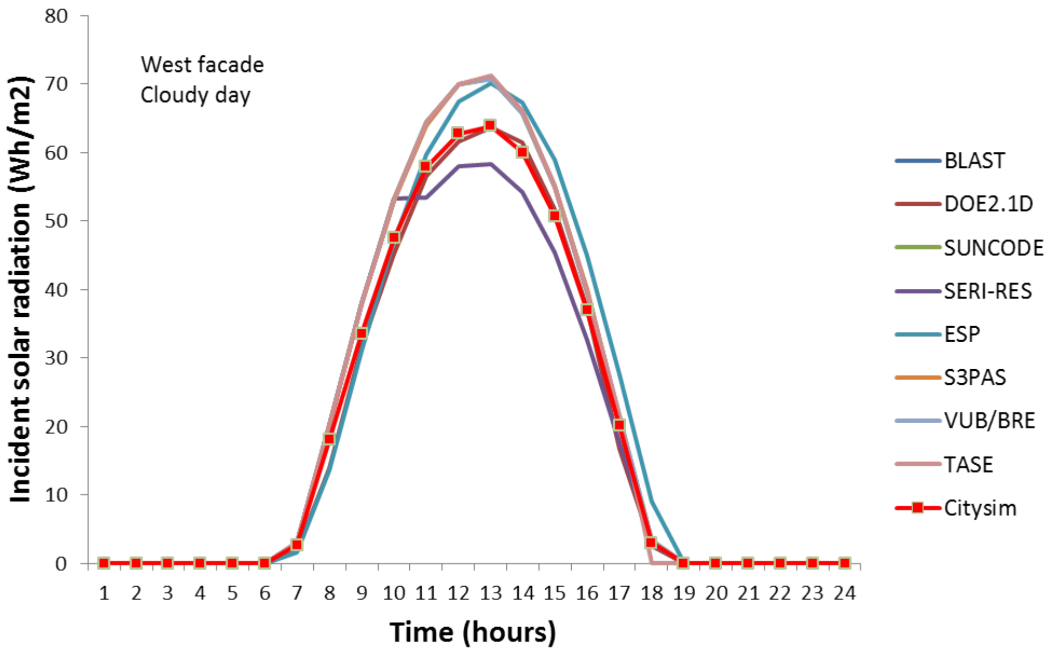

Figure 1.8: Hourly incident solar irradiance on the S (top) and W (bottom) façades for a cloudy day (March 5) - own illustration

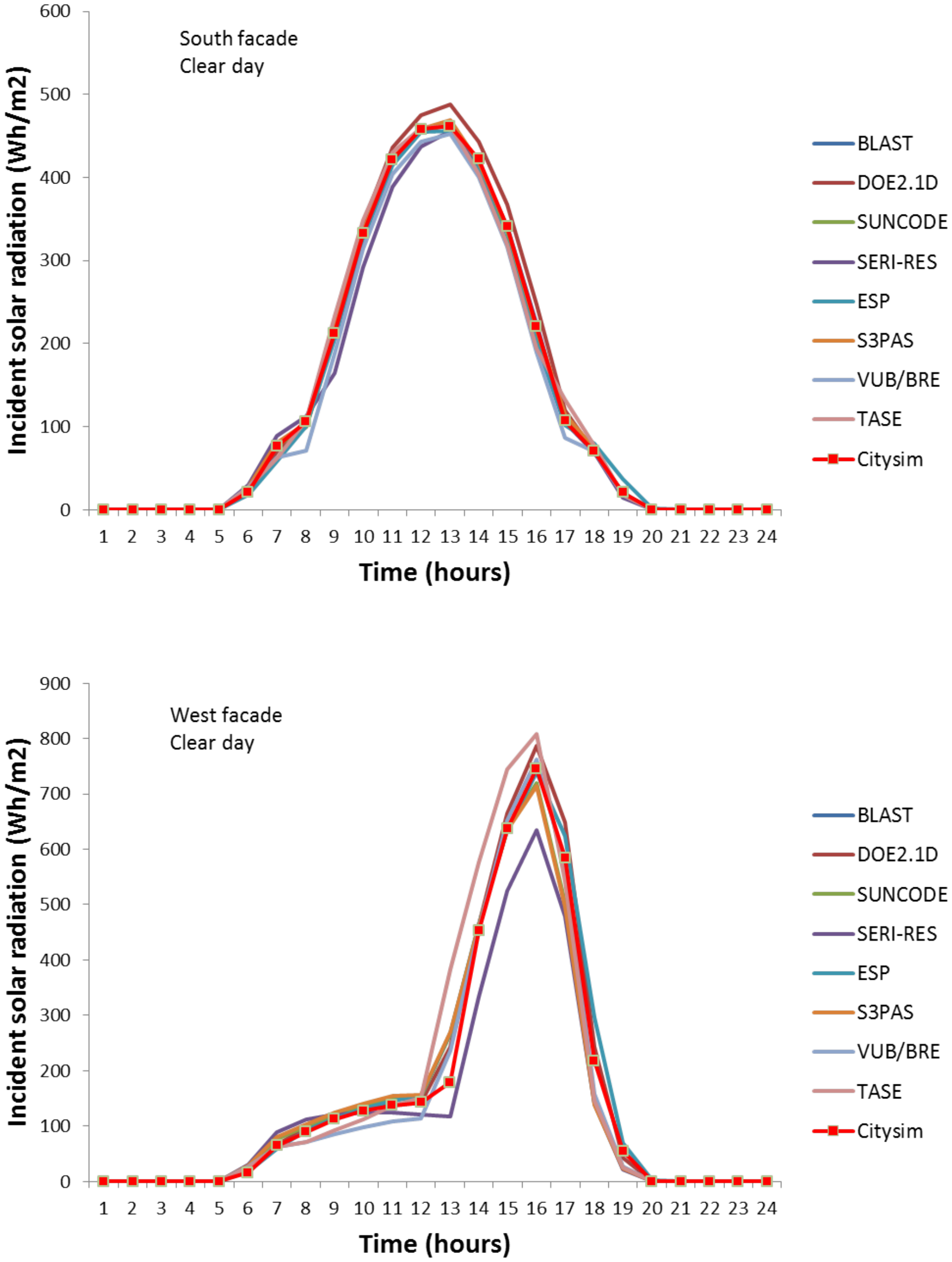

Figure 1.9: Hourly incident solar irradiance on the S (top) and W (bottom) façade for a clear day (July 27) - own illustration

1.6.2 Heating and cooling demand

1.6.2.1 Annual heating and cooling load

Figure 1.10 presents the results for the annual heating and cooling loads and peak heating and cooling demand. All simulated scenarios are here represented with the results of CitySim in the X-axis and all reference programs in the Y-axis. The Bisector is also drawn. Cases 600 and 900 are highlighted as examples. In what follows, the distribution of results for each case is referred to using the word ”cloud”.

In such a graph, a cloud distribution defines the validity range with its maximum and minimum value for one particular test scenario. If the bisector passes through the cloud, results are correct. Otherwise, the bisector passes either below or above the cloud. CitySim simulation results are pessimistic in the former case and optimistic in the latter.

For the annual heating load, clouds are very concentrated close below the bisector which means that reference programs are in good agreement with each other and that CitySim results are very similar to rather pessimistic reference programs like DOE or SERIES. For some cases however, CitySim outputs are above the range as for case 900.

For the annual cooling load, the general cloud concentration appear inferior when compared to results for annual heating load. Most clouds are located close above the bisector. This means that CitySim is in agreement with reference programs and have a tendency to give rather low estimations.

1.6.2.2 Annual peak heating and cooling demand

Similarly than for annual loads, the reference programs are more in agreement with each other for the peak heating than for the peak cooling where results are more dispersed.

The peak heating and cooling demand simulated with CitySim is globally within the validity range. Peak heating and cooling also has a tendency to be respectively on the higher and lower end of the validity range. This is the same tendency as for the annual load discussed in the previous part.

From the analysis of these results dispersion graphs, CitySim was demonstrated to follow globally the reference programs.

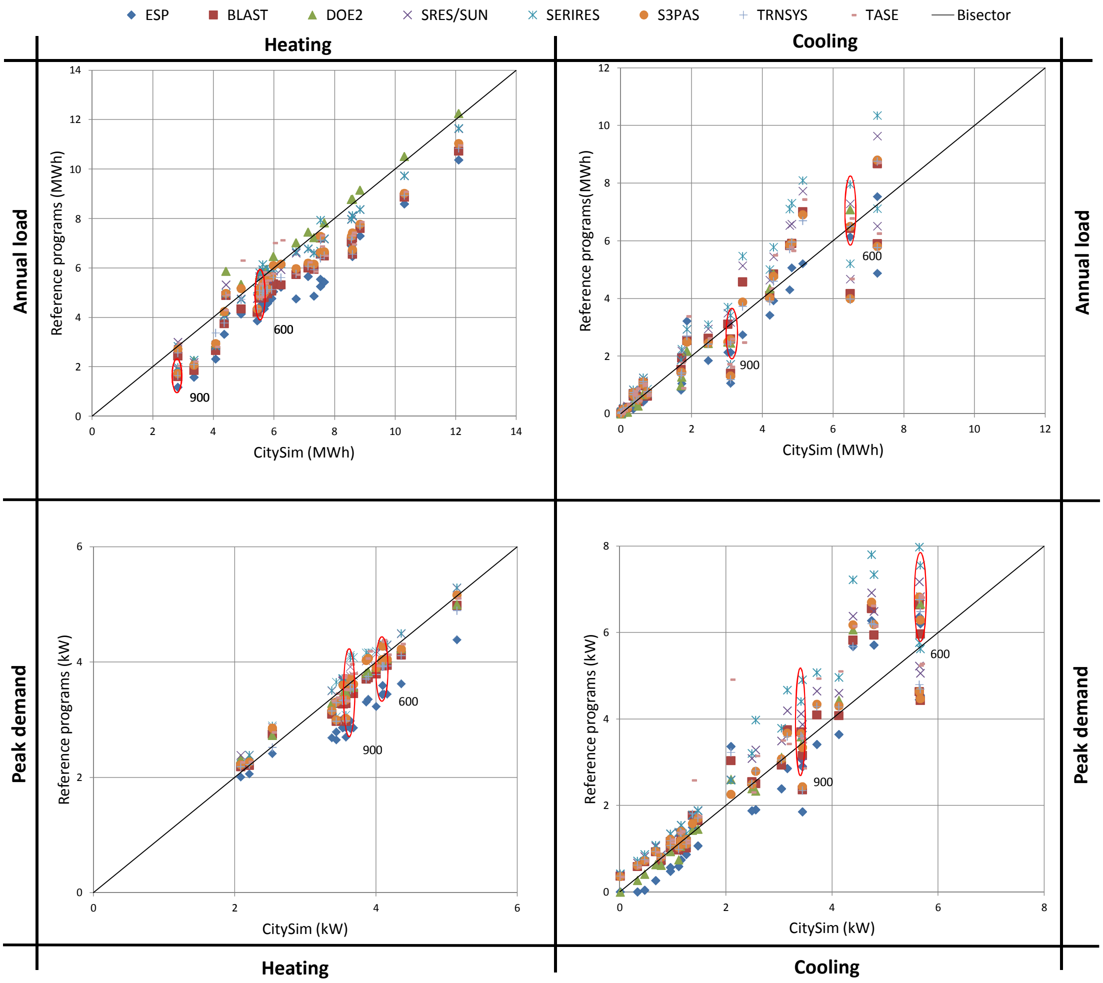

Figure 1.10: Results dispersion for annual heating load (top left), annual cooling load (top right), peak heating demand (bottom left) and peak cooling demand (bottom right) - Cases 600 and 900 encircled - own illustration

1.6.2.3 Daily results

Figure 1.11 presents the daily heating and cooling results obtained for scenario 600 and 900 on the 4^{th} of January. The hours of the day are on the X-axis and the needs are on the Y-axis. Positive and negative values correspond respectively to heating and cooling needs.

The order of magnitude given by CitySim is correct in Case 600 and bigger than for the reference programs in Case 900. In both cases, the heating variations are not completely coordinated between CitySim and the reference programs. The model appears more reactive in CitySim. This behavior can be explained by a too low inertia of the indoor air. Indeed, any change in indoor conditions is, to some extent, absorbed by the inner part of the envelope. Therefore, increasing the inside air thermal inertia decreases the reactivity of the model.

The underestimation of inside air thermal inertia might be caused by CitySim's simplified model of heat conduction and inertia.

In CitySim, the wall is assimilated to a single nod as described in (Lorenz & Masy, 1982) p.6 (cf Figure A.2). The total resistance of the wall R_{out} is divided in two smaller resistance that surround the total heat capacity C_{out}: One to the exterior (R_{p1}) and one to the interior (R_{p2}). The values of these resistance is determined by the accessibility θ_{out}. These three quantities are computed according to Eq. 1.2.

$$\theta_{out} = 1 - \frac{\sum_{k=1}^{n}[\sum_{i=1}^{k-1}(R_i + \frac{R_k}{2}) \cdot C_k]}{R_{out} \cdot C_{out}} \quad R_{p1} = (1-\theta_{out}) \cdot R_{out} \quad R_{p2} = \theta_{out} \cdot R_{out} \quad (1.2)$$

Where k and i represent the layers of the wall

C_k is the capacity of layer k

R_i and R_k are the resitances of layers i and k

R_1 and R_n are the resistance of the outer and inner most layers respectively

Ideally, the wall should be divided into an infinite number of thin layers that would be defined by a specific thermal conductivity and heat capacity(cf Figure A.2). However, this type of modeling is not possible because of computing power limitations. Consequently, considering the envelope as a single nod is a significant assumption. In the case of CitySim, it is justified by a gain in simulation time.

In this model, the capacity of the wall is only accessible to the inside air through the resistance $R_{p2} + \frac{1}{h_i}$. However, in reality, the only resistance that oppose the interaction of the innermost layer is the one of air. This means that the accessibility of the wall capacity by the inside air is smaller than in reality, which explaines the gap observed on Figure 1.11 between CitySim and other programs that model the wall thermal behavior in a complexer way.

This statement is supported by the fact that the problem has a higher impact in the heavyweight case 900 in Figure 1.11.

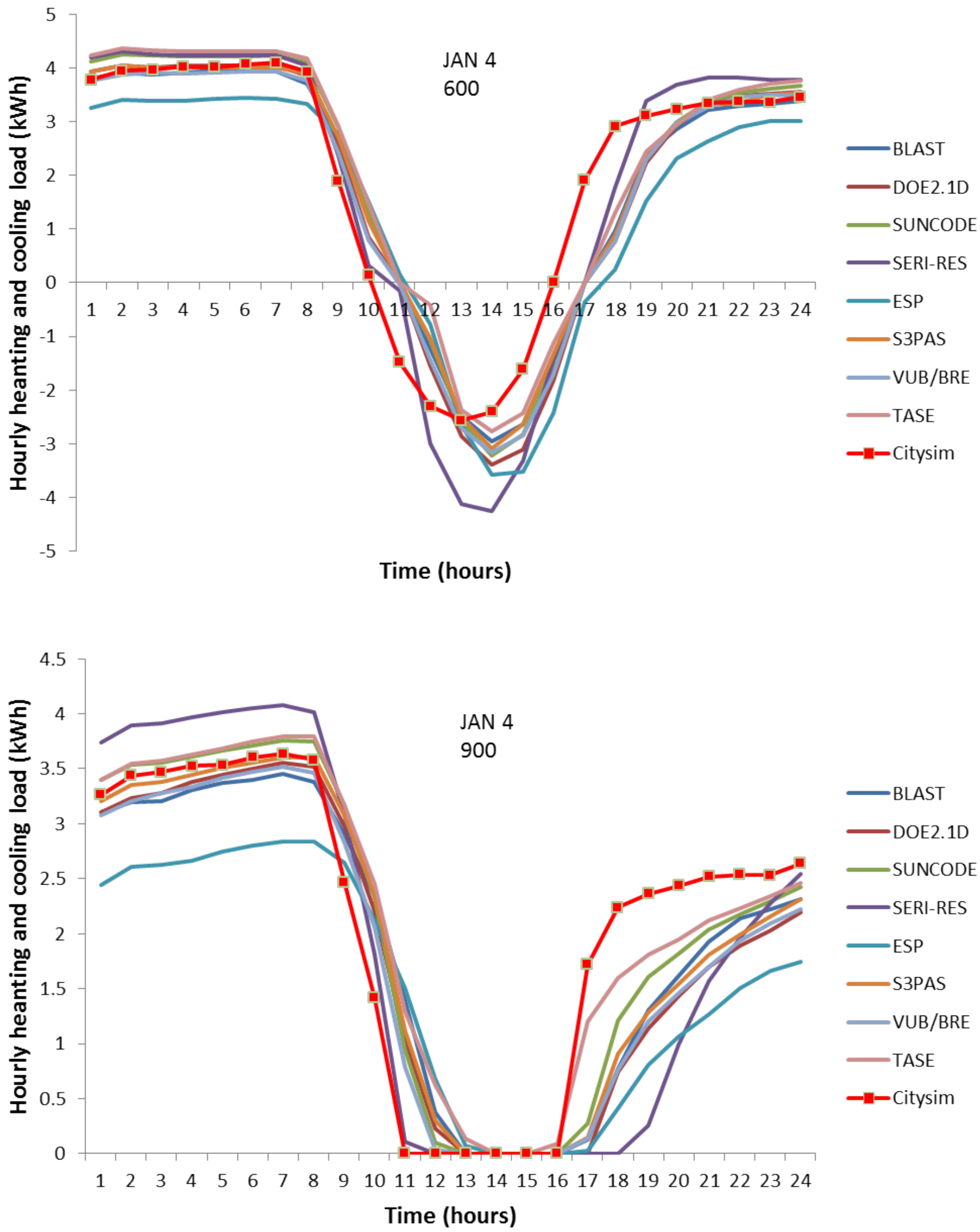

Figure 1.11: Hourly heating (+) and cooling (-) for the low-weight (top) and heavy-weight (bottom) cases on the 4^{th} of January - own illustration

1.6.3 Temperature Variations

Figure 1.12 presents the annual maximum, minimum and average inside temperature for the two free-float cases (600FF and 900FF) and for the sun-zone case (960). In orange are the results given by CitySim. Blue and red present respectively the minimum and maximum values of the validity range defined by the reference programs.

Figure 1.13 presents the distribution of temperature during the year sorted in bins of 1 $^\circ$C for the free-float heavyweight building (900FF). The bins are on the X-axis and the annual occurrence is on the Y-axis.

Finally, Figure 1.14 presents the hourly temperature variation for the two free-float cases (600FF and 900FF) on the 4^{th} of January. The hour of the day is on the X-axis and the inside temperature is on the Y-axis.

CitySim is more reactive to outside temperature changes than other programs.

This statement is illustrated in Figure 1.14 where the inside temperature changes are clearly out of phase between CitySim and the other programs. Also, for the heavyweight building (900FF) in particular, the amplitude of temperature changes is bigger.

Moreover, in Figure 1.12, values given by CitySim for the annual minimum temperature are below the reference range. This means that when the outside temperature drops, the inside temperature decreases quicker in CitySim than in other programs. This tendency is more important in heavy-weight cases 900FF and 960 than for lightweight case 600FF.

Finally, in Figure 1.13, the distribution is globally shifted to colder temperatures and a high peak of occurrence is observed around 24 $^\circ$C. Such a distribution indicates more violent indoor temperature variations.

The above observations show that the variations of inside temperature are larger than in the reference programs. This tendency increases in importance when thermal mass is added in the envelope. This leads to the same conclusion as in paragraph1.6.2.3 that states that the accessibility of the envelope capacity to the inside air is too low.

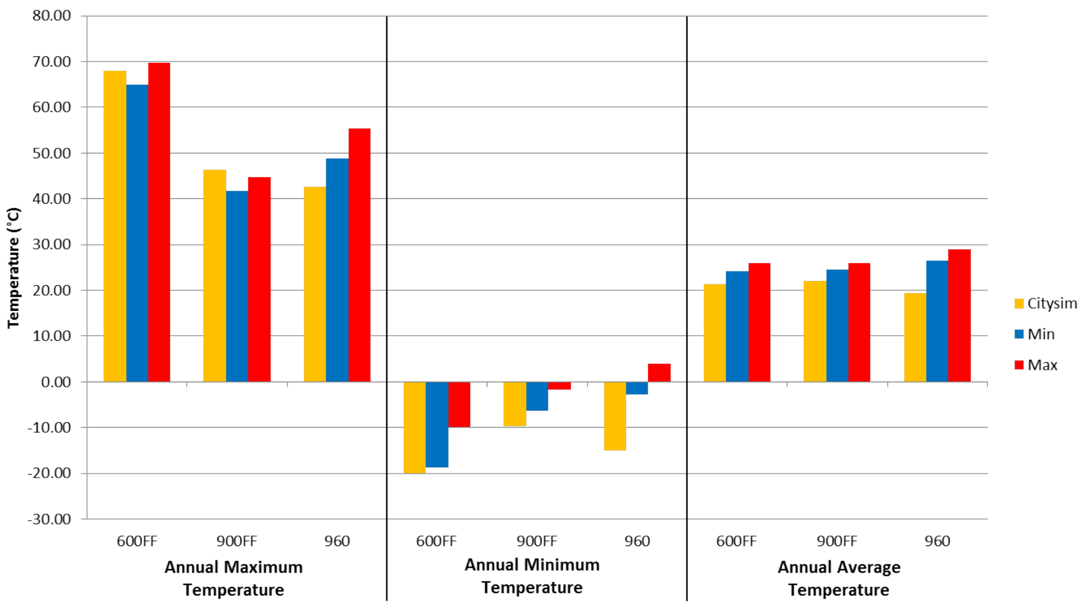

Figure 1.12: Annual maximum (left), minimum (middle) and average (right) temperature for the light-weight (600FF), heavy-weight (900FF) free float cases and the sun-zone case (960) - own illustration

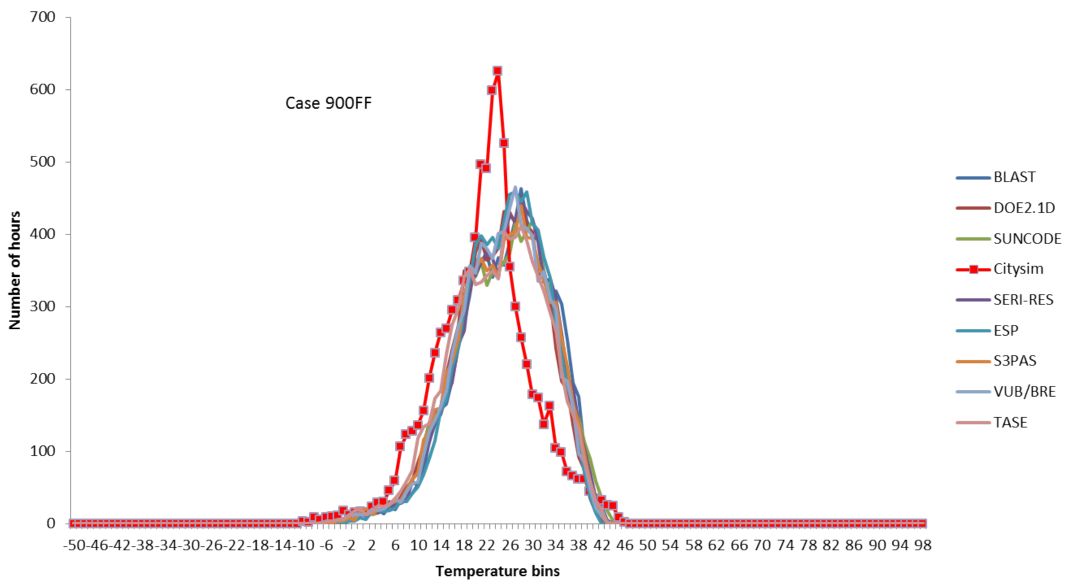

Figure 1.13: Annual occurence of hourly temperature in bins of 1 ° C for the high-mass free-floating case (900FF) - own illustration

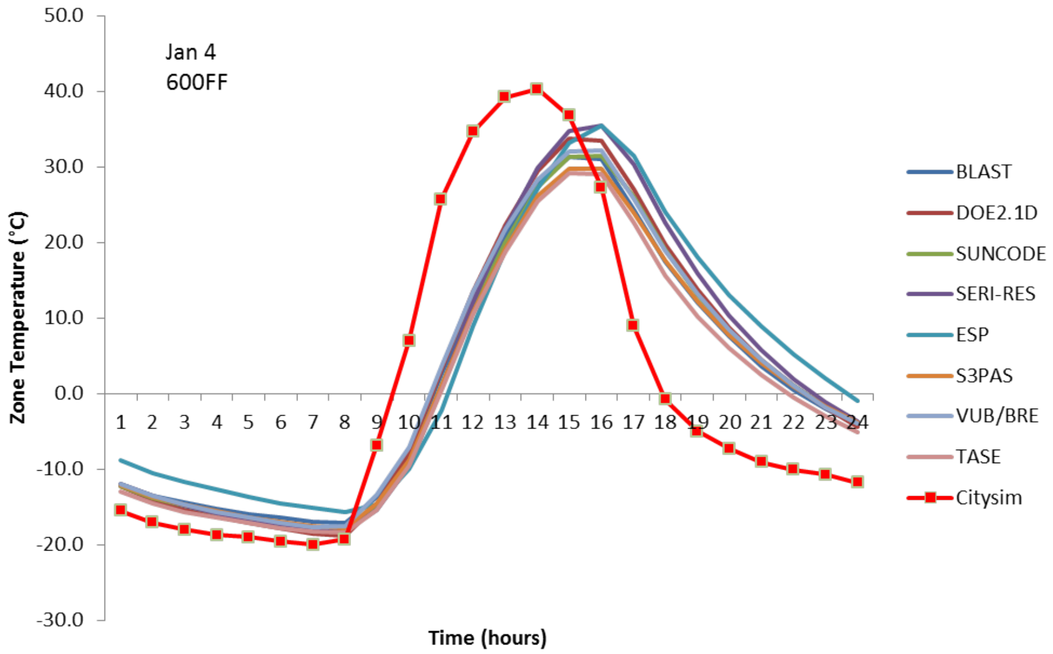

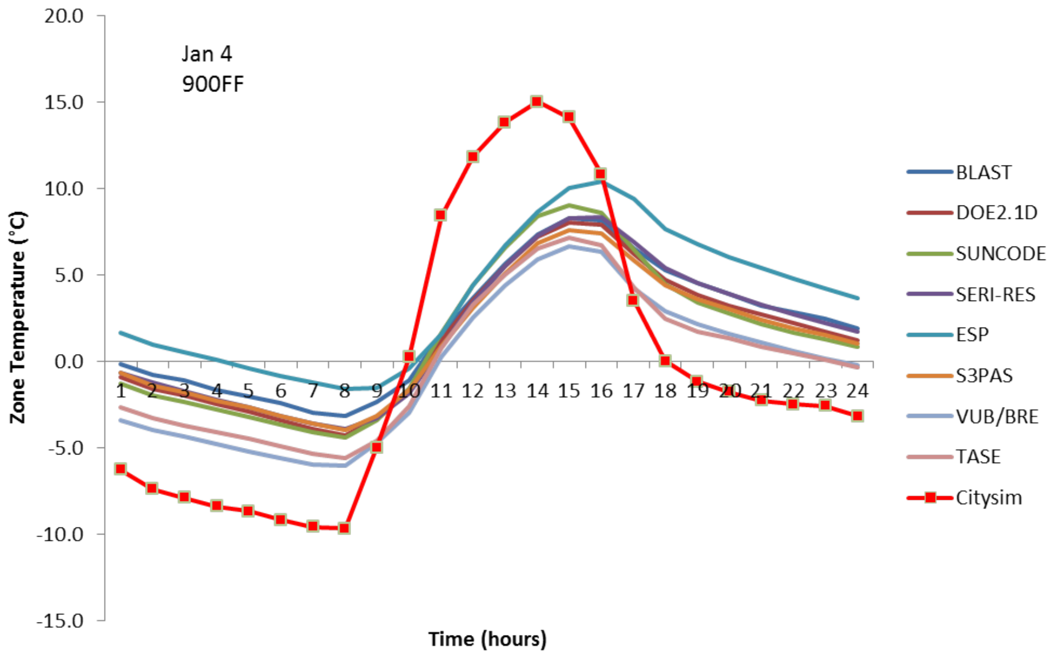

Figure 1.14: Hourly temperature for the low-weight (top) and heavy-weight (bottom) cases on the 4^{th} of January - own illustration

1.7 The BESTEST Method

Tables 1.11 to 1.13 present the results of the BESTEST sequence for annual heating and cooling loads and annual peak heating and cooling demand.

These tables are organized according to the BESTEST sequence presented in paragraph 1.4.3. Table 1.10 is an example of the format used here to quicken results interpretation. Error messages only appear in case of discrepancy.

Table 1.10: BESTEST results color code example

Case#	CitySim	Reference range		Distance
1	Above reference range	Min1	Max1	$\frac{CS_1 - Min_1}{\lvert Min_1 \rvert}$
2	Within reference range	Min2	Max2	0
3	Below reference range	Min3	Max3	$\frac{CS_3 - Max_1}{\lvert Max_1 \rvert}$

1.7.1 Annual heating load

Table 1.11 presents the results for the annual heating load.

The first difference is encountered for Test 610-600, which is above the range by 51%. This might be due to a problem with shading on the south façade, an assumption that is confirmed by Test A12, which is also above the validity range by 75%. Here, the presence of south overhangs increases the heating load by decreasing the solar gains through the glazing. However, this effect is very small due to the high position of the overhangs on the façade and the fact that the sun is low on the horizon during the heating season. According to the BESTEST, the problem might therefore be an over-estimation of the impact of south overhangs. However, this conclusion is jeopardized by observations in Paragraph 1.6.1.1 where consistent values for solar incident and transmitted solar irradiation are observed. The error might therefore be located elsewhere.

A second difference is encountered for Test 630-620, which is 13% below the range. However, the diagnosis case A14 overturns the responsibility of the blinds and leads to Cases A1 to A11 or B1 to B9. Among these diagnosis cases, A2 and B5 indicate that the error can be caused by the definition in CitySim of too high convective exchange coefficients. Indeed, the error appears when high-conductive walls are added to the model. The heat flux through these types of surfaces depends more on external and internal surface coefficients. The fact that Tests A2 and B5 are above the reference range indicates that the values of these coefficients are globally too high. This can be explained by the definition in the IEA BESTEST of fixed combined surface radiative and convective coefficients. In CitySim, the surface radiative and convective coefficients vary according to the surface temperature and wind speed respectively. This illustrates the gap between dynamic and static simulations.

Except for the minor cases mentioned above, CitySim passes successfully all lightweight cases of IEA BESTEST.

The next error is found for Test 900, which is 38% above the reference range. Diagnosis case C1 indicates that the error is located in the definition of building thermal mass. In general, the effect of thermal mass is to decrease the heating demand. Here, this decrease is not sufficient. The effect of thermal mass is therefore under-evaluated. This observation leads to the same conclusion as in Paragraph 1.6 where a rather weak interaction between the wall and the inside air is suspected. The cause of this problem might be the simplified definition of the envelope as a single nod implemented in CitySim as explained in paragraph 1.6.2.3.

Table 1.11: BESTEST sequence applied on results for the annual heating load - own illustration

ANNUAL HEATING [MWH]

Qualification cases	Citysim	MIN	MAX	Distance	error location	Diagnose	Citysim	MIN	MAX	Distance	error location
600	5.525	4.296	5.709	0%		A1 195	4.417	4.167	5.871	0%	Solid conduction
						A2 200-195	3.113	1.085	1.961	59%	Surface convection
						A3a 210-200	1.058	0	1.204	0%	
						A6 230-220	3.507	3.432	3.615	0%	
						A7 240-220	-1.462	-1.341	-1.203	-9%	IHG
						A8 250-220	-1.864	-2.193	-1.448	0%	
						A9 270-210	-2.960	-2.62	-1.948	-13%	South solar transmittance / incidence
						A11 320-270	-0.182	-0.779	-0.649	72%	Thermostat deadband
						or					
						B1 395	2.206	2.062	2.391	0%	
						B5 400-395	2.950	1.916	2.935	1%	Surface convection / IR
						B6 410-400	1.744	1.696	1.798	0%	
						B7 420-410	-1.457	-1.361	-1.222	-7%	IHG
						B8 430-420	-1.177	-1.869	-1.112	0%	
						B9 600-430	-2.139	-2.118	-1.133	-1%	South solar transmittance / incidence
610	5.673	4.355	5.786	0%	South shade	A12 290-270	0.154	0.02	0.088	75%	South shade
610-600	0.148	0.021	0.098	51%							
620	5.745	4.613	5.944	0%		A13 300-270	0.301	0.044	0.59	0%	
620-600	0.220	0.138	0.682	0%							
630	5.978	5.05	6.469	0%	EW shade	A14 310-300	0.305	0.201	1.349	0%	
630-620	0.233	0.267	0.551	-13%							
900	2.825	1.17	2.041	38%	Mass/South solar Interaction	C1 800-430	-0.341	-0.649	-0.501	32%	Basic mass
900-600	-2.700	-3.837	-3.126	14%		C2 900-800	-4.499	-5.356	-3.698	0%	
910	3.361	1.575	2.282	47%	Mass/South shade Interaction	C3 910-610	-2.312	-3.532	-2.78	17%	Mass/s.Shade Interaction A12
910-900	0.536	0.179	0.442	21%							
920	4.363	3.313	4.3	1%	Mass/EW solar Interaction	C4 920-620	-1.382	-1.689	-1.297	0%	
920-900	1.538	2.07	2.505	-26%							
930	4.912	4.143	5.335	0%	Mass/EW shade Interaction	C5 930-630	-1.066	-1.273	-0.712	0%	
930-920	0.549	0.595	1.08	-8%							
960	4.075	2.311	3.373	21%	Multiple						
960-900	1.250	0.775	1.718	0%							

1.7.2 Annual cooling load

Table 1.12 present the results for the annual cooling load.

The first difference is found for Test 620-600, which is 3% above the reference range. There might be a problem with the solar incident or transmitted irradiation on east or west facades. This is confirmed by diagnosis case A13, which is above the validity range by 13%. Placing windows on east and west instead of south surfaces decreases significantly the annual cooling load by reducing solar gains in comparison to south oriented windows. Here, this decrease is too low which means that solar gains through windows located on east and west façades are overestimated according to the BESTEST method. However, it was shown in Paragraph 1.6.1.1 that annual incident and transmitted values for solar irradiation are correct. Moreover, the difference for the qualification tests is rather small. The cause for these discrepancies is then located elsewhere most probably. Test A2 indicates a problem with surface convection coefficients similar to previous tests.

The next discrepancy is found for Test 900-600, which is above the reference range by 12%. As with annual heating load, adding thermal mass to the building decreases the annual cooling load. Test 900-600 shows that this decrease is too small. The influence of thermal mass is therefore insufficient. This diagnosis is confirmed by Case C1. The same conclusion applies as for the annual heating load: the interaction between the building thermal mass and the inside air is too weak.

However, the impact of both surface coefficients and thermal mass problems is much smaller in the case of the annual cooling load in comparison to the annual heating load. This difference in impact can be partly explained by a difference in heating and cooling periods duration. The heating season is much longer than the cooling season: there are 7048 hours below the set-point and 495 above. Therefore, a systematic error implemented in the code has more impacts on the heating load.

Table 1.12: BESTEST sequence applied on results for the annual cooling load - own illustration

ANNUAL COOLING [MWH]											
Qualification cases	Citysim	MIN	MAX	Distance	location	Diagnose	Citysim	MIN	MAX	Distance	location
600	6.482	6.137	7.964	0%		A1 195	0.486	0.264	0.51	0%	
						A2 200-195	0.258	0.156	0.2412	7%	Surface convection
						A3a 210-200	-0.398	-0.408	0.008	0%	
						A6 230-220	0.286	0.268	0.304	0%	
						A7 240-220	0.290	0.229	0.412	0%	
						A8 250-220	1.518	1.752	3.027	-13%	Ext solar abs / incidence
						A9 270-210	6.904	7.342	9.515	-6%	South solar transmittance / incidence
						A11 320-270	-2.422	-3.055	-2.467	2%	Thermostat deadband
						or					
						B1 395	0.000	0	0.016	0%	
						B5 400-395	0.006	0	0.045	0%	
						B6 410-400	0.010	0	0.026	0%	
						B7 420-410	0.048	0.011	0.105	0%	
						B8 430-420	0.374	0.371	0.732	0%	
						B9 600-430	6.045	5.595	7.28	0%	Cavity
610	4.312	3.915	5.778	0%		A12 290-270	-2.113	-2.324	-1.283	0%	
610-600	-2.170	-2.227	-1.272	0%							
620	4.210	3.417	5.004	0%	EW incidence/transmittance	A13 300-270	-2.474	-3.25	-2.834	13%	EW Solar Incidence /Transmittance
620-600	-2.273	-2.96	-2.341	3%							
630	3.020	2.129	3.701	0%		A14 310-300	-1.334	-3.31	-1.266	0%	
630-620	-1.189	-1.845	-0.984	0%							
900	3.100	2.132	3.415	0%	Mass/South solar Interaction	C1 800-430	-0.255	-0.55	-0.367	31%	Basic mass
900-600	-3.382	-4.624	-3.833	12%		C2 900-800	2.918	2.019	3.193	0%	
910	1.701	0.821	1.872	0%		C3 910-610	-2.612	-3.924	-3.094	16%	Mass/s.Shade Interaction A12
910-900	-1.400	-1.561	-0.832	0%							
920	2.470	1.84	3.092	0%	Mass/EW solar Interaction	C4 920-620	-1.739	-1.912	-1.476	0%	
920-900	-0.630	-0.323	0.016	-95%							
930	1.722	1.039	2.238	0%		C5 930-630	-1.298	-1.463	-0.827	0%	
930-920	-0.748	-1.174	-0.682	0%							
960	0.366	0.4113	0.803	-11%	Multiple						
960-900	-2.734	-2.697	-1.644	-1%							

1.7.3 Annual peak heating demand

Table 1.13 presents the results for the annual peak heating demand.

CitySim results are within the validity range in all tests. Discrepancies appear for Test 910-900 and 930-920 where fins and overhangs are added to the model. However, the change in peak heating is negligible. The influence of overhangs and fins on the peak heating demand is weak because peak heating occurs during the night (4^{th} of January at 07:00 for case 195). At that moment, shading devices only influence the heating needs by decreasing radiative IR losses. This effect on heating is rather small.

The results are shown to be consistent despite the problem in thermal mass observed previously on annual loads. This leads to the conclusion that discrepancies on annual loads are due to a small systematic error that occurs in every calculations. Diagnose Tests A2 and B5 suggest that the error could be due to high surface coefficients.

1.7.4 Annual peak cooling demand

Table 1.14 presents the results for the annual peak cooling demand.

A first discrepancy appears in qualification Test 600, which is below the validity range by 5%. The BESTEST procedure indicates that the problem might be in basic heat transfers. The diagnosis Tests A2 and B5 are above the reference range by 40% and 11% respectively. Both indicates that defined surface coefficients are too high when compared to the BESTEST.

The cooling requirements mainly depend on the solar gains. For instance, peak cooling occurs on October 17^{th} at 13:00 for Case 600. At this moment, the outside and inside temperatures are $24.4\,^{\circ}$C and $25.8\,^{\circ}$C respectively. The beam solar irradiance is 958 $\frac{W}{m^2}$. This means that the inside temperature is above the outside temperature even during the cooling period because of solar gains. Moreover, the effect of solar gains on the inside temperature is strong as cooling appears to be necessary even within the set-point, the maximum inside temperature being 27 $^{\circ}$C.

The above observations explain the result obtained for Case 600. The peak is too low because the heat of solar gains is evacuated outside through the envelope. This is the case because surface coefficients defined in CitySim are globally higher.

Table 1.13: BESTEST sequence applied on results for the annual peak heating demand - own illustration

ANNUAL HOURLY PEAK HEATING LOADS [KW]											
Qualification cases	Citysim	MIN	MAX	Distance	error location	Diagnose	Citysim	MIN	MAX	Distance	error location
600	4.090	3.437	4.354	0%		A1 195	2.082	2.004	2.385	0%	Solid conduction
						A2 200-195	1.356	0.647	1.119	21%	Surface convection
						A3a 210-200	0.137	-0.057	0.050	174%	Exterior IR
						A6 230-220	1.569	1.519	1.811	0%	
						A7 240-220	-0.200	-0.200	-0.180	0%	
						A8 250-220	-0.036	-0.007	0.005	-414%	Ext solar abs / incidence
						A9 270-210	-0.047	-0.025	0.218	-88%	South solar transmittance / incidence
						A11 320-270	-0.049	-0.009	0.000	-444%	Thermostat deadband
						or					
						B1 395	2.206	2.062	2.391	0%	
						B5 400-395	1.369	0.805	1.318	4%	Surface convection / IR
						B6 410-400	0.783	0.757	0.885	0%	
						B7 420-410	-0.200	-0.200	-0.180	0%	
						B8 430-420	-0.043	-0.001	0.011	-4200%	Ext solar abs / incidence
						B9 600-430	-0.025	-0.029	0.217	0%	Cavity
610	4.090	3.437	4.354	0%		A12 290-270	0.000	-0.008	0.000	0%	
610-600	0.000	-0.011	0.000	0%							
620	4.092	3.591	4.379	0%		A13 300-270	0.004	-0.008	0.259	0%	
620-600	0.002	-0.008	0.240	0%							
630	4.092	3.592	4.278	0%		A14 310-300	0.000	-0.013	0.001	0%	
630-620	0.000	-0.021	0.003	0%							
900	3.635	2.850	3.797	0%		C1 800-430	-0.114	-0.215	-0.113	0%	
900-600	-0.455	-0.587	-0.414	0%		C2 900-800	-0.366	-0.378	-0.107	0%	
910	3.681	2.858	3.801	0%	Mass/South shade Interaction	C3 910-610	-0.409	-0.579	-0.223	0%	
910-900	0.046	0.003	0.019	137%							
920	3.862	3.308	4.061	0%		C4 920-620	-0.230	-0.318	-0.150	0%	
920-900	0.227	0.192	0.458	0%							
930	3.887	3.355	4.064	0%	Mass/EW shade Interaction	C5 930-630	-0.205	-0.579	-0.223	8%	Mass/EW shading Interaction
930-920	0.025	0.027	0.127	-7%							
960	2.531	2.410	2.896	0%	Multiple						
960-900	-1.104	-1.018	-0.440	-8%							

Table 1.14: BESTEST sequence applied on results for the annual peak cooling demand - own illustration

ANNUAL HOURLY PEAK COOLING LOADS [KW]

Qualification cases	Citysim	MIN	MAX	Distance	error location	Diagnose	Citysim	MIN	MAX	Distance	error location
600	5.666	5.965	6.812	-5%	Basic heat transfer	A1 195	0.779	0.616	0.853	0%	Solid conduction
						A2 200-195	0.471	0.212	0.336	40%	Surface convection
						A3a 210-200	-0.295	-0.387	0.016	0%	
						A6 230-220	0.514	0.480	0.536	0%	
						A7 240-220	0.200	0.179	0.200	0%	
						A8 250-220	1.141	1.043	3.699	0%	
						A9 270-210	4.686	5.475	6.625	-14%	South solar transmittance / incidence
						A11 320-270	-0.852	-0.726	-0.586	-17%	Thermostat deadband
						or					
						B1 395	0.006	0.000	0.421	0%	
						B5 400-395	0.322	0.000	0.291	11%	Surface convection / IR
						B6 410-400	0.137	0.035	0.151	0%	
						B7 420-410	0.211	0.195	0.233	0%	
						B8 430-420	0.692	0.637	1.657	0%	
						B9 600-430	4.298	4.193	5.772	0%	Cavity
610	4.394	5.669	6.146	-22%	South shade	A12 290-270	-0.895	-0.561	-0.086	-60%	South shade
610-600	-1.272	-0.811	-0.116	-57%							
620	4.130	3.634	5.096	0%	EW incidence/transmittance	A13 300-270	-1.926	-2.952	-1.938	1%	EW Solar Incidence /Transmittance
620-600	-1.536	-2.560	-1.716	10%							
630	3.418	3.072	3.704	0%		A14 310-300	-0.562	-1.504	-0.344	0%	
630-620	-0.712	-0.842	-0.371	0%							
900	3.442	2.888	3.567	0%	Mass/South solar Interaction	C1 800-430	-0.257	-1.220	-0.397	35%	Basic mass
900-600	-2.224	-3.355	-2.810	21%		C2 900-800	2.331	2.099	3.519	0%	
910	2.562	1.896	3.147	0%		C3 910-610	-1.832	-3.773	-2.883	36%	Mass/s.Shade Interaction A12
910-900	-0.880	-1.122	-0.310	0%							
920	3.046	2.385	3.505	0%		C4 920-620	-1.084	-1.591	-1.106	2%	Mass/EW Shading Interaction
920-900	-0.396	-0.517	0.048	0%							
930	2.491	1.873	2.546	0%		C5 930-630	-0.927	-1.242	-1.036	11%	Mass/EW shading Interaction
930-920	-0.555	-0.721	-0.387	0%							
960	1.143	0.953	1.403	0%							
960-900	-2.299	-2.401	-1.935	0%							

1.8 Discussion

The usefulness of applying the IEA BESTEST procedure to CitySim can be questioned.

Certifying CitySim using the IEA BESTEST would mean that this program is consistent with the state-of-the-art of building simulation in 1995. This raises two main interrogations. First, the purely software-to-software approach of the IEA BESTEST does not ensure that results are consistent with the reality. Second, the building simulation sector has evolved significantly since 1995 and there are no guaranties that the current versions of the reference programs, if they are still on the market, still produce the same reference results.

As to the first interrogation, it can be said that the goal of the BESTEST is above all to trap bugs and faulty algorithms within the program code by developing a set of tests that can be quickly and cheaply performed. Moreover, the reference programs had already benefited from several decades of development and real applications when the IEA BESTEST was released which gives them a certain credibility through experience. As to the second interrogation, the founder of the BESTEST claim that if evolutions of the BESTEST are necessary, future developments will remain backward compatible.

To conclude, the application of the IEA BESTEST might allow to identify problems within the CitySim code but it appears necessary to apply a more recent version of the BESTEST or another certification method to confirm CitySim's validity.

The cases defined in the BESTEST were not perfectly implemented in CitySim.

Several BESTEST cases are not considered here because their definition is not feasible in CitySim. For instance, all cases that consider changes in the interior LW emissivity or SW reflectance are neglected as CitySim assumes that all is absorbed as heat. This means that there are possible errors on the amplitude of the solar or IR effect.

The weather data used in simulations contains values external to the IEA BESTEST. Some data such such as the relative humidity and the precipitations were obtained from Meteonorm. Others such as the diffuse horizontal irradiance were calculated based on available weather information. The weather file is therefore not completely consistent and might cause discrepancies.

Some properties of the materials used in simulation were modified in order to avoid fatal errors of CitySim during simulation. It is the case for the density of the fibreglass quilt and the foam insulation whose values were modified from 12 to 250 $\frac{kg}{m^3}$ and 10 to 40 $\frac{kg}{m^3}$ respectively. However, this particular difference should not strongly influence the results as the thermal mass of these materials is located outside.

The convective and radiative coefficients are defined by a fixed value in the BESTEST. By contrast, CitySim computes these parameters dynamically based on weather data. These coefficients have a significant influence on heat fluxes through high conductive surfaces such as windows. Discrepancies are therefore to be expected in the BESTEST results.

Finally, the definition of the windows located on the south wall is not completely the same. In CitySim, these windows were added by defining of a global glazing ratio on the total surface. However, splitting the surface to get closer would change the solar gains by modifying the effect of the overhangs.

To summarize, there are gaps between the definition of the different BESTEST cases and their implementation in CitySim.

Finally, parts of the information is not extracted from the results. It is the case for the annual peak heating and cooling demand or the extreme inside temperature variations that are not extracted with date and hour of occurrence. This reduction in information quality decreases the conclusions solidity.

1.9 Conclusion

In this work, CitySim was confronted to the IEA BESTEST certification procedure. The interest here is to improve the trustability of CitySim outputs and to promote its spreading into the design community.

The IEA BESTEST proposes a certification method based on the comparison of the candidate programs with a set of reference programs that represent the state-of-the-art of building simulation. It is focused on building envelope and tests various outputs that are solar irradiance, heating and cooling demand and inside temperature variations.

Paragraph 1.6.1.1 shows that the irradiation model of CitySim for daylight incidance and transmittance is in complete agreement with the reference programs used in this BESTEST suite. This is true at annual and hourly scale.

Concerning heating and cooling, CitySim results are shown in Paragraph 1.6.2 to have a tendency toward high values for heating and low values for cooling. This is true for annual loads and annual peak demand. At hourly scale, CitySim appears to be more reactive than the reference programs.

This last conclusion is also found analysing CitySim results for inside temperature variations in Paragraph 1.6.3.

The cause of these problems was found by using the BESTEST sequential approach. Two main sources of discrepancies were found:

1. The influence of the envelope thermal mass on the regulation of the inside air is weaker in CitySim. Temperature variations are too high in free-float cases and the decrease in annual heating load is too small. A solution to this problem could be to divide the building envelope into several nods corresponding to different layers or to divide the building into zones

2. The BESTEST procedure often returns a problem in the definition of surfaces convective and/or radiative coefficients. In the BESTEST, these coefficients are defined as fixed values while they are dynamically computed in CitySim with the surface temperature, cloud cover fraction, and environment for instance. This difference is decisive in the case of high conductive surfaces such as windows, for which heat fluxes depend more on these coefficients. This effect is found in all result categories.

1.10 Future work

Several elements of the CitySim model can still be improved.

The weather data that was used is not completely based on original data from the NREL. Missing data, such as the humidity ratio, precipitations and diffuse horizontal irradiance should be obtained from the NREL in later simulations.

The windows could be drawn in the walls instead of assuming a global glazing ratio. This would improve the quality of the results by modifying the solar gains when shadings are involved.

This work is a basis for a more comprehensive BESTEST analysis of CitySim.

The annual peak heating and cooling demand should be integrated in order to verify not only the magnitude but also the temporal consistency of CitySim outputs. This should also be done for the maximal and minimal temperatures for free-float cases.

Moreover, the impact of interior radiative coefficients should be analysed in order to verify that related assumptions taken in CitySim are consistent.

Other aspects of building energy simulations such as heating and cooling supply also need to be addressed. This could be done by applying other BESTEST suites.

The application of the BESTEST highlighted several possible improvements for CitySim.

On the one hand, the implementation of a multi-nod model for the envelope would allow to strengthen the influence of the wall capacity on the inside air. On the other hand, this change is also likely to modify the envelope external layer temperature and therefore impact the surface radiative behavior. It would also increase the simulation time, further investigations should be pursued to determine if CitySim would then be enough time efficient for urban scale simulations.

More complex set-point strategies such as set-back can be interesting for the simulation of particular energy savings during idle periods such as holidays, week-ends or even nights. However, this concept would also require the definition of some smart planning to avoid a large and sudden increase of the required heating or cooling power at the end of the idle period. This local peak would happen because energy conversion systems have to bring the inside air back to normal comfort conditions.

Part 2

Simulation of EPFL heating demand with CitySim

2.1 Introduction

In Chapter 1, the consistency of CitySim outputs is verified using the BESTEST method. Now, it is applied to simulate the heating demand of the EPFL campus.

The creation of an energy hub on the EPFL requires the ability to simulate energy fluxes within the campus. The present study focuses on the heat demand and supply.

First, a model of the campus is developed in CitySim. Then, this model is used to simulate the hourly heating demand of EPFL. Finally, the annual heating load and peak heating demand are extracted from the simulation results and analysed in four steps. (i) The simulated and monitored annual heating load are compared to validate the model. (ii) The distributions of the annual and peak heating loads are compared. (iii) The differences in specific consumption for the different buildings are studied. (iv) The potential benefits of energy saving scenarios are investigated.

2.2 Methodology

2.2.1 CitySim model development

This Paragraph details all the assumptions made during the development of the EPFL model. The development is mainly supported by the EPFL Infrastructure and Housing Deparment (DII) plan database and SIA norms.

The climate used in simulations is obtained from meteonorm for the location of Ecublens. It contains hourly values for the elements presented in Table 2.1.

Table 2.1: CitySim weather file required entries

Element	**Symbol**	**Unit**
Diffuse horizontal irradiance	G_{Dh}	$\frac{W}{m^2}$
Beam normal irradiance	G_{Bn}	$\frac{W}{m^2}$
Air temperature	T_a	$^\circ$ C
Wind speed	FF	$\frac{m}{s}$
Wind direction	DD	$^\circ$
Relative humidity	RH	-
Precipitations	RR	mm
Cloud cover fraction	N	Octas

The original geometry of the EPFL model was developed by Dr Claudio Carneiro (Carneiro, 2011) using the Light Detection And Ranging technology (LiDAR). This initial model was then simplified by Silvia Coccolo in order to allow CitySim simulations.

The following changes are applied on Coccolo's model version for this study.

- Division of buildings into floors with an assumed height of 4m
- Definition of Air Change per Hour (ACH). Values of ACH are determined using the surface occupied by laboratories in each building.
- Setting of the heating system with an infinite power and a limited period of operation from August 31^{st} to May 1^{st}.

- Definition of the envelope typologies based on the plan database of the DII
- Introduction of Internal Heat Gains (IHG) according to the SIA 2024 norms

2.2.2 Simulation results analysis

In this part, outputs from the simulation of the EPFL model are analysed. Results are presented in four different parts.

First, simulation results are compared with the monitored annual heating load. EPFL monitored consumption is provided by the DII building per building for the year 2013. This verification is crucial because it shows how trustworthy simulated heating loads are. Results are presented in a dispersion graph. Indicators for results validation are the correlation factor with a linear regression and the proximity of the latter with the graph bisector. Outliers are then highlighted and their specific cases is analysed.

Results for the annual heating load and the peak heating demand of all EPFL buildings are presented together in ascending order. Ranking differences between the two graphs are analysed through the comparison of two particular buildings. Then, this difference in behavior is studied using the Peak to Average Ratio (PAR) to highlight the reasons of changes in the ranking.

Afterwards, the differences in behavior of EPFL buildings are studied from the point of view of the specific heating consumption. Various norms are also represented for comparison. The main goal here is to determine the main parameters that determine the energy demand.

Finally, results obtained for the following energy saving scenarios are presented.

- Absence of IHG
- Walls retrofit for buildings of the first construction period with rockwool insulation thicknesses of 5, 10 and 15 cm
- Reduction of the set-point by 1 °C
- Replacement of all windows with efficient double glazing and triple glazing

Results are analysed in different ways: (i) Comparison between buildings for each scenario, (ii) Comparison between scenarios for chosen buildings and (iii) Comparison between the heating load and the peak demand.

2.3 CitySim model development

2.3.1 Climate

Ecublens weather is extracted from meteonorm. This program produces values based on an average of several years. Its main characteristics are summarized in Table 2.2.

Table 2.2: Summary of used climate for the site of Ecublens

Element	CitySim	Unit
Mean annual wind speed	1.94	$\frac{m}{s}$
Mean annual air temperature	10.28	$^\circ$C
Minimum annual temperature (12.01 22:00)	-9.5	$^\circ$C
Maximum annual temperature (21.07 18:00)	30	$^\circ$C
Maximal annual wind speed (21.03 21.00)	16.3	$\frac{m}{s}$
Mean annual relative humidity	75.84	%
Direct normal solar irradiation annual total	1179.42	$\frac{kWh}{m^2.y}$
Diffuse horizontal solar irradiation	591.78	$\frac{kWh}{m^2.y}$

Figure 2.1 presents the evolution of the outside temperature[1]. The yearly minimum and maximum temperatures are -2.3 $^\circ$C in Januray and 24.6°C in July respectively. If dates correspond, both values are less extreme than the ones presented in Table 2.2. A rather pessimistic tendency is therefore expected in the results.

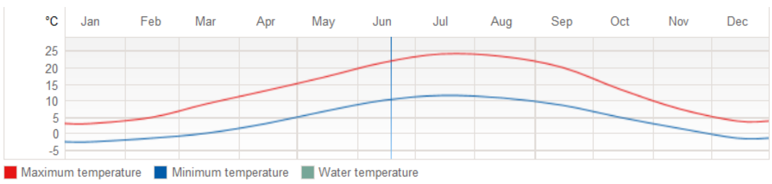

Figure 2.1: Evolution of the temperature during the year for Ecublens - Source meteovista)

[1]These data were found on the website of meteovista

2.3.2 Geometry

The basis of the EPFL 3D model was laid by Dr Claudio Carneiro (Carneiro, 2011) using the LiDAR technology, which consists in measuring distances by illuminating a target with a laser and analyzing the reflected light.

This model was then simplified by Silvia Coccolo because it included too many small details. The interest of simplifying the model was to decrease the simulation time with CitySim. A simplified simulation would still allow the study of many different variants.

Each building is divided into floors. This division is necessary because CitySim is using a simplified simulation model. It applies to a whole surface what happens at its geometric center. Dividing the model into floors increases the simulation time but it allows to take into consideration the fact that surfaces at different heights are subject to different conditions such as solar irradiance and IR interactions. This fact is illustrated in Figure 2.2.

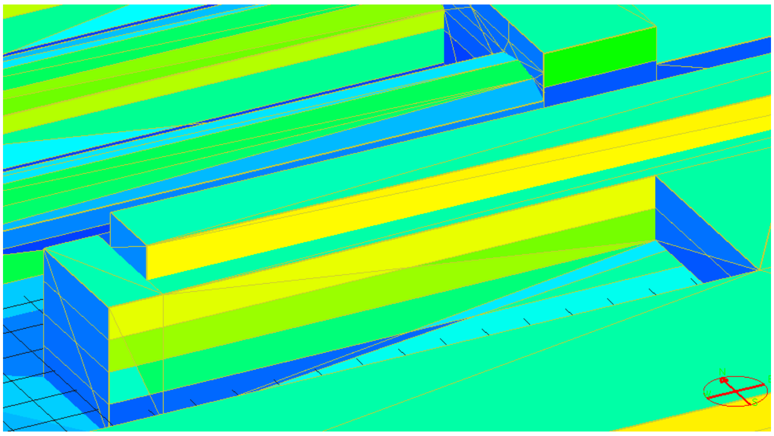

Figure 2.2: CitySim output for the irradiance received by the south surface of building AI on the 13^{th} of December at 13:00 - own illustration

The number of floors (n) of each building is obtained from the interior volume (V_{int}) and the ground occupation surface (S_g) using Eq. 2.1.

$$n = nint(\frac{V}{S_g \cdot h}) \tag{2.1}$$

where a floor height (h) of 4m is assumed.

The final model includes 252 buildings or sub-buildings. The envelope of these buildings is composed of nearly $13'700$ surfaces.

Buildings are differentiated by their glazing to wall ratio (GR). Values of GR are either determined using the façade elevation plans from the DII or assumed after visual inspection. Values of GR are assumed homogeneous for a single building. Buildings belonging to the same construction period are assumed, with a few exceptions, to have the same GR. Examples of this method are given in Appendix B.3.

The treated floor area $S_{treated}$ is calculated for each building using Eq.2.2.

$$S_{treated} = n \cdot S_g \tag{2.2}$$

The obtained values for $S_{treated}$ are confronted with the real values obtained from (DII EPFL, 2008). This comparison shows that most of the time, $S_{treated}$ is underestimated by less than 20%. The results of this comparison are in Appendix B.2

The list of all buildings classified by zone and with their general characteristics can be found in Appendix B.1. Figure 2.3 presents an annotated plan of the EPFL model with building names.

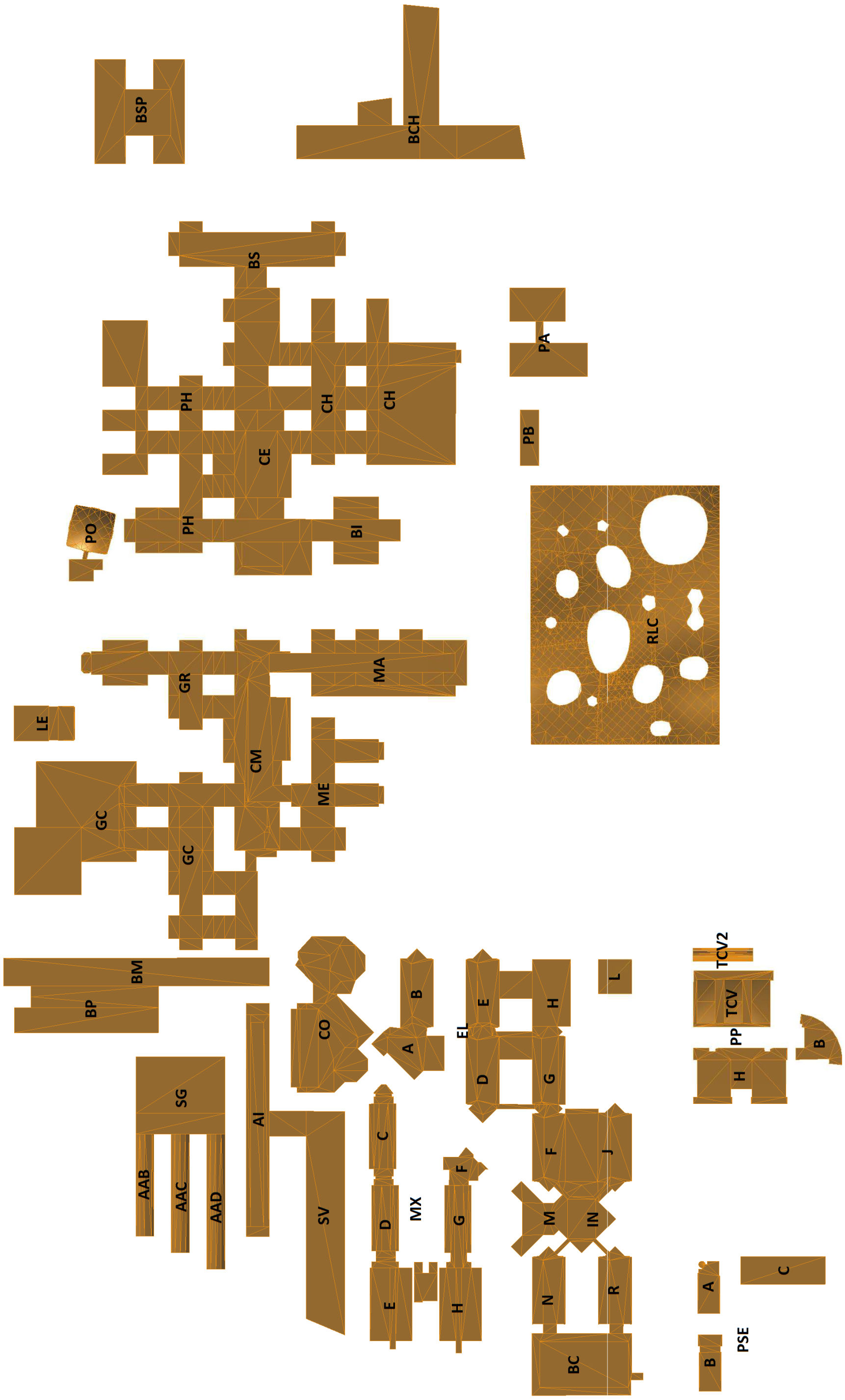

Figure 2.3: Top view of the EPFL on Rhinoceros with added building names - own illustration

2.3.3 Air Change per Hour

In CitySim, the value of air infiltration is the fraction of the volume that is replaced every hour, the unit is $[h^{-1}]$. This value is building specific.

Two types of rooms are implemented in the model: offices and laboratories. This distinction is crucial because laboratories require a far higher air renewal rate than offices. The ACH of each building is determined using the building fraction occupied by laboratories (x_{labs}) according to Eq. 2.3.

$$ACH[h^{-1}] = (1 - x) \cdot ACH_{offices} + x \cdot ACH_{Labs} \tag{2.3}$$

In the norm SIA 2024 (SIA, 2006), the ACH is defined in $[\frac{m^3}{m^2 \cdot h}]$, that is the volume of new air that is required every hour per m^2 of treated floor.

ACH recommended values by norm SIA 2024 are 10 $\frac{m^3}{m^2 \cdot h}$ for special rooms and 1.2 $\frac{m^3}{m^2 \cdot h}$ for offices [1].

The conversion between $\frac{m^3}{m^2 \cdot h}$ and h^{-1} is done using Eq. 2.4

$$ACH_i[h^{-1}] = \frac{ACH_i[\frac{m^3}{m^2 \cdot h}]}{h} \tag{2.4}$$

where i is either laboratory or office and h is the floor height defined earlier.

All EPFL buildings are considered without laboratory surfaces except the one specified in Table 2.3

Table 2.3: Description of highly ventilated buildings

Building	Laboratory area portion[2]	ACH [h-1]
CH	20%	0.74
PH	21%	0.762
SV	40%	1.18
AI	37%	1.114
BM	30%	0.96

[1] The value during the day is considered too high. Consequently, the chosen consumption is the overall between ACH during the day and the night

[2] These values are mainly extract from (Helms, 2009)

Here, there is no distinct ACH for building parts used by restaurants. This could have an impact on the heating consumption. as removing smells in restaurants means higher ACH. The simulated consumption of concerned buildings will therefore probably be lower than the monitored consumption.

2.3.4 Heating system

The defined heating system in this model is a simple boiler of infinite capacity. The efficiency of the heating distribution network within the building is assumed to be 0.95. In reality, the EPFL is heated by a heat pump but the interest is strictly the building heating consumption. The optimal energy conversion system is determined in the next Part 3.

The setpoint is defined by a minimum temperature of 21.5 ˚C and an "infinite" maximal temperature of 100 ˚C. The heating system only operates from August 31^{st} to May 1^{st} according to (Helms, 2009).

2.3.5 Envelope definition

In CitySim, the building envelope is composed of three different wall-types: Wall, roof and floor, which are homogeneous for a single building.

Two envelope typologies are defined. The first typology corresponds to the aluminum facades of the first construction period. The second represents buildings of the second construction phase. The definition of these typologies was extracted from the plan database ARCHIBUS managed by DII. Printscreens of the source plan found on ARCHIBUS are in Appendix B.4.

Table 2.4 summarizes the U-values of the different wall-types defined in the model.

Table 2.4: Summary of the U-values of the two construction period

Construction period	Wall	Roof	Floor
1st	0.36	0.36	0.24
2nd	0.29	0.29	0.53

The definition of the two envelope typologies can be found in Tables B.3 and B.4. The used materials are described with their names, thickness (m), thermal conductivity

λ ($\frac{W}{m.K}$), density ρ ($\frac{kg}{m^3}$) and specific heat Cp ($\frac{J}{kg.K}$).

The interaction with the sun is determined by two coefficients: the shortwave reflectance ($\epsilon_r SW$) and the long-wave emissivity (ϵ_{IR}). The former describes the share of incident solar irradiation that is reflected by the wall, while the rest is absorbed. The latter describes the IR self-emitting behavior of the surface that depends on the environment and the temperature of the considered surface.

The values of these coefficients are are specific to the envelope typology and are included in Tables B.3 and B.4.

The sources are wageningenur.nl for ϵ_{SW} and LESOSAI for ϵ_{IR}.

The renovation scenario consists in replacing the aluminium modules of the first construction period with rockwool insulation of various thicknesses and 2 cm of rendering. Table 2.5 presents the evolution of the U-value depending on the insulation thickness.

Table 2.5: Evolution of the U-value depending on the insulation thickness

Insulation thickness	Wall
Basecase	0.36
5 cm	0.25
10 cm	0.19
15 cm	0.15

This transformation is presented in Table B.5. The thermal properties of the rendering are extracted from the materialsdb used in LESOSAI [1]. This renovation also changes the value of radiative coefficients. New values were found on the website of Hindawi.

[1] In the materialsdb, this material is called "Enduit mortier extérieur"

2.3.6 Occupants and equipments

Occupants and equipments are implemented in CitySim through the definition of a maximal number of occupants N_{max}, daily schedules $\alpha_h \in [0, 1]$ and a yearly schedule $\epsilon_y \in [0, 1]$.

N_{max} defines the peak power of IHG. α_h describes the daily variation of IHG where h is the hour of the day. Finally, ϵ_y is a multiplication coefficient that varies the IHG depending on the season and day of the week.

Two types of rooms are considered: self-service restaurants or offices as defined in SIA 2024 (SIA, 2006). The maximal density (ρ_i) and daily schedule (α_h) where i is either occupants or equipments are extracted from this norm. Table 2.6 presents the density of occupants and equipments of the two types of rooms.

Table 2.6: Occupants and equipments density for restaurants and offices (SIA, 2006)

Type	ρ_{occ} ($\frac{m^2}{people}$)	ρ_{equ} ($\frac{W}{m^2}$)
Offices	14	7
Restaurant	2	2

Only one schedule can be defined per day and per building in CitySim. The two schedules for equipments and occupants have to be combined into a single schedule (α_h^c).

For each hour of a day, the total emitted power (P_h) is calculated using Eq. 2.5 .

$$P_h[W] = P_{occ,h} + P_{(qu,h} = S_{treated} \cdot (\rho_{occ} \cdot \alpha_h^{occ} + \rho_e \cdot \alpha_h^{equ}) \tag{2.5}$$

where $P_{occ,h}$ is the heat emitted at hour h by occupants

$P_{equ,h}$ is the heat emitted at hour h by equipments

$S_{treated}$ is the treated floor area of the building defined in Paragraph 2.3.2

For all buildings of the same type (self-service restaurant or office), the schedule is the same as the only parameter that varies between them is the treated floor area.

α_h^c is obtained using Eq. 2.6

$$\alpha_h^c = \frac{P_h}{max(P_h)} \tag{2.6}$$

The daily combined schedule obtained with this method is represented in Figure 2.4.

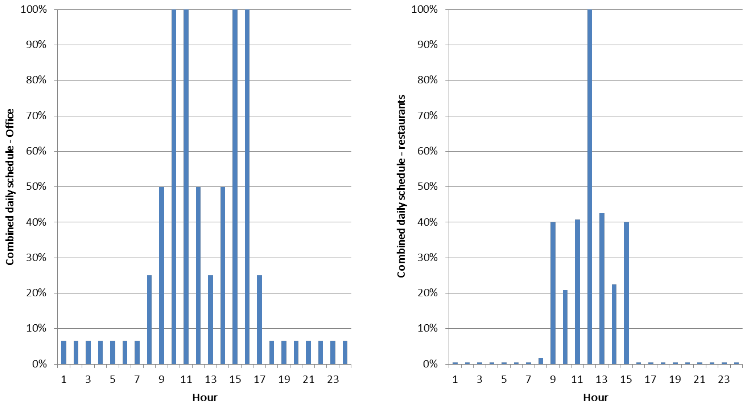

Figure 2.4: Combined Schedules for offices and restaurants - own illustration

N_{max} is defined as a number of occupants assuming that every person emit constantly 90 W. It is calculated using Eq.2.7

$$N_{max} = \frac{max(P_h)\ [W]}{90\ [W/pers]} \tag{2.7}$$

Finally, the yearly schedule (ϵ_y) is used to differentiate Christmas, summer, weekends and course periods with specific coefficients presented in Table 2.7.

Table 2.7: Value of the yearly schedule coefficient depending on the period of the year

Period	ϵ_y	Dates
Courses	1	Jan. 13^{th} - Jul. 27^{th} and Sep. 17^{th} - Dec. 21^{st}
Summer	0.5	Jul. 28^{th} - Sep. 16^{th}
WE	0	-
Christmas	0	Dec. 18^{th} - Jan. 12^{th}

ϵ_y applies to both restaurants and offices. Its values are chosen arbitrarly based on the assumption that most people do not work during Christmas and that a large part of occupants is on holiday during summer. The dates are inspired by the academic calendar of EPFL.

2.4 Simulation results

2.4.1 Model calibration with monitored energy consumption

In Figure 2.5, the simulated results (X-axis) are compared to the monitored heating consumption of EPFL buildings for 2013 (Y-axis).

On this graph, each blue dot corresponds to one particular building. The blue line is the linear regression of the cloud. The dark line is the bisector of the graph which means the points where the simulation results are equal to the monitored consumption. If results are correct, the cloud should be concentrated around this dark line.

The correlation factor is rather high ($R^2 = 0.80$) which means that the cloud of points is close to forming a straight line. The bisector (dark line) and the cloud linear regression (blue line) are almost confounded. Moreover, the equation of the cloud linear regression is $y = 1.0176x$ which is very close to y=x, the equation of the bisector. For these reasons, the results can be considered as acceptable. Some buildings are however diverging.

If buildings are located below the bisector, it means that the simulation gives pessimistic results in comparison to the monitored consumption. It is the other way around for buildings located above the bisector.

LC is located below the bisector. This building is recent (2012) and was designed to respect the Minergie Standard. It is equipped with double-flux ventilation, has high-performance windows and presents a very thick insulation against the ground. Therefore, assuming that LC has the same air renewal and envelope type as other buildings on the campus is a very pessimistic assumption.

For AI, the simulation is too optimistic. This building houses laboratory activities linked to life sciences. In such buildings, the regulation of the inside air conditions requires high air renewal rates ((Helms, 2009) p.20). One could argue that the air renewal is underestimated even with the assumption presented in Paragraph 2.3.3. This statement is supported by the fact that the same effect is observed for buildings MX, which houses material science activities, PPB, research on plasmas, PH, physics and SV, again life-sciences.

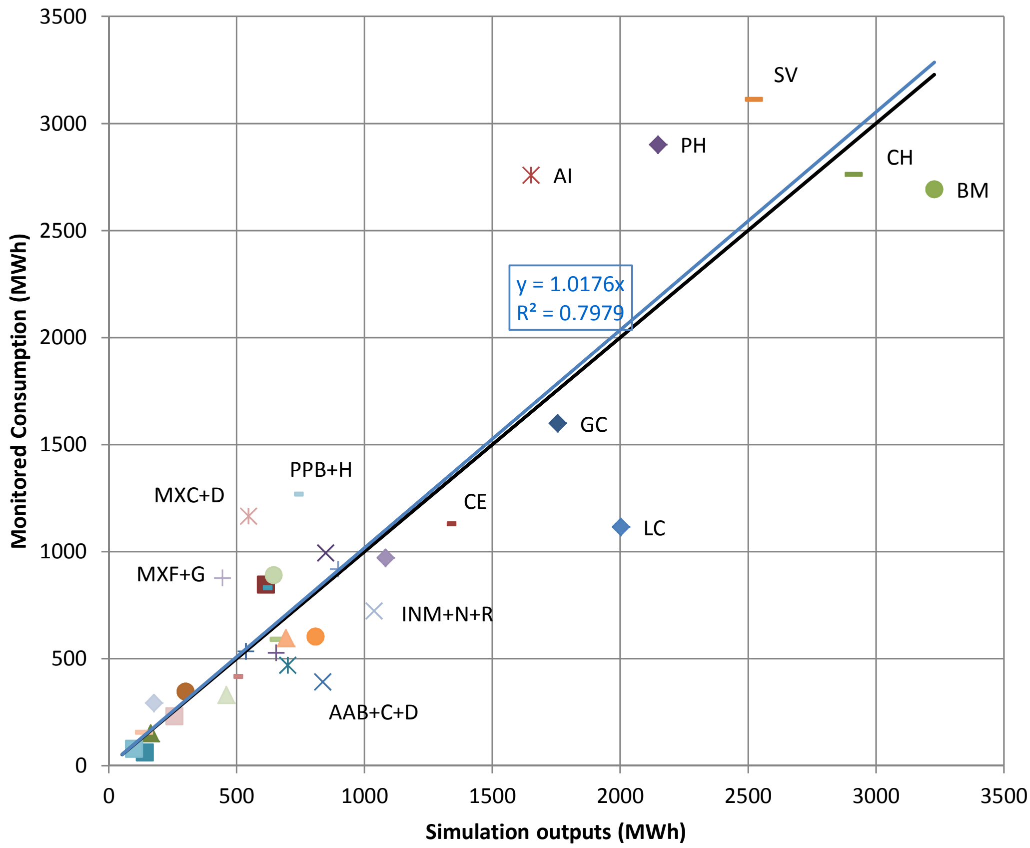

Figure 2.5: Dispersion graph of monitored energy consumption and simulation results, bisector (dark line) and linear regression of the cloud (blue line) - own illustration

2.4.2 Annual load and peak demand

Figure 2.7 presents the results obtained for annual and hourly peak heating demand. In these graphs, buildings were ranked in decreasing order.

The ranking in the two graphs is not the same. Buildings whose ranking changes are highlighted in red. For instance, this is the case for buildings CE and BSP. The simulation results for these two buildings are summarized in Table 2.8.

Table 2.8: Comparison between buildings CE and BSP

Building name	Annual load (MWh)	Annual peak (kW)
CE	1 325	539
BSP	1 245	556

The annual load is higher for CE than for BSP whereas it is the other way around for the annual peak demand.

The BSP is located on the eastern border of EPFL. It has the shape of a flat H where the middle bar is a large 7 floor high tower. CE is a long building (around 200m) with only three floors. The GR is higher on BSP (70%) than on CE (36%). Although the glazing is the same, the envelope is different. The BSP is defined as part of the 2^{nd} construction period while CE belongs to the 1^{st} construction period (cf Paragraph 2.3.5). Finally, BSP is isolated whereas CE is surrounded by PH, BS, CH and BI. Figure 2.6 presents the situation of these two buildings.

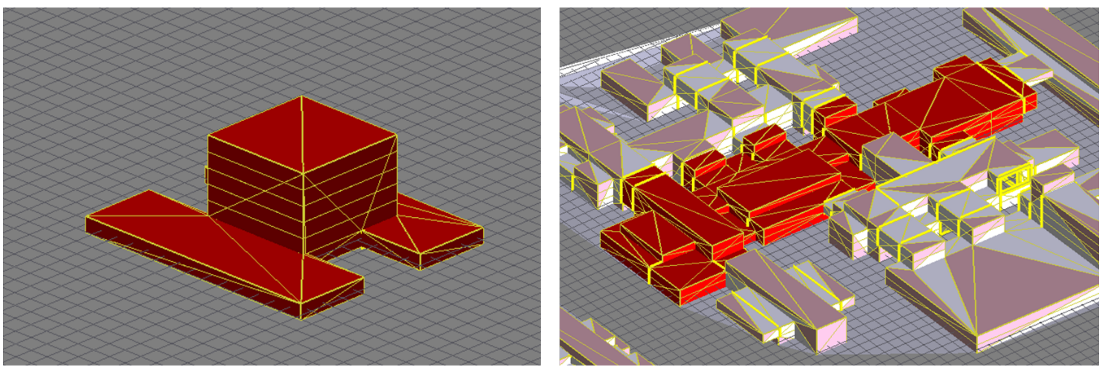

Figure 2.6: Situation of BSP (right) and CE (left) buildings - own illustration

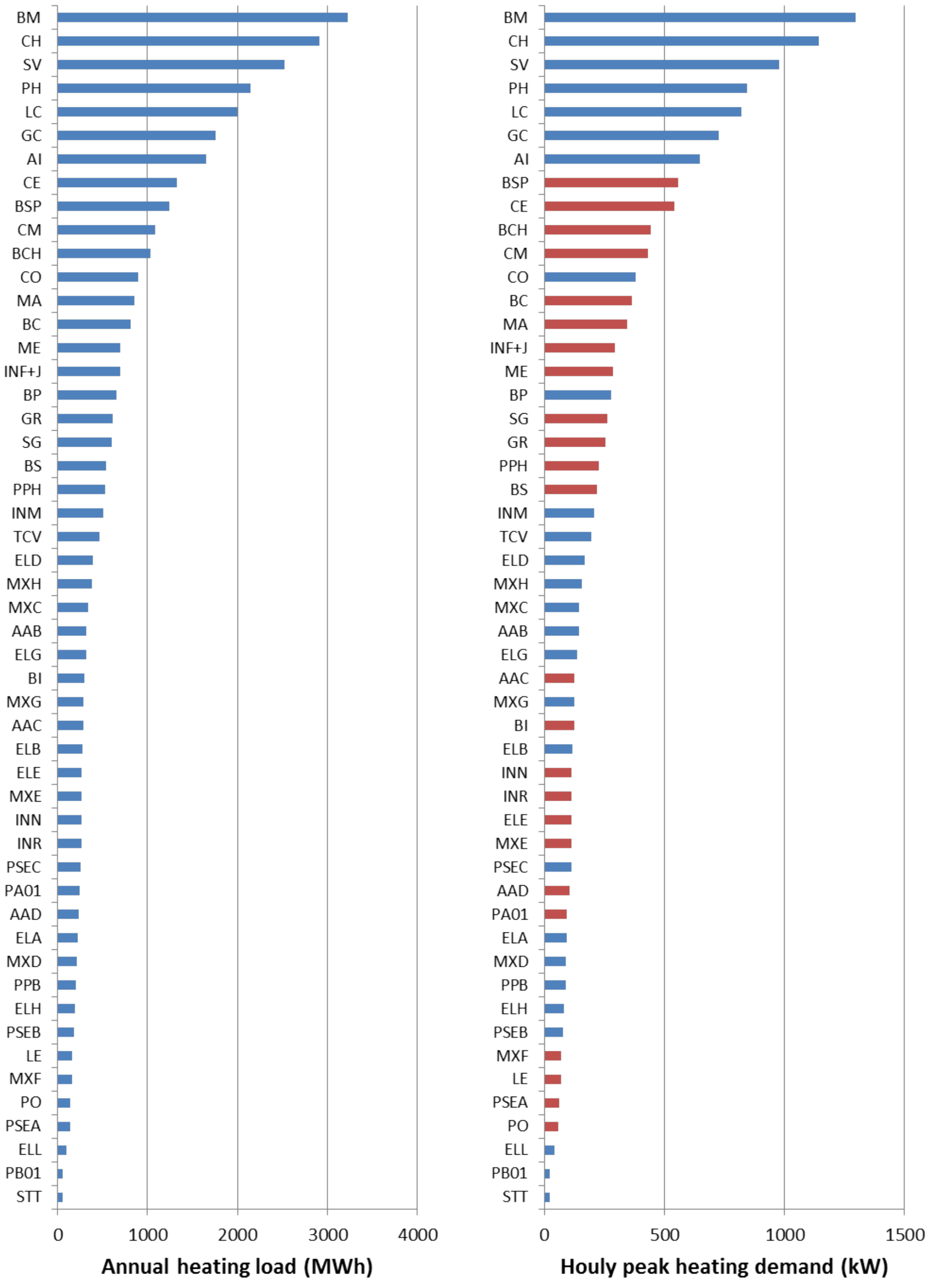

Figure 2.7: Simulation results for annual (left) and hourly peak (Right) heating demand - own illustration

The observations above together with the consumption values in Table 2.8 illustrate that buildings respond differently to a similar external stress. To understand these differences in behavior, Figure 2.8 presents the Peak to Average Ratio (PAR).

$$PAR = \frac{Hourly\, peak\, heating\, demand\, (kW)}{Hourly\, Average\, heating\, demand\, (kW)} \tag{2.8}$$

This quantity is often used in telecommunications (Wulich *et al.*, 2008) and (Lim *et al.*, 2009). Its application here aims to identify parameters that could have an influence on the correlation between the hourly peak heating demand and the annual heating load. The conclusions drawn here would however require further confirmation.

All values on Graph 2.8 are included in the interval [3.19 - 3.94], which means that the peak heating demand is 3.19 to 3.94 times higher than the average consumption. This interval is quite narrow which means that the peak demand and average demand are globally correlated. However, significant variations are observed. On this graph, a higher value means that the heating effort is more intensive relatively to the average demand. This difference in behavior could be explained by the variation of the glazing ratio (GR), as buildings with high GR (BC, BCH, BSP, AAD, AAC and AAB) dominate the ranking (dark blue). By contrast, the lower end is occupied by buildings with smaller (PA and PB) or nil (STT) GR. Moreover, there is a separation between buildings belonging to the first period of construction (red) that are defined with a GR = 36% and buildings from the second period of construction (blue) that are defined with a GR = 40%, the latter being ranked higher than the former. These observations show that the gap between peak demand and the average demand seems to increase with the glazing ratio. This change in the building thermal behavior might be explained by the solar gains through the glazing and that decreases the building needs during daytime. However, the impact of solar gains on the peak demand is limited as it occurs during the night.

Finally, buildings defined with higher air renewal rates are clustered at the bottom of the ranking. This shows that ventilation does not affect the building dynamic behavior in a similar way as windows. This difference is explained as follows. The ventilation creates a constant air flow between indoor and outdoor. The outdoor air temperature is influenced by many parameters among which the solar irradiance. This explains that the solar gains through windows have a stronger impact on the building thermal behavior than ventilation that is only indirectly influenced by solar irradiation.

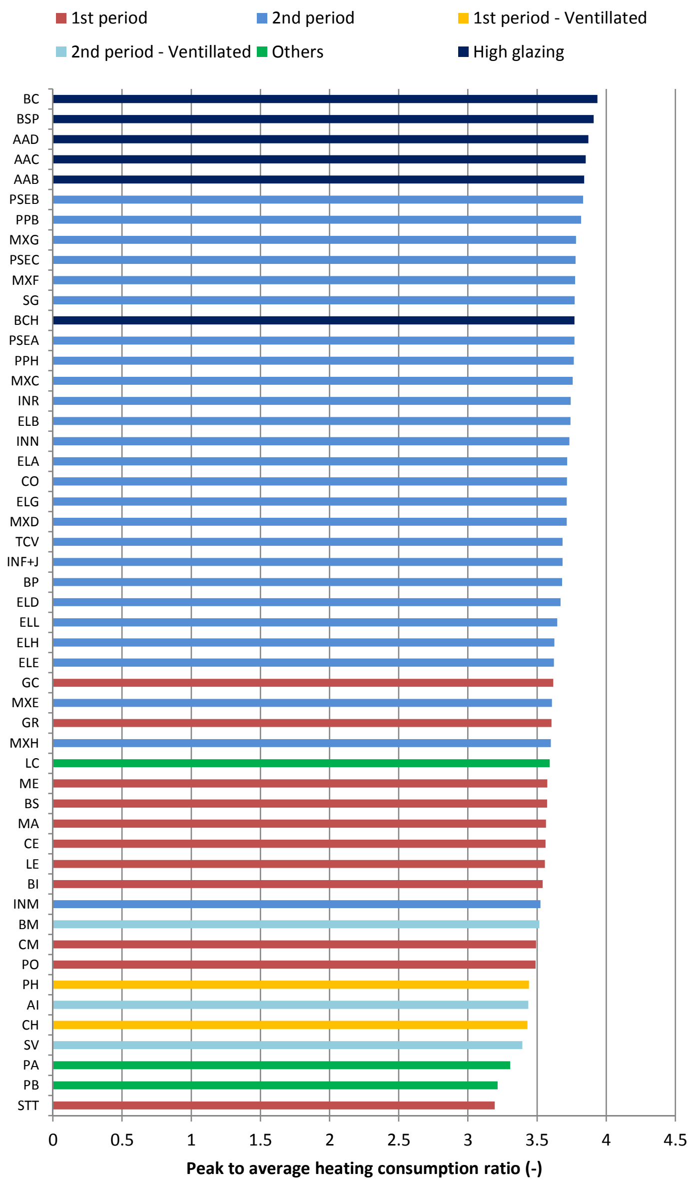

Figure 2.8: Peak heating demand to annual heating load ratio $(-)$ - own illustration

2.4.3 Building specific consumption

Figure 2.9 presents the results for the specific consumption of EPFL buildings in $\frac{kWh}{m^2}$. The determination of the treated floor area is explained in Paragraph 2.3.2. The choice of colors is the same as in Figure 2.8.

Various norms are also represented for comparison. The maximal consumption for administrative Minergie-P and Minergie buildings is hatched in green. The designations *new*, *retrofitted* and *existing* describe respectively the maximal consumption of new, retrofitted and existing high-school buildings as defined by norm SIA 180/4 as shown in (DII EPFL, 2008) p. 16.

Most EPFL buildings are located within the requirements for retrofitted and new high-school buildings. On the high end of this interval are buildings with a high glazing ratio (AA c,b and d) and isolated buildings (LE and ELL).There is no clear separation between buildings from the first and second period of construction.

Buildings with high ACH (SV, AI, BM, PH and CH) are clustered at the top of the ranking around the requirements for existing high-school buildings. This shows the decisive impact of ventilation on the heating demand at EPFL. This correlation is illustrated in Table 2.9 where the building with the highest ACH also has the highest specific consumption.

Table 2.9: Value of ACH and specific consumption for highly ventilated buildings

Building name	ACH [h^{-1}]	Specific consumption [$\frac{kWh}{m^2}$]
CH	0.74	116
PH	0.762	123
BM	0.96	144
AI	1.114	164
SV	1.18	168

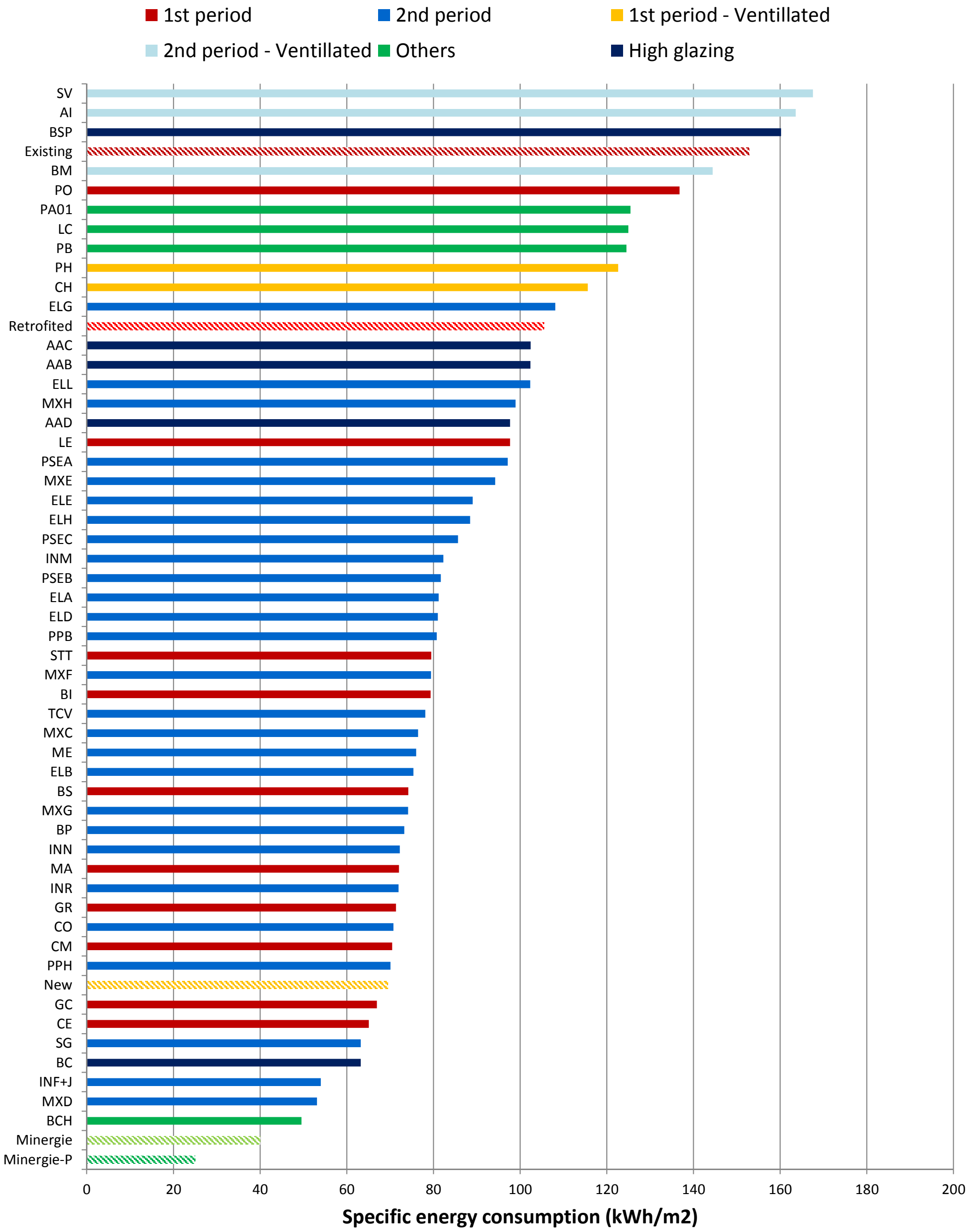

Figure 2.9: Specific consumption per building ($\frac{kWh}{m^2}$) - own illustration

The importance of geometry is also illustrated in this graph. PO, PA, LC and PB are all located high on the ranking. These buildings are the only ones on the campus with a single floor. This "flat" shape is not energy efficient because the inside volume is small in comparison to the exterior surface used to enclose it.

The influence of glazing on energy consumption is balanced by two phenomena. On the one hand, windows present rather high thermal conductivities in comparison to a normal wall and therefore are often the source of high thermal losses. On the other hand, windows are transparent and can decrease the heating demand by allowing solar gains.

In Figure 2.9, the impact of windows can be highlighted through the example of two particular buildings, BSP and BCH. These buildings only differ through location and geometry (cf Figure 2.3). However, their specific consumption is very dissimilar. The BSP is very high on the ranking while the BCH is the best building of EPFL in terms of specific consumption. The gap might be explained by a difference in solar gains. BCH benefits from significant solar gains due to its long and high shape. Moreover, the sun is not obstructed by any other building. By contrast, BSP has equally oriented glazing surfaces to the four directions as it corresponds more or less to a square tower. This means that windows oriented to the north cause relatively more losses than in BCH. Moreover, the BSP is located north of BCH and is therefore partially obstructed during the heating season because the sun is low on the horizon.

Similarly, BC is much lower on the ranking than AAb, c and d. This could be due to a difference in solar gains as BC benefits from large solar inputs particularly on its west façade while AA buildings are in the shadow of the AI building and are also shading each other.

The situation of all these different buildings can be seen in Figure 2.10.

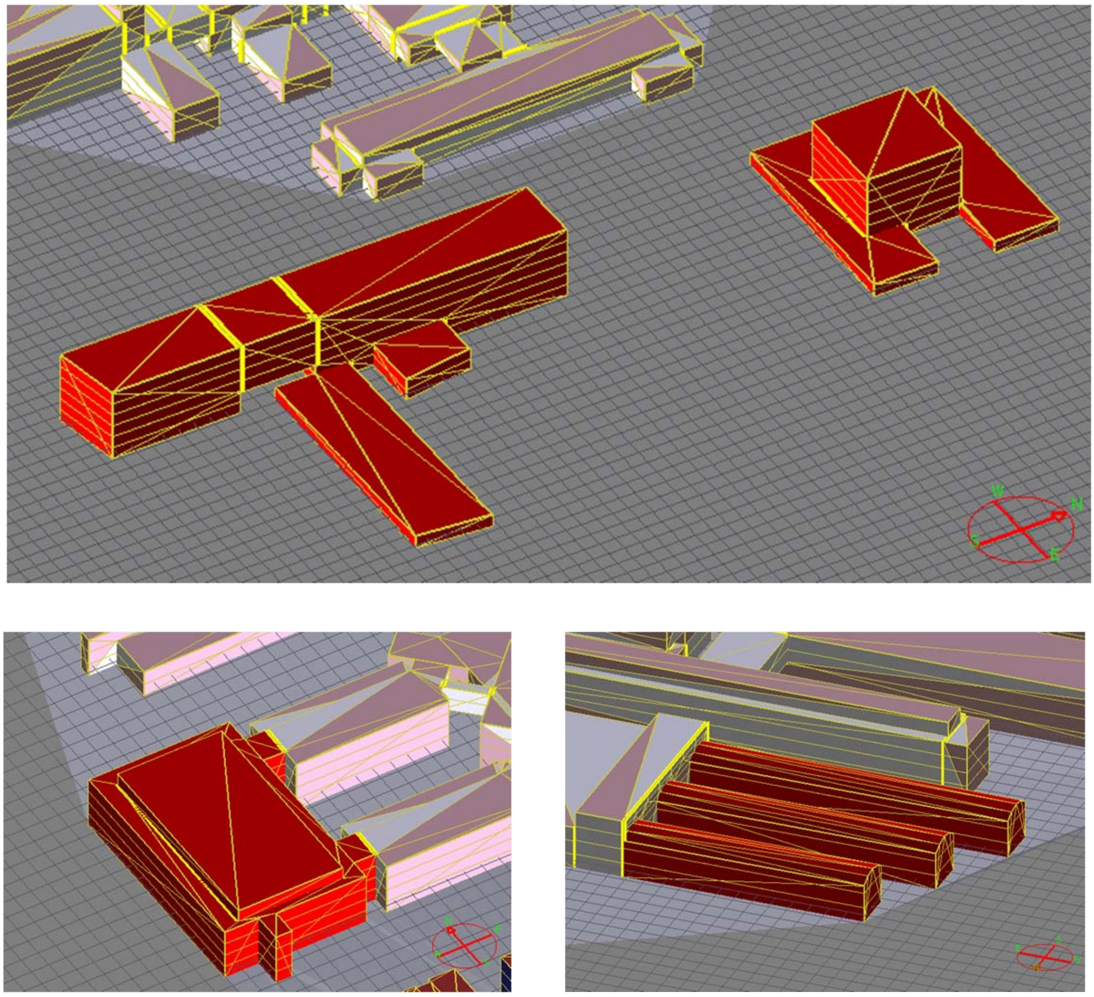

Figure 2.10: Situation of BCH and BSP (top), BC (bottom left) and AA buildings (bottom right) - own illustration

2.4.4 Energy saving scenarios

In this part, the potential benefits of energy saving scenarios are investigated. First,the IHG are removed to quantify their influence on the heating needs. Then, the impact of insulating the old buildings from the first year of construction is studied. Afterward, the set-point of all buildings is decreased by 1 °C. Finally, windows are replaced by efficient double glazing or triple glazing. All these results can be found in Appendix B.5.

The absence of IHG provokes a heating load increase of 9% on average. The smallest impact of IHG is found for SV (2%) and is explained by the low impact of IHG when compared to the large losses through ventilation. This diagnosis is verified in the case of AI (6%). These two buildings have the highest ACH on the campus (cf Table 2.9). The highest impact of IHG is found for the SG (15%).

Renovation scenarios are considered for buildings of the first construction period. Figure 2.11 presents the evolution of the annual load and the peak demand for different buildings of the first construction period.

The annual load is quickly decreasing when 5 cm of insulation are added in all cases. Savings obtained by adding more insulation are less substantial. In absolute value, the highest gains are obtained for GC (104 MWh). However, the relative decrease to the base-case is maximum for ME (9%).

This last difference might be due to solar gains. GC is oriented to the north while ME is toward the south (cf Figure 2.3). Therefore, ME benefits from more relative solar gains. Increasing the insulation thickness reduces the conduction losses and so the transfer of solar gains to the outside. This means that buildings that rely on solar gains for heating might benefit more than others from a retrofit. However, this statement would need confirmation as it is not observed between buildings MA (oriented to the south) and GR (oriented to the north).

The evolution of the annual load and the peak demand are very different. The latter decreases much slower than the former with increasing insulation thickness. Moreover, the peak heating is even observed to increase by 0.2% for the GC and when 5 cm of insulation are added.

The low decrease of the peak demand when compared to the annual value can be explained as follows. The walls of the first construction period already include 10 cm of rock-wool ($\lambda = 0.04\frac{W}{m^2 \cdot K}$). Therefore, the addition of even more insulation is not likely to provoke a high change in the dynamic behavior of the building but only slightly decreases the heat transfer through the envelope. However, the systematic addition of such small heat savings might well lead to a significant reduction of the annual load.

As to the increase of the peak heating described above, the cause might be building losses through IR. The IR emmissivity of the walls is increased from 0.2 with aluminium façades to 0.85 after insulation. The peak demand occurs during the night (22:00) when the sky is clear (N=0 octas). In these conditions, the losses through IR are larger.

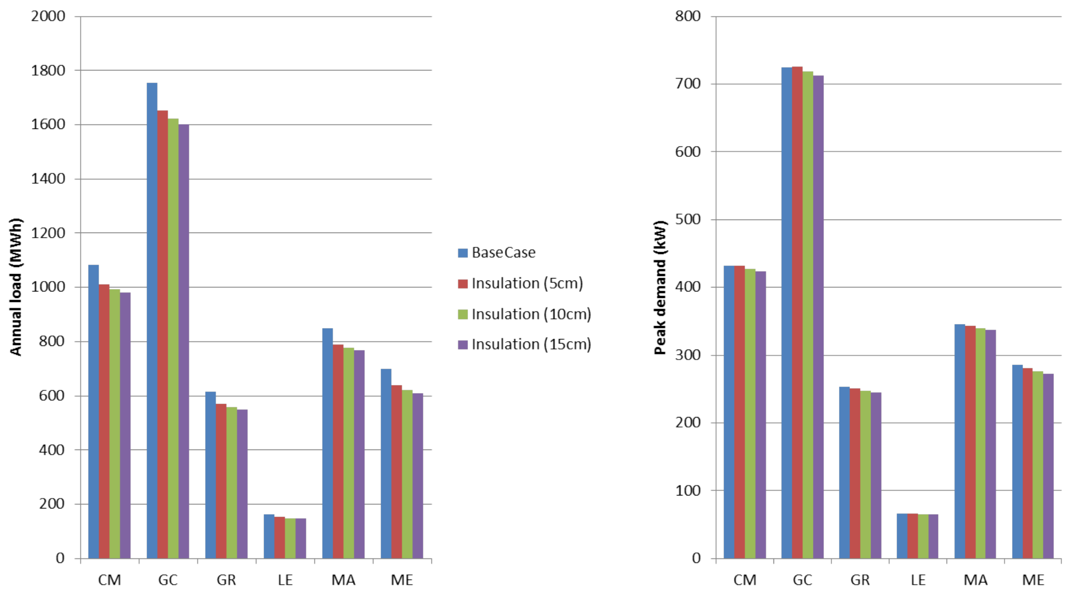

Figure 2.11: Evolution of the annual load (left) and peak demand (right) with building insulation of various thickness - own illustration

The decrease of 1 °C of the set-point leads to a decrease of the annual heating needs from -6% to -8% with an average of 7%. The result of the peak load is a general decrease of 3% in all cases. The conclusion is that savings obtained with a reduction of the set-point do not depend significantly on the characteristics of the building as the change in consumption is rather homogeneous for all EPFL buildings.

Windows replacement with efficient double glazing modifies the heating load by -2% for SV, PA and PB to -12% for AAb and c. In the case of SV building, the weak impact of windows replacement is due to a high ACH that decreases the impact of windows on the heating load. This remains true for other buildings with high ACH such as CH (-3%), PH (-3%), AI (-3%) and BM (-4%). The small impact on PA and PB is due to their rather small GR (25%) and their "flat" shape. The high impact of windows replacement on the performace of the AA buildings is due to their high glazing ratio (70%) and obstruction of the sun by each other and by the AI. These observations are confirmed by results for triple glazing replacement where the difference in impact between highly ventilated and glazed buildings is much larger (SV: -4% and AAC: -46%).

Figure 2.12 presents the evolution of the annual load and the peak demand with glazing of various performances for some buildings of the first construction year. By contrast with Figure 2.11, the annual load follows much more the peak demand. This is because windows are highly conductive, moreover, windows have no thermal mass and are therefore very sensitive to any changes in the outdoor conditions. This leads to the conclusion that windows have a much stronger impact on the dynamic behavior of buildings.

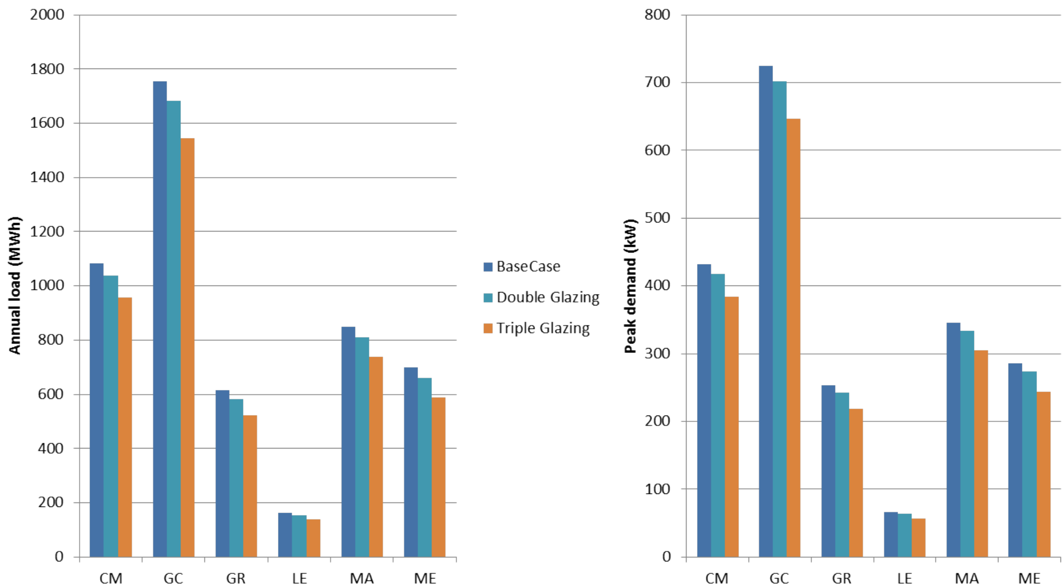

Figure 2.12: Evolution of the annual load (left) and peak demand (right) with glazing of various performances - own illustration

2.5 Discussion

The correspondence of a model with reality is always limited.

Building energy consumption is influenced by a large number of parameters. In the scope of the present work, many of these are assumed with limited guaranty of consistency with reality and often no way to estimate their actual impact on the simulation outputs.

For instance, the simulation results are compared with the monitored consumption of EPFL buildings in 2013. However, no comprehensive comparison of the weather file used in simulations and the actual weather of 2013 is performed.

This possible difference with reality can be discussed with regard to all the other assumptions. To quote other examples, the model of the envelope in three homogeneous wall-types is simplistic, the IHG are determined using the treated floor area and the SIA norm. The former is shown to be rather far from the truth in some cases (cf Appendix B.2) and the latter cannot take into account the stochastic behavior of people. The value of the setpoint is global and assumed at 21.5 $^\circ$C based on literature (Helms, 2009), however, it does not allow to distinguish unheated building zones such as the staircases. Most windows at EPFL can be opened and are equipped with shading devices, however, those are not defined in the model. The assumption of a 95% efficiency heating distribution network within each building is arbitrary.

The purpose of this work is above all to show that consumption values of acceptable consistency can be obtained even at the cost of heavy assumptions.

The analysis of the results also has its limitations.

The validation of the model is not complete as some annual consumptions of EPFL buildings are not obtained (PA or BCH for example). Moreover, buildings are only compared based on absolute values, it might be revealing to study the relative error.

In Paragraph 2.4.3, the differences between buildings with same definition but different specific consumptions is not analysed (for instance the MX, EL or IN).

In Paragraph 2.4.2, the annual load and the peak demand are shown not to be completely correlated. However, these differences in behavior are analysed by observing tendencies in variations of the PAR. This parameter is mainly used in telecommunications and had not yet been applied to buildings. The conclusions obtained here would therefore require further investigations to determine if this analysis is consistent or not.

Finally, only a handful of energy saving scenarios are investigated with the parametric analysis presented here. Present conclusions are guidelines that highlight operations with significant potential impact. The finding of an optimal solution requires a more advanced work.

2.6 Conclusion

The creation of an energy hub on the EPFL campus requires the ability to predict the heating consumption of its different buildings. This work demonstrates that it is possible to simulate acceptable annual heating loads despite the inherent complexity of this particular study object. Outliers can be explained by either pessimistic or optimistic assumptions taken in the model definition.

The annual heating load and hourly peak heating demand are shown to be uncorrelated. The PAR is computed for all buildings with the intent to identify the cause of this difference in behavior. The findings are that solar gains through windows decrease the average load but have no influence on the peak heating. Therefore, the value of the PAR increases with the GR. By contrast, increasing the ACH reduces the value of the PAR. The explaination might be that the impact of solar on the ventilation is indirect.

Considering the building specific consumption, ventilation is shown to drastically increase the building energy consumption. The single floor geometry adopted by buildings PA, PB, PO and LC appears to be inefficient from an energy point of view. Finally, differences in windows orientation and buildings inter-shading are shown to provoke extreme variations in heating requirements through differences of solar gains.

Some energy saving scenarios were applied to buildings of the campus. The evolution of the annual heating load and the peak heating demand according to each scenaariocan be found in Table 2.10

The impact of IHG is to decrease the heating load. However, the amplitude of this decrease depends on several different parameters among which the ventilation is important.

For the renovation scenarios of buildings from the first construction year, an insulation thickness of 5 cm allows significant savings. This is not the case for thicker insulation. The solar gains might cause differences in the savings obtained for various renovated buildings. Also, the peak demand decreases much slower with the insulation thickness than the annual load. This fact could be explained by the heat conductance properties of the wall and by the increased losses through IR after renovation.

The savings obtained with a decrease of the set-point do not appear to significantly depend on buildings characteristics.

Changing the glazing quality has a small impact on buildings with high ACH but a very high impact on buildings that are both highly glazed and sun obstructed. This difference increases with the quality of the glazing. Finally, the changes in annual load and peak demand are correlated with the renovation of windows. This means that the glazing has a more direct impact on the building dynamic behavior than walls. The difference is explained by the high conductance and the low thermal mass of the former.

Table 2.10: Global savings obtained with the different energy saving scenarios

	Annual Load		Peak demand	
	GWh	%	MW	- %
Basecase	35.3	-	14.5	-
Empty	39.0	10%	14.4	0%
Insulation (5cm)	34.7	-2%	14.5	0%
Insulation (10cm)	34.6	-2%	14.5	0%
Insulation (15cm)	34.5	-2%	14.4	0%
Setpoint (20.5C)	32.9	-7%	14.0	-3%
Double glazing	33.8	-4%	14.0	-3%
Triple glazing	31.0	-12%	12.9	-11%
Best case	28.3	-20%	12.5	-14%

2.7 Future work

There is still a large potential for improvements in the development of the model.

First, it seems important to obtain the weather data of 2013. In the best case, these data should be used in simulation. If this is not possible, a comprehensive analysis between simulation and real weather files should be performed in order to predict tendencies in the results.

The model should be divided into more different envelope typologies. Activities should be better characterized in order to set more realistic values of ACH and IHG. The number of floors of each building shoud be determine according to visual observation computed with an assumed floor height.

The parameters mentioned above are only examples of all those that can still be implemented in the model. However, this implementation should only involve one parameter at a time in order to estimate the model sensitivity.

Many paths of analysis remain unexplored.

The annual load of some EPFL buildings should be acquired (PA, BCH, etc) in order to ensure an approximate consistency of the model for all buildings.

In this publication, only the heating needs are studied. It would be revealing to analyse the inside air temperature profile to control if the comfort conditions are met inside the building, especially outside the heating period.

It might be interesting to study clusters of buildings like the MX, IL or EL complexes to understand why these buildings have different heating profiles whereas they share the exact same definition.

Other energy saving scenarios could be applied on the model. For instance, the impact of insulating buildings from the second year of construction should be considered.

It would be interesting to see how the definition of a heating storage system affects the heating profile and in particular the peak heating. This analysis should be done for different categories of buildings such as elevated, flat, highly glazed or ventilated ones.

Part 3

Programs intercommunication: CitySim and Python Energy Integration

3.1 Introduction

Previously, the heating demand of the EPFL campus was simulated on an hourly basis. Now, the interest is to show the possibility to link CitySim to an optimization tool, Python Energy Integration (PEI), that can determine the optimal way to supply this heat by defining a particular energy conversion system: PEI's purpose is equipment sizing with the help of optimization models using energy integration technics.

In PEI, a Mixed Integer Linear Programming (MILP) algorithm is used to determine the optimal characteristics of a heating conversion system based on energy demand, potential renewable energy sources and different energy conversion technologies. Its goal is either cost or cumulated exergy demand minimization.

To link CitySim and PEI, the outputs of the former must be treated to meet the input requirements of the latter. This work was already done between PEI with Bsol, another building energy simulation program (Pfeiffer, 2014). The task here is to adapt the communication code between these two programs to make it consistent with CitySim.

3.2 Methodology

3.2.1 CitySim outputs pre-treatment

The hourly heating profile of all the different buildings of EPFL campus is extracted. They are labelled as *MachinePower* in CitySim result files (cf assumptions 2.3.4).

The goal is to be able to optimize the super structure of the EPFL heating system where heat is supplied by only one centralized energy conversion unit (DII EPFL, 2008) p. 9/52. Therefore, the whole data is concatenated on every hour of the year. After that, the data is in the form of matrix 3.1.

Matrix 3.1 is transformed into the n-by-p matrix 3.2 where $n = 365$ and defines days of the year while $p = 24$ is the hour of the day.

The potential renewable energy sources considered in this work is solar thermal. The hourly production of 1 m^2 of solar panels on various temperature levels is computed in (Pfeiffer, 2014) for the Verbier ski resort. Calculations are adapted with the weather file used in CitySim for Ecublens.

The solar thermal profile is added to matrix 3.2 to form matrix 3.3 were column 1 to 24 describe the heating needs and column 25 to 48 describe the solar profile. These two groups are normalized according to their respective peak values. In this way, the input data for the clustering is standardized: all values are between 0 and 1.

$$\begin{pmatrix} q_1 \\ q_2 \\ \vdots \\ q_{8760} \end{pmatrix} \tag{3.1}$$

$$\begin{pmatrix} q_{1,1} & \cdots & q_{1,24} \\ q_{2,1} & \cdots & q_{2,24} \\ \vdots & \ddots & \vdots \\ q_{365,1} & \cdots & q_{365,24} \end{pmatrix} \tag{3.2}$$

$$\begin{pmatrix} q_{1,1} & \cdots & q_{1,24} & q_{1,25} & \cdots & q_{1,48} \\ q_{2,1} & \cdots & q_{2,24} & q_{2,25} & \cdots & q_{2,48} \\ \vdots & \ddots & \vdots & \vdots & \ddots & \vdots \\ q_{365,1} & \cdots & q_{365,24} & q_{365,25} & \cdots & q_{365,48} \end{pmatrix} \tag{3.3}$$

3.2.2 CitySim outputs clustering

Matrix 3.3 contains many values. PEI is not able to process that much data at a reasonable computing cost. Therefore, it is necessary to reduce the number of inputs.

This is possible using a clustering algorithm. These kind of methods are comprehensively described in literature (Gan *et al.*, 2007). Clustering algorithms are used is many different fields such as image compression (Nikam *et al.*, 2011), biology or archeology (Gordon, 1999).

There are mainly two families of clustering algorithms: hierarchical and partitional. The clustering method used here belongs to the patitional methods and is called k-medoids. Its goal is to reduce a number n of distinct objects to a number k ($k < n$) of clusters where similar elements of n are regrouped. In the context of the present work, n is a set of 365 days among which k typical days are chosen. Similar applications of clustering algorithms can be found in (Domínguez-Muñoz *et al.*, 2011) and (Rager *et al.*, 2013).

k-medoids was preferred to other methods like the k-means because it is less sensitive to outliers and noise (Singh, 2011). Moreover, the k-medoids is more effective in term of computation time as it does not require the distance matrix to be recalculated at each iteration (Reynolds *et al.*, 2004). Finally, the result of this algorithm is a set of real days whereas the k-mean method produces average days that are not real.

The application of the k-medoids method is organized in two distinct phases (i) the computation of the distance matrix and (ii) application of the clustering procedure.

For (i), it is necessary to define the criteria that determines the distance or dissimilarity between two days. Here, it is defined as the squared Euclidean distance expressed by Eq. 3.4.

$$d(i,j) = (\sum_{p=1}^{48} |q_{i,p} - q_{j,p}|^2) \tag{3.4}$$

The squared Euclidean distance is chosen because it increases the differences between objects. Therefore, an extreme object such as peak demand is more likely to be taken into consideration.

The distance between two objects depends on heating and solar values.

Using Eq. 3.4, the dissimilarities between all objects (days in this context) is computed and arranged in a n-by-n symmetric matrix (cf Mat 3.5).

$$\begin{pmatrix} 0 & d(1,2) & \dots & d(1,365) \\ \vdots & 0 & \dots & \vdots \\ \vdots & \vdots & \ddots & d(364,365) \\ sim & \dots & \dots & 0 \end{pmatrix} \tag{3.5}$$

The clustering total cost (Co) is computed using Eq. 3.6. This notion is used in the clustering process.

$$Co = \sum_{i=1}^{k} Co_i = \sum_{i=1}^{k} \sum_{l_i=1}^{J_i} d(i, l_i) \tag{3.6}$$

Where k Number of medoids/clusters
Co_i Specific cost for clustering around centroid i
l_i Element of j linked to centroid i
J_i Group linked centroid i

For (ii), the algorithm operates as follows.

1. A set i ($i = 1, ..., k$) of days is randomly selected, they are called medoids
2. All other objects j ($j = 1, ..., 365 - k$) are associated to the medoid i with the smallest $d(i, j)$ and form k clusters. The total cost Co is computed according to Eq. 3.6.
3. Within each cluster, the best position for the medoid is recalculated. A new combination of medoids i' is obtained
4. All other objects j' are associated to the medoid i' with the smallest $d(i', j')$, forming new clusters. The new total cost Co' is calculated. If $Co' < Co$ the change is maintained

Steps #3 and #4 are repeated until no change.

On the one hand, applying this technic avoids to calculate the clustering cost of all the possible combinations of typical days. This number is huge (i.e. $\binom{6}{365} = 3.15 \cdot 10^{12}$)

and the task would be time intensive. On the other hand, applying this technic only once is likely to generate a local minimum of the total cost.

Therefore. the operation is repeated X times. In this way, all total cost minimum are likely to be detected as the initial combination of typical days is randomly chosen. The global minimum can then be deduced by comparison. However, this approach is heuristic as it assumes that a series of X tests is enough to find all minimum. The solution is not guarantied optimal. $X = 100'000$ has shown to produce acceptable clustering results (Pfeiffer, 2014).

Another main disadvantage of this clustering method is that the number k of clusters is defined by the user. Indeed, all values of k don't lead to a natural partitioning of the data. For example, if data is regrouped in 3 distinct groups but the user defines k=4, one of the three group is split without necessity. By contrast, if the user defines k=2, two of the three groups are meaninglessly linked.

To choose a consistent value, the clustering optimal solution is computed for $k = 4$ to $k = 10$. The best value is then chosen by assessing the clustering quality using specific indicators : the annual error, the silhouette and the number of times the optimal solution was chosen. These parameters are described below.

The annual error (AE) describes the error made on the total year. It is computed according to Eq. 3.7. The optimal value is 0. AE can be either negative or positive.

$$AE\,[\%] = \frac{\sum_{j=1}^{365} q_d - \sum_{i=1}^{k} (w_i \cdot q_i)}{\sum_{d=1}^{365} q_{o,d}} \tag{3.7}$$

Where j are the days of the year

q_d is the sum of heating needs during day d

q_i is the sum of heating needs during typical day i

The definition of the silhouette is given in (Rousseeuw, 1987). It is an indicator of the intra-cluster tightness and inter-cluster separation. Its value varies from -1 to 1. 1 being the ideal and corresponding to the situation were all objects are near their respective medoids and far from others.

The number of times that the optimal solution is found ($Nb \in [1, X]$) corresponds to the number of times that the clustering operation described above ended on the same minimum total clustering cost. If Nb is close to the number of runs made, one can be sure to have identified a global optimum. Whereas when Nb is small or even 1, there is no way to determine if the found solution is a local or global minimum. This is one drawback of the heuristic approach.

After clustering, a weight w_i (whole number) is associated to each typical day i of the optimal distribution. This weight represents the frequency of occurrence of i during the year. The sum of all w_i is equal to 365.

At that point, the number of considered hours for optimization is down from 8760 to $k * 24$. This number is reduced even further by clustering together similar hours within each typical day according to the same method. The result is a set t_i of typical hours specific to each typical day i each associated with a particular duration d_{i,t_i}.

3.2.3 Energy Integration

Previously, the heating needs of the whole campus are reduced to typical days. After clustering, the heating needs are described as a set of cold streams specific to each selected day i and hours t_i. Each stream is defined with given entering and outgoing temperature (respectively T_{in} and T_{out} with $T_{in} > T_{out}$) and a heat flux (q [kW]).

The goal of energy integration is to determine a set of hot streams produced by utilities that fulfill the requirements of the cold streams in an optimal way.

This is done using a MILP algorithm, PEI that is more comprehensively described in (Pfeiffer, 2014). A MILP is defined with a continuous objective function such as the cumulated energy efficiency, the total cost or CO_2 emissions and a set of discrete constraints such as thermodynamic laws, space, time or technology.

In this case, the objective function is the Life Cycle Exergy (LCEx). LCEx is composed by two elements:

- The construction and deconstruction exergy consumptions of the utility
- Operating exergy consumption including preceding steps (i.e. oil refinement) and succeeding steps (i.e. ash disposal)

In (Pfeiffer, 2014), PEI is subject to the following constraints.

1. Energy balance (1^{st} law of thermodynamics): the entering energy (utilities) is equal to the energy that leaves the system (heating needs) plus the stored energy
2. Heat Cascade (2^{nd} law of thermodynamics): this constraint ensure that it is the entering energy that is devalued to provide the required energy services
3. Time constraints: the utilities have to follow the schedule of the heating needs.
4. Technology availability: allow only the utilities that are bought to operate

3.3 Results

3.3.1 Clustering results

Figure 3.1 presents the variation of the annual error, the silhouette and the number of times the optimal solution was found in function of k.

The annual error is maximum for k=4. In this case, the annual load is overestimated by 5.63%. The second higher value is for k=5 that overestimates the consumption by 2.42 %. The closer value to 0 is obtained for k=6 (-0.19%) and then for k=8 (-0.37%).

The silhouette is maximum for k=5 (0.41[-]) and globally decreases regularly with k. This means that the more typical days are chosen, the less consistent are the clusters definitions. In other words, the choice of more typical days provoke a situation where many days are located in between two different clusters. However changes are rather small from k=6 to 10.

Finally, the optimal solution is only found once for k=10 and twice for k = 9. It is higher in all the other cases.

The most consistent value of k is chosen based on the above observations. k = 4 and k = 5 are eliminated by the annual error. The variations of the silhouette are low and do not appear decisive on the decision process. k = 9 and k = 10 are eliminated as Nb is very low in these two cases. The chosen value is k = 6 because the PEI simulation time is shorter than with k = 7 or k = 8. Moreover, the annual error is minimized for k = 6.

Table 3.1 presents the distribution of the typical days with associated weight for the k = 6. As an example, Figure C.1 and C.2 present the hourly evolution of original and clustered heating and solar data for typical day 340.

These days are well-distributed with the seasons: There are two days in Winter (5, 64), two days in Spring (82 and 135), one day in Summer (176) and one day in Autumn (340). Two days without heating are chosen (135 and 176). This is due to the definition of the dissimilarity matrix that increases the importance of extremes. In the case of the heating, there are two extremes, the peak demand and 0. The latter is much larger than the former. Therefore, several days without heating are chosen to minimize the global error made on representing this particular extreme.

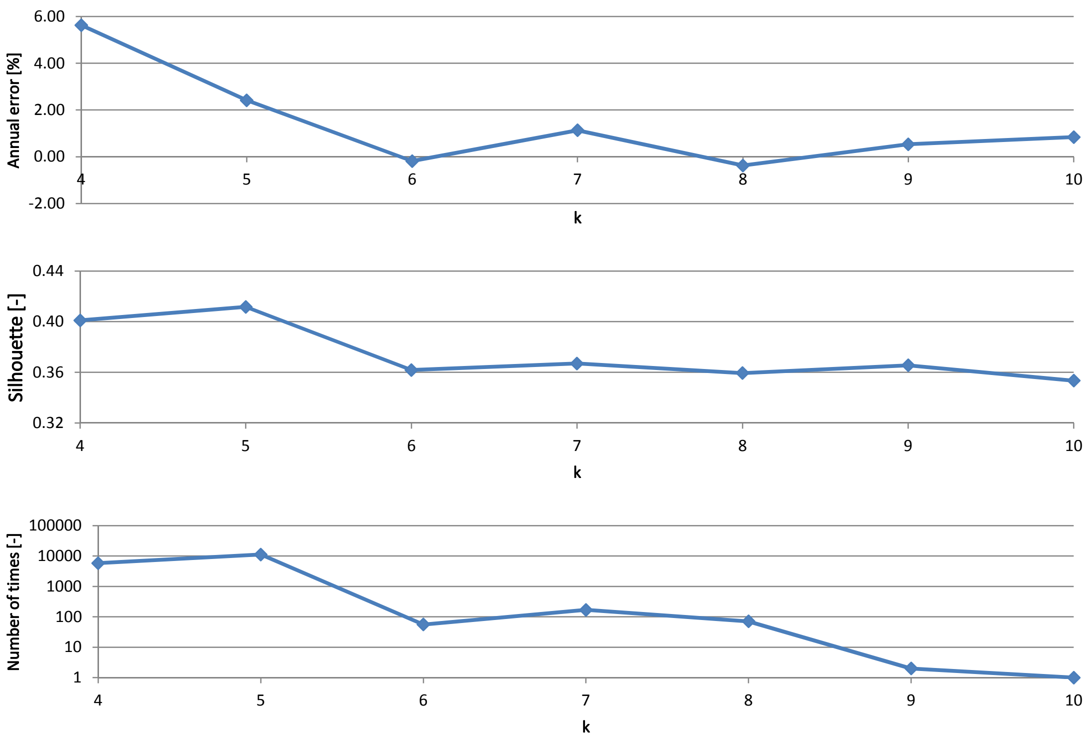

Figure 3.1: Variation of the annual error, the silhouette and the number of times the optimal solution is found in function of k - own illustration

Table 3.1: Distribution of typical days with associated weight depending on the value of k

k	d_y	d_m	Month	W	D	w_i
6	5	05	January	1	5	61
	64	04	March	10	1	77
	82	22	March	12	5	36
	135	14	May	20	2	61
	176	24	June	26	1	75
	270	26	September	39	4	55

Figure 3.2 presents the original and clustered heating load duration curves.

In this figure, the original data profile is divided into three main parts: one near vertical, a second decreasing oblique and a third horizontal and equal to 0. The first part corresponds to the peak heating and the third to the period where the heating is off. This shape is not similar to others found in literature (Rager *et al.*, 2013), (Pfeiffer, 2014) or (Domínguez-Muñoz *et al.*, 2011). In those publications, the load duration curve generally has the shape in $f(x) = \frac{1}{x}$. The specific shape observed here might be due to the limitations imposed on the heating period. Currently, loads that would occur after or before the heating period are not simulated. These potential loads might impact strongly the lower part of the heating load duration curve.

The clustered and original load duration curve are globally well fitted. However, the peak demand is not achieved. This could be due to the solar data that are shown to provoke the choice of two typical days when the heating is not operating. To obtain a better fit of the typical days with the heating profile, one should give a specific weight to the heating data in matrix 3.3.

Figure 3.3 presents the yearly heating profile.

The absence of the peak in the typical days is here also in evidence.

One can notice that the heating needs fall abruptly at the end of the heating period whereas a more gradual evolution would be normally expected. The explanation could be that the outside temperatures are still quite low when the heating system is turned off. In this case, this would mean that the heating period is not well defined. This hypothesis is supported by observations as many EPFL offices are equipped with personal electric space heaters.

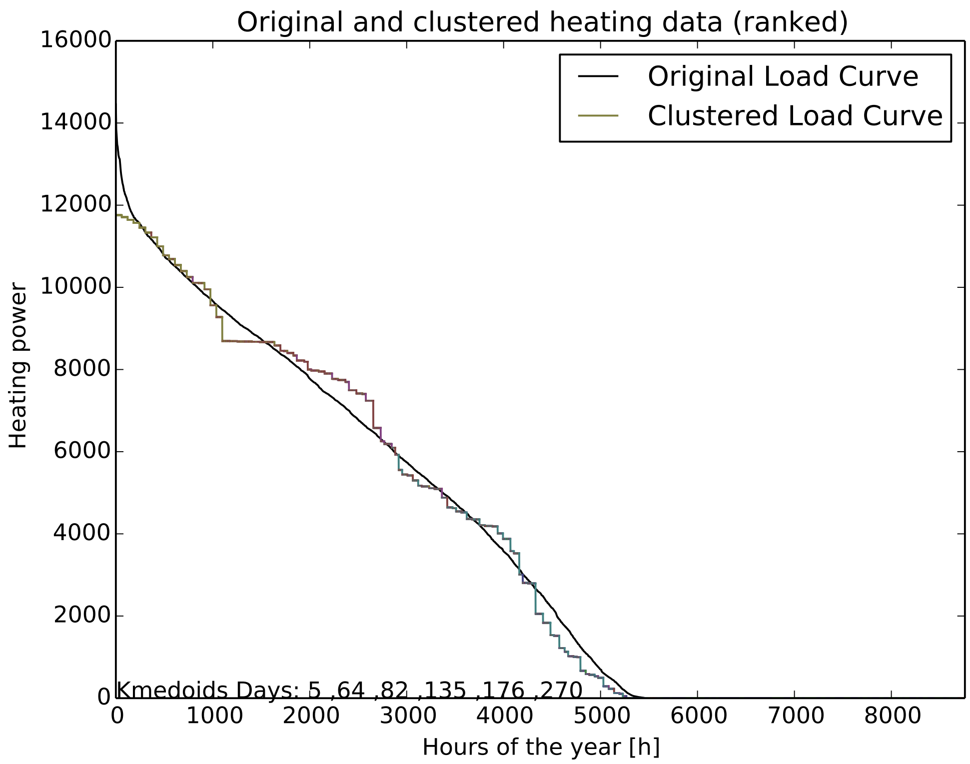

Figure 3.2: Original and clustered heating load duration curves - own illustration

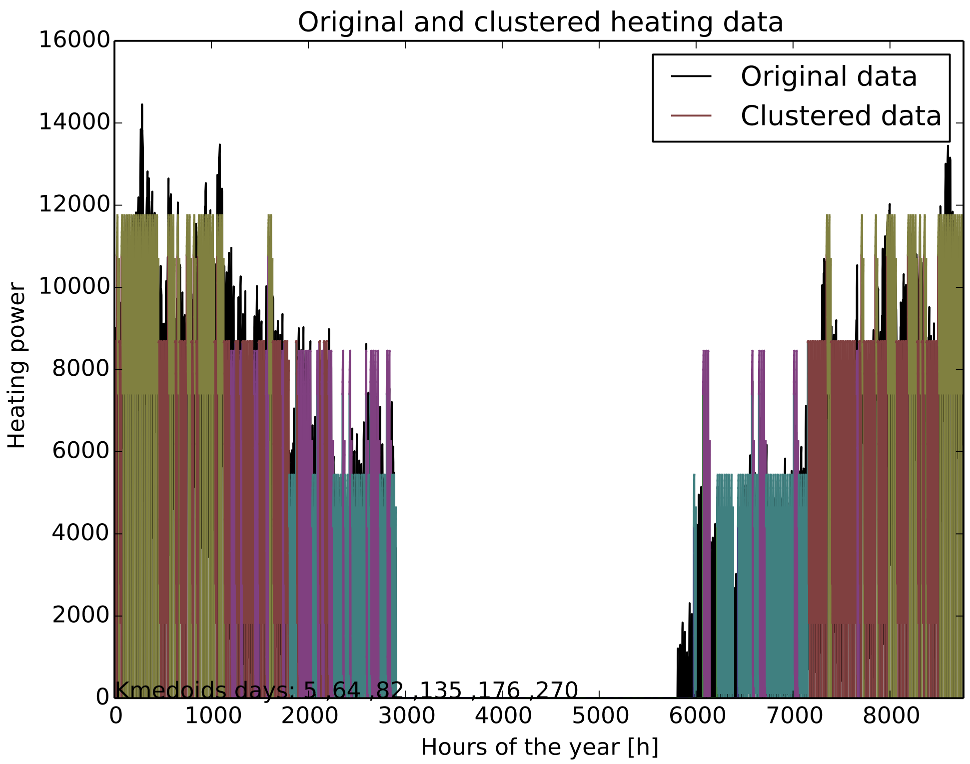

Figure 3.3: Original and clustered yearly heating profile - own illustration

3.4 Discussion

In this part, CitySim results are prepared. However, PEI simulations could not be performed due to the limited time available for this part of the project.

The results obtained with CitySim are assumed to represent the needs that an energy conversion system would need to fulfill to the Campus. However, these simulation results do not include the losses through the heating distribution system. The demand is therefore most probably underestimated in comparison to what a central heating system would need to provide in reality for the EPFL.

The heating needs are concatenated on every hour of the year. However, some building that were simulated with CitySim such as BCH, BSP, PA and PB are not included in the heating distribution system of the EPFL while several others such as ODY and several buildings of PSE are not modelled. Moreover, the campus is in reality divided into two distinct heating temperature levels. The first construction period of the campus is defined with an entering heating temperature of 65 $^\circ$C. The rest with 50 $^\circ$C. CitySim results should therefore be divided accordingly in PEI simulations.

The peak heating demand is not achieved. the equipments total capacity is therefore likely to be underestimated. However, the sizing of heat pumps is never done on the peak capacity because that would be far too expensive. At EPFL, the capacity for the peak load is ensured by two turbines and the base load by a heat pump. Moreover, to represent the data correctly, the peak heating could be added manually. The absence of the peak in the clustered results is therefore not disqualifying for their application to plan the energy conversion sizing.

Only three indicators are involved in the selection process of k. Consequently, possible optimal solutions might be removed.

The objective function of the linear optimization is the life cycle exergy. However, decisions are often taken on the total cost of equipments. These two functions are likely to lead to the different decisions.

3.5 Conclusion

In this work, CitySim and PEI are linked using the k-medoids clustering method.

This method consists in reducing the hourly heating predictions of CitySim for the whole year to a set of k typical days. This reduction is necessary because working with the whole set of yearly data would be too time intensive.

This methodology is applied on the results obtained in Part 2 for heating needs of EPFL buildings. These are coupled with the hourly heat production of solar thermal panels in the climate of Ecublens. This is done to include solar thermal as one of the possible heat sources in the design of the optimal energy conversion system of the EPFL campus. Solar data have to be clustered because they are, same as heating, time dependant.

The k-medoids method requires beforehand the definition of the total number of clusters. However, all values of k don't lead to a natural partitioning of the data. Therefore, the optimal value of k is determined with a benchmark. The clustering quality is estimated using several indicators such as the silhouette, the annual error or the number of times that the optimal solution was found. The chosen value of k according to these indicators is 6. The corresponding set of typical days includes two days without heating. This is due to the definition of the dissimilarity matrix that increases the importance of extremes such as 0. And the fact that solar that peaks outside of the heating period.

Then, the clustered data are compared with the original CitySim outputs using the yearly heating profile and the heating load duration curve for $k = 6$. The main observations are that the clustered and original data are in general well-fitted. However, the peak heating is not included in the results. This result is once more explain by the differences of evolution with the solar.

The heating load duration curve is shown to have a non-standard shape when compared to those in literature. Moreover, the yearly heating profile is shown to fall abruptly at the end of the heating period. Both of these observations are explained by the limitations imposed on the heating period. At EPFL, this restriction on the heating period results in the multiplication in offices of personal electric heaters that are energetically very inefficient. The heating period should therefore be extended in the model.

3.6 Future work

First, the clustered heating profile of the campus should be simulated with PEI to obtain initial results on the size of equipments and on the variations of the objective function according to the scenarios considered.

Other treatments could be applied on CitySim outputs.

For each building, a coefficient corresponding to the losses through EPFL heating distribution system could be applied on CitySim results. The value of this coefficient would be building specific and would vary depending on spacial parameters such as the distance to the energy conversion unit.

Then, buildings that are not attached to the heating system should be removed from calculations. Remaining buildings should be sorted in two categories representing the two different temperature levels of use on campus.

Some outputs of CitySim remain unconsidered.

The maximum possible area of solar thermal collectors should extracted from the characteristics of CitySim model. The solar irradiance on each surface of the model is calculated by CitySim. Solar thermal input could be directly calculated from these values instead of using an external method.

The usage of the clustering algorithm might be improved

Other parameters should be used in order to verify the clustering quality. For instance, the load duration curves for several values of k could be compared. Also, the results for the chosen k could be checked with a calendar inspection.

In (Domínguez-Muñoz *et al.*, 2011), the peak days are extracted before the algorithm starts and considered by default as typical days. This could be an interesting solution to ensure that the clustering optimal solution includes the peak heating load.

Currently, both heating and solar are standardized according to their respective peaks. A particular weight could be applied on these inputs in order to meet a particular objective. For instance, if implementing renewable is a priority, the solar profile could be set to vary between 0 and 2 while the heating varies between 0 and 1. That would make that a difference in solar irradiance more important than a difference in heating demand. The solar profile would in this case be better represented.

General conclusion

First, the large-scale building energy simulation tool, CitySim is certified reliable using the IEA BESTEST certification procedure. The main conclusions are that CitySim produces consistent hourly and annual values for buildings heating and cooling energy consumption. However, the model in CitySim is more reactive than in other programs. The BESTEST sequential procedure allows to identify that the cause of these small discrepancies are the simplified thermal model of the building envelope and the definition in CitySim of higher surfaces coefficients.

Afterwards, CitySim was used to simulate dynamically the heating consumption of EPFL buildings. This work demonstrates that it is possible to simulate acceptable annual heating loads despite the inherent complexity of this particular study object. The air renewal rate, solar gains and building geometry were shown to be major factors of influence on the heating demand. The savings obtained with a decrease of the set-point do not appear to significantly depend on buildings characteristics. Walls retrofit and windows replacement are shown to have similar impacts on the annual heating load but different effect on the peak demand. This difference is explained by windows high conductance and low thermal mass.

Finally, CitySim is linked to Python Energy Integration (PEI). This program determines the optimal sizing of the energy conversion system based the heating profiles generated by CitySim-like programs. The communication methodology consists is reducing the year to a set of k typical days using the k-medoids clustering method. It is applied to the hourly heating results obtained in Part 2. The analysis of the chosen typical days reveals that the peak heating is not taken into account and that the limitations on the heating period have a strong influence on the load duration curve.

To summarize, CitySim is shown to be a consistent tool for the The contribution of this work to the IDEAS4cities project in the creation process of energy hubs is

This work supports the choice of CitySim in the IDEAS4cities project for the simulation of heating demand and supply. It is shown to provide outputs that are similar to more complex programs.

results obtained in this part support the choice of CitySim as the main building energy simulation tool used in the IDEAS4cities project.

To summarize, CitySim is an efficient tool for the creations of energy hubs as its results are shown comparable to those of more complex programs. When applied to the case of the EPFL, CitySim heating predictions are shown to be close to the actual monitored heating values. Finally, CitySim's outputs are usable by other programs.

References

Carneiro, C. (2011). Extraction of Urban Environmental Quality Indicators using LiDAR-Based Digital Surface Models. **5050**.

Delsante, A. (2004). A VALIDATION OF THE ACCURATE SIMULATION ENGINE USING BESTEST. Tech. Rep. April, The Australian Greenhouse Office.

DII EPFL (2008). Bilan des énergies du site de l'EPFL à Ecublens 2007. Tech. Rep. Septembre, EPFL, Ecublens, Switzerland.

Domínguez-Muñoz, F., Cejudo-López, J.M., Carrillo-Andrés, A. & Gallardo-Salazar, M. (2011). Selection of typical demand days for CHP optimization. *Energy and Buildings*, **43**, 3036–3043.

Gan, G., Ma, C. & Wu, J. (2007). *Data Clustering: Theory, Algorithms, and Applications*. SIAM: Society for Industrial and Applied Mathematics, Philadelphia, 1st edn.

Gordon, A. (1999). *Classification 2nd Edition*. Chapman & Hall/CRC.

Helms, T. (2009). Energy System Analysis of a University Campus.

IEA (2008). World Energy Outlook 2008. Tech. rep., International Energy Agency, Paris, France.

Judkoff, R. & Neymark, J. (1995a). Home Energy Rating System Building Energy Simulation Test (HERS BESTEST) Volume 1 Tier 1 and Tier 2 Tests User s Manual. NREL/TP-472-7332a. Tech. rep., National Renewable Energy Laboratory, Golden, Colorado.

Judkoff, R. & Neymark, J. (1995b). Home Energy Rating System Building Energy Simulation Test (HERS BESTEST) Volume 2 Tier 1 and Tier 2 Tests Reference Results. NREL/TP-472-7332b. Tech. rep., National Renewable Energy Laboratory, Golden, Colorado.

Judkoff, R. & Neymark, J. (1995c). International Energy Agency building energy simulation test (BESTEST) and diagnostic method. NREL/TP-472-6231. Tech. rep., National Renewable Energy Laboratory, Golden, Colorado.

Judkoff, R. & Neymark, J. (1997a). Home Energy Rating System Building Energy Simulation Test for Florida (Florida-HERS BESTEST) Volume 2 Tier 1 and Tier 2 Tests Reference Results. NREL/TP-550-23124b. Tech. Rep. August, National Renewable Energy Laboratory, Golden, Colorado.

Judkoff, R. & Neymark, J. (1997b). Home Energy Rating System Building Energy Simulation Test for Florida (Florida-HERS BESTEST): Volume 1 Tier 1 and Tier 2 Tests User's Manual. NREL/TP-550-23124a. Tech. rep., National Renewable Energy Laboratory, Golden, Colorado.

Judkoff, R. & Neymark, J. (1998). The BESTEST Method for Evaluating and Diagnosing Building Energy Sloftware. 175–192.

Judkoff, R. & Neymark, J. (2002). International Energy Agency Building Energy Simulation Test and Diagnostic Method for Heating, Ventilating, and Air Conditioning Equipment Models (HVAC BESTEST) Volume 1: Cases E100-E200. NREL/TP-550-30152. Tech. Rep. January, National Renewable Energy Laboratory, Golden, Colorado.

Judkoff, R. & Neymark, J. (2004). International Energy Agency Building Energy Simulation Test and Diagnostic Method for Heating, Ventilating, and Air-Conditioning Equipment Models (HVAC BESTEST): Volume 2: Cases E300-E545. NREL/TP-550-36754. Tech. Rep. December, National Renewable Energy Laboratory, Golden, Colorado.

Judkoff, R. & Neymark, J. (2013). Twenty Years on !: Updating the Iea Bestest Building Thermal Fabric Test Cases for Ashrae Standard 140. In *13th Conference* *of International Building Performance Simulation Association*, 63–70, Chambéry, France.

Judkoff, R. & Wijsman, A. (2009). IEA BESTEST In-Depth Diagnostic Cases for Ground Coupled Heat Transfer Related to Slab-on-Grade Construction.

Judkoff, R., Wortman, D., Doherty, B. & Burch, J. (2008). A Methodology for Validating Building Energy Analysis Simulations.

Judkoff, R., Polly, B., Bianchi, M. & Neymark, J. (2010a). Building Energy Simulation Test for Existing Homes (BESTEST-EX) Phase 1 Test Procedure: Building Thermal Fabric Cases. NREL/TP-550-47427. Tech. Rep. August, National Renewable Energy Laboratory, Golden, Colorado.

Judkoff, R., Polly, B., Bianchi, M. & Neymark, J. (2010b). Example Procedures for Developing Acceptance-Range Criteria for BESTEST-EX. NREL/TP-550-47502. Tech. Rep. August, National Renewable Energy Laboratory, Golden, Colorado.

Kämpf, J. (2009). *On the Modelling and Optimisation of Urban Energy Fluxes*. Ph.D. thesis, EPFL.

Lim, D., Heo, S. & No, J. (2009). An overview of peak-to-average power ratio reduction schemes for OFDM signals. *Journal of Communications and Networks*, **11**, 229–239.

Lorenz, F. & Masy, G. (1982). Méthode d'évaluation de l'économie d'énergie apportée par l'intermittence de chauffage dans les bâtiments. Traitement par différences finies d'un modèle à deux constantes de temps. Tech. rep., Laboratoire de Physique du Bâtiment, Université de Liège, Liège, Belgium.

Morel, N. (2004). Description of the LESO Building.

Nikam, V., Kadam, V. & Meshram, B. (2011). Image Compression Using Partitioning Around Medoids Clustering Algorithm. **8**, 399–401.

Pfeiffer, B. (2014). Identification of optimal Heat Supply Concepts for the Ski Resort of Verbier by Means of MILP and Heat Integration.

REFERENCES

Rager, J., Dorsaz, C. & Maréchal, F. (2013). ECOS : Integrated energy planning for new districts. In *International Conference on Efficiency, Cost, Optimization, Simulation and Environmental Impact of Energy*, Guilin, China.

Reynolds, A., Richards, G. & Rayward-Smith, V. (2004). The Application of K-medoids and PAM to the Clustering of Rules. *Springer*, pp. 173–178.

Rousseeuw, P.J. (1987). Silhouettes: A graphical aid to the interpretation and validation of cluster analysis. *Journal of Computational and Applied Mathematics*, **20**, 53–65.

SIA (2006). SIA 2024 - Condition d'utilisation standard pour l'énergie et les installations du bâtimment.pdf. Tech. rep.

Singh, S. (2011). K-means v / s K-medoids : A Comparative Study.

Strachan, P., Kokogiannakis, G. & Macdonald, I. (2008). History and development of validation with the ESP-r simulation program. *Building and Environment*, **43**, 601–609.

UN (2011). World Urbanization Prospects The 2011 Revision. Tech. rep., United Nations, Department of Economic and Social Affairs, Population Division, New York, United States.

Walter, E. (2013). Simulation of the EPFL Heating Demand. Tech. rep., LESO-PB, EPFL, Lausanne, Switzerland.

Wulich, D., Goldfeld, L. & Tsouri, G. (2008). Peak to Average Power Ratio in Digital Communications. Tech. Rep. 2, Ben-Gurion University of the Negev, Beer-Sheva, ISRAEL.

Appendix A

Appendix on part 1

A.1 Definition the envelope typology in the BESTEST

Table A.1: Lightweight walls definition

Element	Thickness (m)	λ ($\frac{W}{m \cdot K}$)	ρ ($\frac{kg}{m^3}$)	Cp ($\frac{J}{kg \cdot K}$)
Wall				
Wood Sidings	0.009	0.14	530	900
Fibreglass quilt	0.066	0.04	250	840
Plaster Board	0.012	0.16	0.95	840
Roof				
Roofdeck	0.019	0.14	530	900
Fibreglass quilt	0.1118	0.04	250	840
Plaster Board	0.01	0.16	950	840
Floor				
Insulation	1.003	0.04	1	1
Timber flooring	0.025	0.14	650	1200

Table A.2: Heavyweight walls definition

Element	Thickness (m)	λ ($\frac{W}{m \cdot K}$)	ρ ($\frac{kg}{m^3}$)	Cp ($\frac{J}{kg \cdot K}$)
		Wall		
Wood Sidings	0.009	0.14	530	900
Foam insulation	0.0615	0.04	40	1400
Concrete Block	0.1	0.51	1400	1000
		Roof		
Roofdeck	0.019	0.14	530	900
Fibreglass quilt	0.1118	0.04	250	840
Plaster Board	0.01	0.16	950	840
		Floor		
Insulation	1.007	0.04	1	1 ¡2¿
Concrete slab	0.08	1.13	1400	1000

A.2 Definition of the shadings

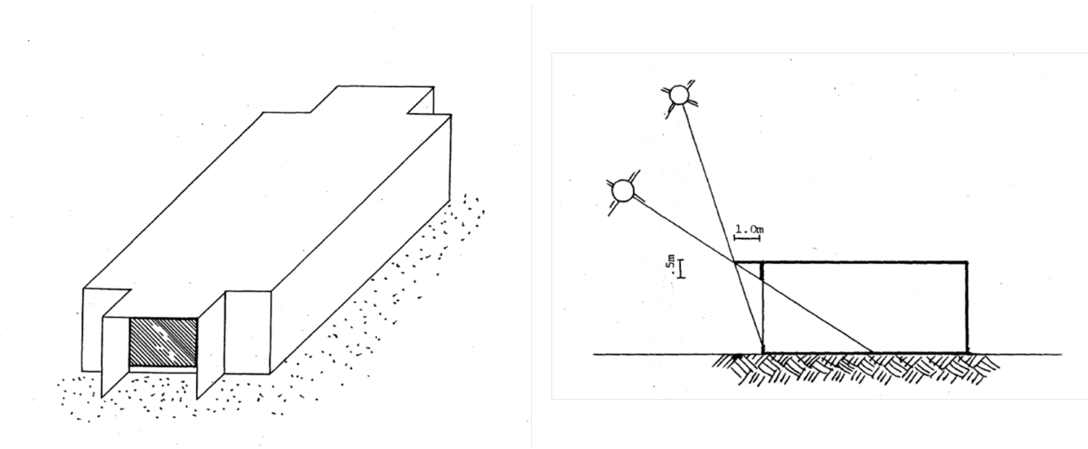

Figure A.1: Positioning of the shadings is cases 1.0MHV (left) and 1.0MH (right) - extracted from Judkoff & Neymark (1995c)

A.3 Illustration of Citysim thermal model

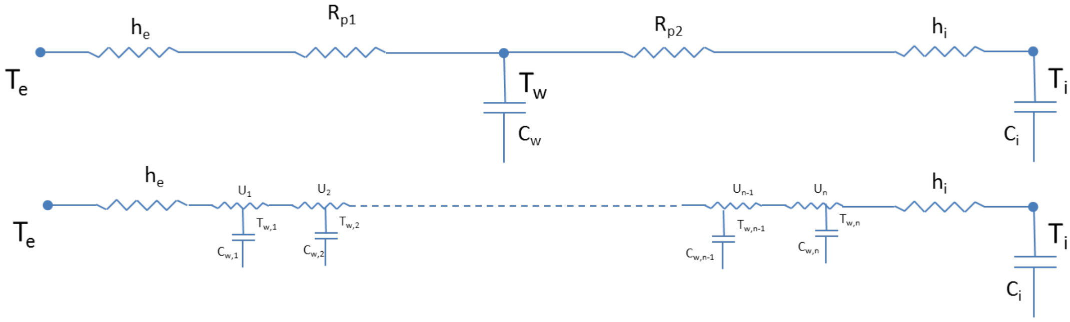

Figure A.2: Schema of Citysim (top) and ideal thermal model - own illustration

A. APPENDIX ON PART 1

Appendix B

Appendix on part 2

B.1 Simulation data

Table B.1 summarizes the input data of the EPFL model. In order to avoid repetitions, neighboring buildings in this tabular are clustered when they share the same definition for a particular parameter.

Table B.1: Data input - own table

Zone	Building	# Sub-building [-]	Treated surface (m2)	Volume (m3)	GR [-]	U-value (W/m2.K)	gvalue [-]	ACH [h-1]	Envelope
C	CM	17	15'358	55'956	0.36	1.3	0.5	0.3	1st
	GC	16	26'212	103'357					
	GR	10	8'618	33'610					
	LE	3	1'673	7'260					
	MA	17	11'771	45'905					
	ME	11	9'201	36'731					
E	BI	5	3'784	14'758					
	BS	8	7'232	27'446					
	CE	19	20'352	74'895					
	CH	21	25'191	97'848				0.74	
	PH	21	17'508	67'673				0.762	
	PO	1	1'035	5'237				0.3	
	STT	1	658	2'568	0.00				
N	AAB	1	3'145	34'979	0.70				2nd
	AAC	1	2'761	95'155					
	AAD	1	2'377	37'901					
	AI	5	10'090	12'461	0.40			1.114	
	BM	1	22'352	10'941	0.47			0.96	
	BP	2	8'931	9'400	0.38			0.3	
	SG	2	9'588	39'555	0.30				
	SV	2	15'057	62'090	0.30			1.18	
S	LC	1	16'017	6'852	0.70	0.7	0.61	0.3	
	PA	1	1'975	1'134	0.25	1.3	0.5		
	PB	1	445	79'633	0.25				
UNIL	BCH	5	20'774	80'045	0.70				
	BSP	3	7'774	31'562					
W	BC	2	12'799	48'428	0.70				
	CO	7	12'677	49'492	0.40				
	ELA	2	2'707	10'827					
	ELB	2	3'593	14'014					
	ELD	7	4'880	19'034					
	ELE	3	3'020	11'779					
	ELG	3	2'905	11'329					
	ELH	1	2'196	8'564					
	ELL	1	965	3'764					
	INF+J	7	12'829	36'298					
	INM	6	6'166	23'664					
	INN	2	3'674	14'090					
	INR	2	3'674	14'090					
	MXC	5	4'402	17'206					
	MXD	4	3'952	15'442					
	MXE	3	2'853	11'425					
	MXF	3	1'966	7'711					
	MXG	3	3'882	15'228					
	MXH	6	3'804	15'253					
	PPB	1	2'502	6'075					
	PPH	2	7'498	8'639					
	PSEA	1	1'424	13'073					
	PSEB	1	2'160	28'013					
	PSEC	1	2'998	22'313					
	TCV	2	5'885	10'010					

B.2 Treated floor area - comparison between the model and DII publications

This comparison is done in order to validate the values of $S_{treated}$ that are used in part 2.3.6 to compute the IHG and in part 2.4.3 to compute buildings specific consumption.

The real values for $S_{treated}$ are the one used by the DII to compute the specific consumption of buildings in DII EPFL (2008). It is not available for all buildings therefore, the comparison is only partial but gives an idea of the methodology validity.

Using Figures B.1 and B.2, the building absolute and specific consumption is obtained for 2007. Then, the treated floor are is simply obtained using Eq. B.1.

$$S_{treated} = \frac{Absolute\, kWh}{Specific\, \frac{kWh}{m^2}} \tag{B.1}$$

Results are then compared with the reference results. This comparison can be illustrated on Table B.2. Simulated values that differ of more than 20% are highlighted in blue if inferior and red if superior.

As expected, the assumptions presented in part 2.3.2 to calculate $S_{treated}$ lead to significant disagreement with the values computed using data from the EPFL DII. However, this difference is below 20% is most cases. Moreover, it is not possible to extract $S_{treated}$ for all EPFL buildings. Consequently, the used $S_{treated}$ are the one of the model.

Table B.2: Comparison results for real and modelized treated surface - own table

Zone	Building	DII (m2)	Model (m2)	Difference (%)
C	CM	18'048	15'358	-18%
	GC	25'688	26'212	2%
	GR	9'825	8'618	-14%
	LE	1'513	1'673	10%
	MA	13'578	11'771	-15%
	ME abc	9'659	9'201	-5%
E	BI	4'412	3'784	-17%
	BS	9'947	7'232	-38%
	CE	16'226	20'352	20%
	CH+STT	28'169	25'849	-9%
	PH	23'007	17'508	-31%
	PO	737	2'070	64%
N	AI	17'253	10'090	-71%
	BM	19'137	25'545	25%
	BP	10'068	8'931	-13%
	SG+AA	17'807	18'654	5%
W	BC	17'005	12'799	-33%
	CO	11'382	14'361	21%
	ELA	2'779	3'025	8%
	ELB	3'945	3'593	-10%
	ELD	5'227	4'880	-7%
	ELE	3'277	3'020	-9%
	ELG	3'229	2'905	-11%
	ELH	1'736	2'196	21%
	ELL	1'324	965	-37%
	INF+J	9'257	9'944	7%
	INM+N	11'014	9'840	-12%
	INR	4'043	3'674	-10%
	MXC	5'465	4'402	-24%
	MXD	5'005	3'952	-27%
	MXE	3'665	3'046	-20%
	MXF+G	6'801	5'848	-16%
	MXH	4'508	4'286	-5%
	PPB	3'008	2'502	-20%
	PPH	7'514	7'498	0%
	TCV	5'919	6'216	5%

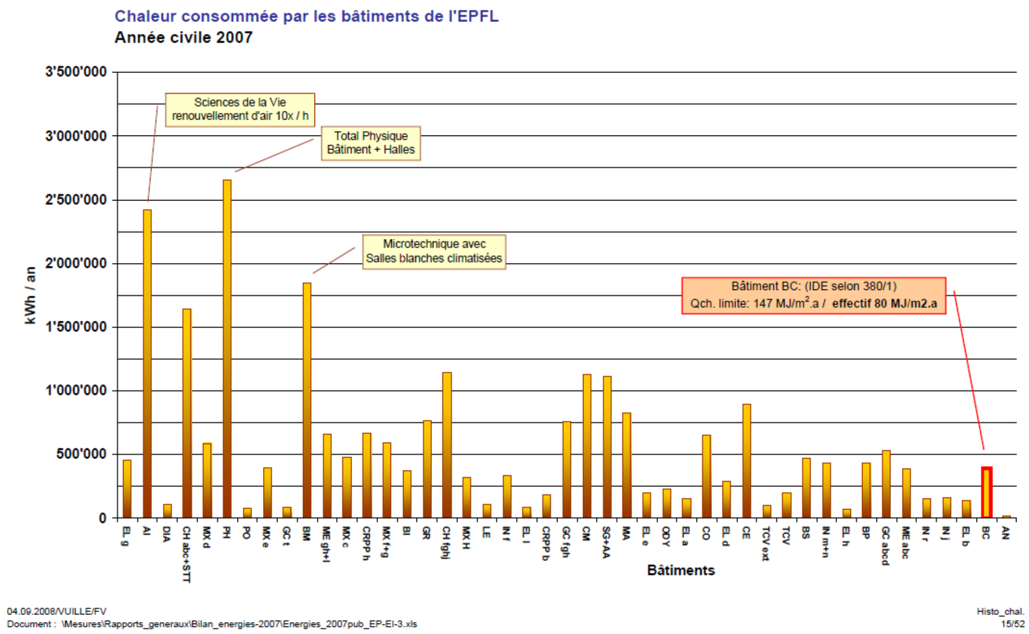

Figure B.1: Absolute consumption of EPFL buildings (2007) $\frac{kWh}{an}$ - Source DII EPFL (2008)

B.3 Glazing ratio determination

The GR of EPFL buildings are obtained from the analysis of the plans provided by the DII. The method consists in simply measuring the area occupied by windows and comparing to the total surface area of the façade.

B.4 Print-screen of source wall types

The walltypes defined in the model were extracted from the plan database of the DII. The following pictures summarizes the documentation found for the different construction period. The definition of the floors for the second period couldn't be found. Therefore, their composition was assumed to be similar the one defined in Morel (2004) p.4.

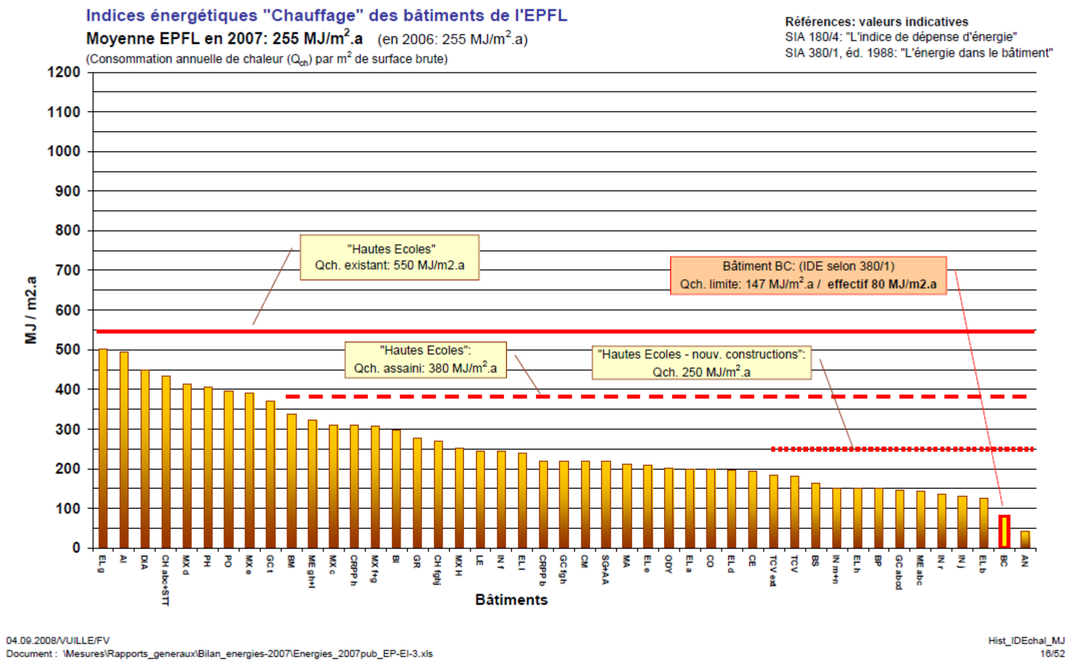

Figure B.2: Specific consumption of EPFL buildings (2007) $\frac{kWh}{m^2.an}$ - Source DII EPFL (2008)

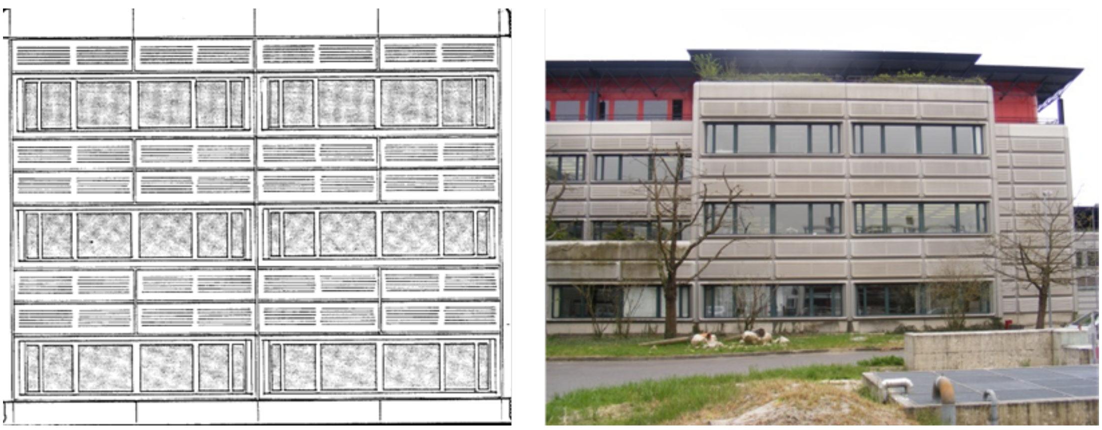

Figure B.3: Plan (left) and picture (right) of the environmental sciences building north façade, assumed to be the representative of the 1^{st} period of construction, GR=36% - Source: DII plan database, own picture

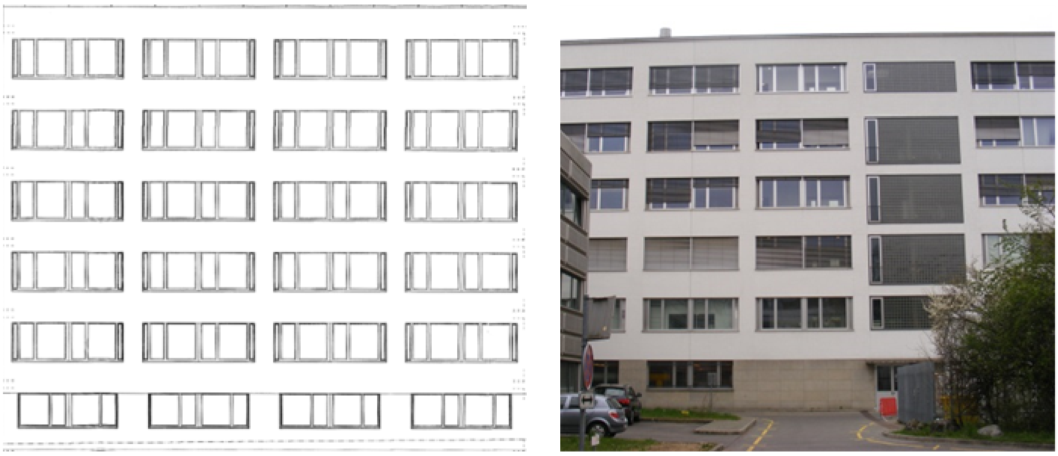

Figure B.4: Plan (left) and picture (right) of the microtechnology building, GR = 47% - Source: DII plan database, own picture

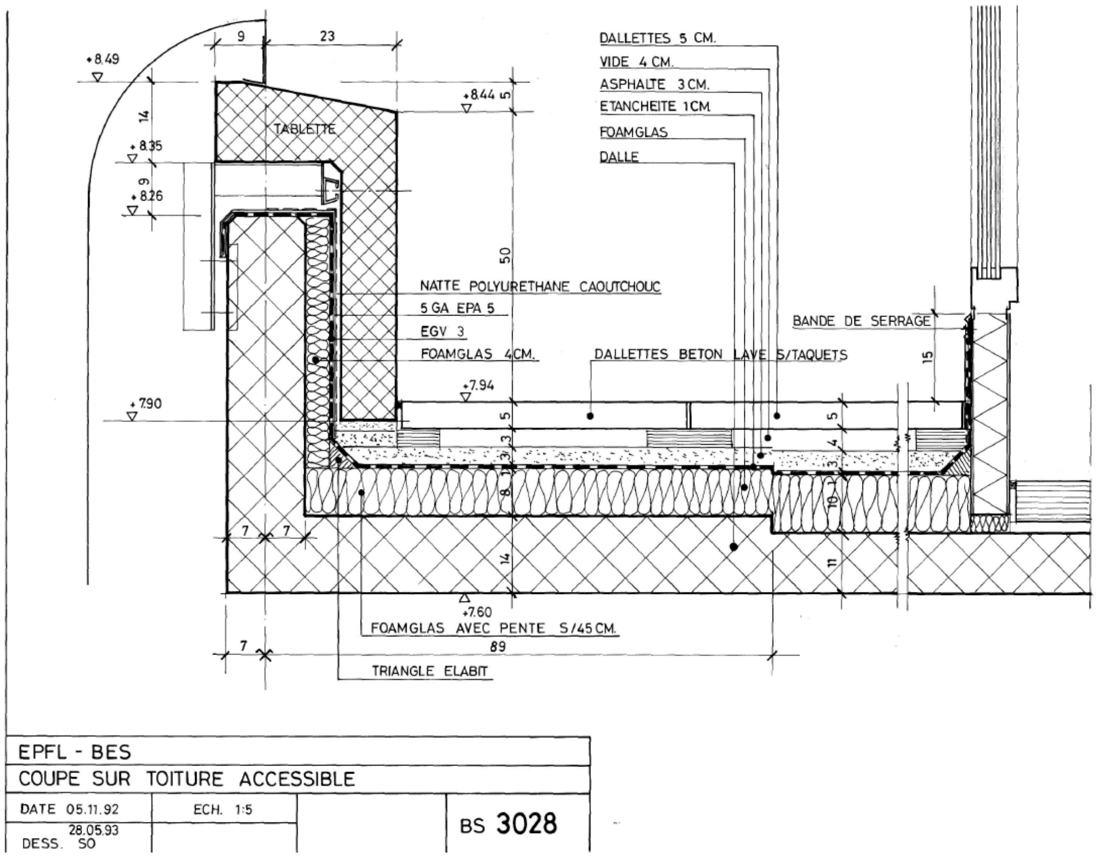

Figure B.5: Roof typology for the first period of construction - Source: DII plan database

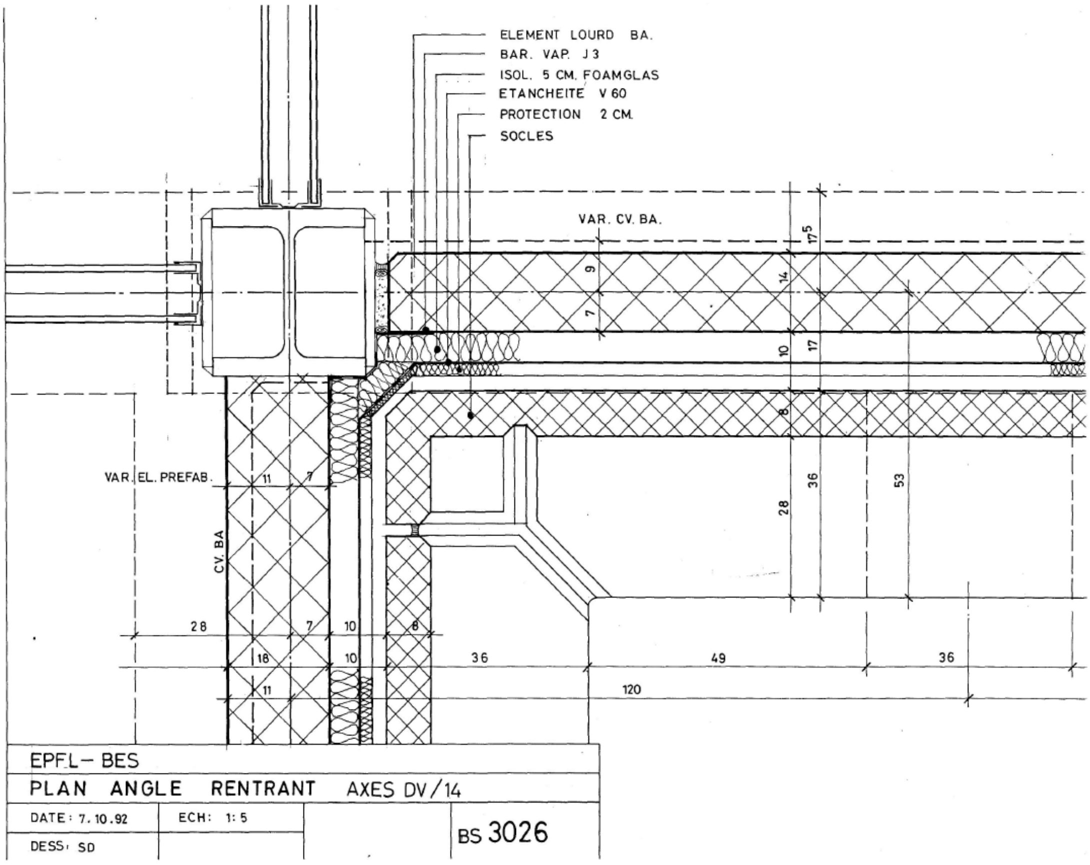

Figure B.6: Wall typology for the first period of construction - Source: DII plan database

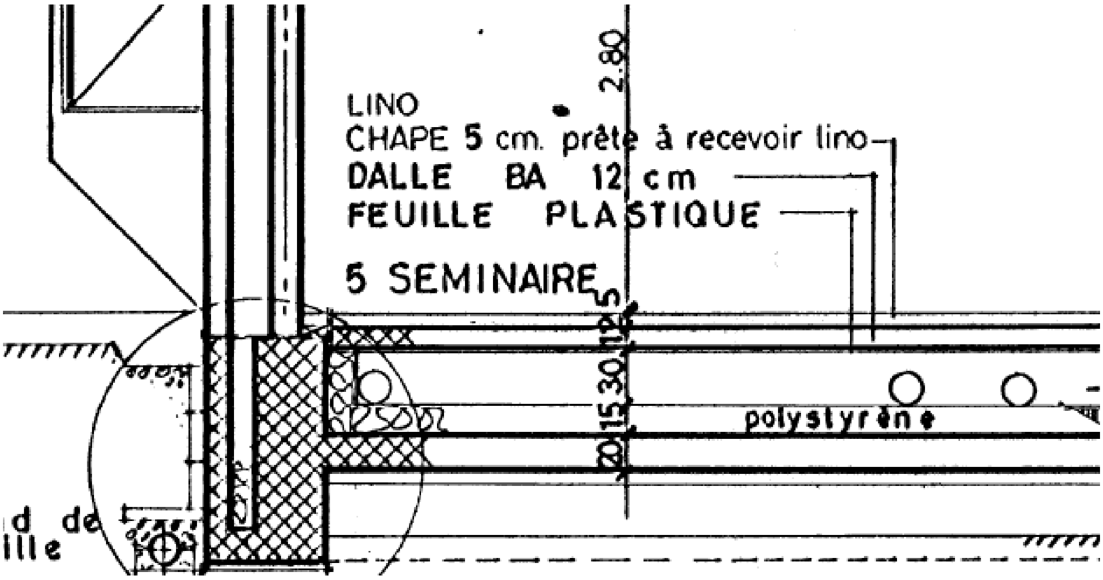

Figure B.7: Floor typology for the first period of construction - Source: DII plan database

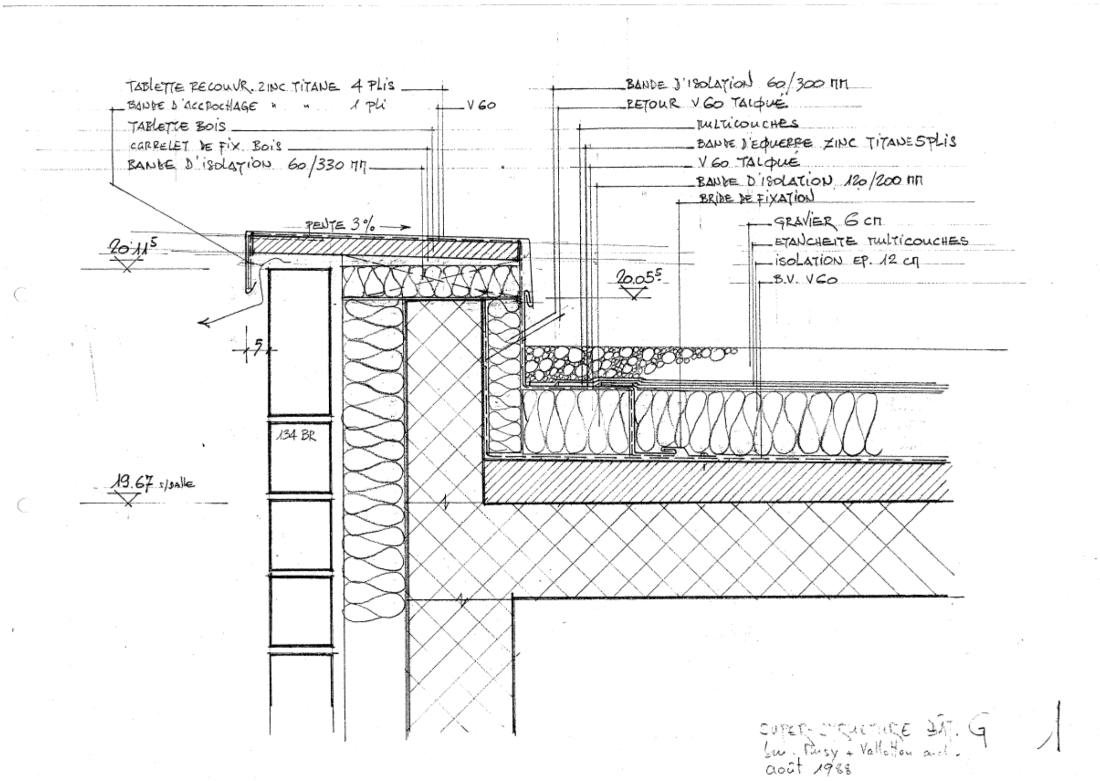

Figure B.8: Roof typology for the first period of construction - Source: DII plan database

Table B.3: Envelope definition for the 1^{st} construction period - Aluminium facades

Material	Thickness (m)	λ ($\frac{W}{m.K}$)	ρ ($\frac{kg}{m^3}$)	Cp ($\frac{J}{kg.K}$)
Wall				
Aluminium	0.002	200	2700	900
Air	0.28	999	1.23	1000.8
Concrete	0.08	2.1	2400	849.6
Rockwool	0.1	0.04	100	601.2
Concrete	0.18	2.1	2400	849.6
Roof				
Concrete	0.05	2.1	2400	849.6
Air	0.04	999	1.23	1000.8
Asphalt	0.03	0.7	2150	1101.6
Foamglass	0.1	0.04	100	601.2
Concrete	0.11	2.1	2400	849.6
Floor				
Concrete	0.2	2.1	2400	849.6
Rockwool	0.15	0.04	100	601.2
Air	0.3	999	1.23	1000.8
Concrete	0.25	2.1	2400	849.6
Irradiance Coefficients				
(ϵ_{SW})	0.9			
(ϵ_{IR})	0.2			

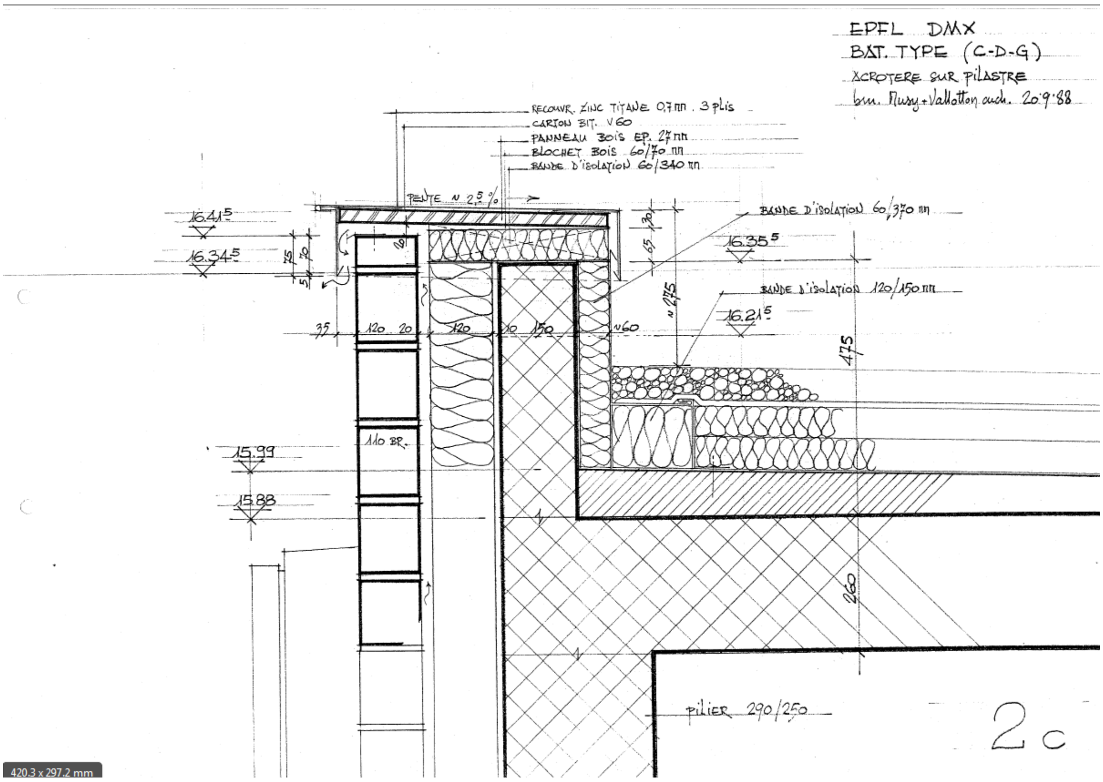

Figure B.9: Wall typology for the first period of construction - Source: DII plan database

Table B.4: Envelope definition for the 2^{nd} construction period - Clay facades

Material	Thickness (m)	λ ($\frac{W}{m.K}$)	ρ ($\frac{kg}{m^3}$)	Cp ($\frac{J}{kg.K}$)
Wall				
Clay brick	0.06	0.35	900	900
Rockwool	0.12	0.04	100	601.2
Concrete	0.25	2.1	2400	849.6
Roof				
Roof gravel	0.06	0.7	1900	799.2
Rockwool	0.12	0.04	100	601.2
Concrete	0.35	2.1	2400	849.6
Floor				
Rubber	0.01	0.17	1200	1200
Mortar	0.06	1	1700	1000
Rockwool	0.06	0.04	100	601.2
Concrete	0.25	2.1	2400	849.6
(ϵ_{SW})	0.2			
(ϵ_{IR})	0.93			

Table B.5: New definition of the wall after the renovation of the first construction period

Material	Thickness (m)	λ ($\frac{W}{m.K}$)	ρ ($\frac{kg}{m^3}$)	Cp ($\frac{J}{kg.K}$)
Wall				
Rendering	0.02	0.87	1800	1101.6
Insulation	0.05-0.15	0.04	100	601.2
Concrete	0.08	2.1	2400	849.6
Rockwool	0.1	0.04	100	601.2
Concrete	0.18	2.1	2400	849.6
(ϵ_{SW})	0.35			
(ϵ_{IR})	0.85			

B.5 Results for the energy saving scenarios

B. APPENDIX ON PART 2

Table B.6: Summary of the results of the energy saving scenarios - own table

	Simulation results	BaseCase		Empty				Insulation (5cm)				Insulation (10cm)				Insulation (15cm)				SetPoint (-1°C)				Double Glazing				Triple Glazing			
	Building	Annual (MWh)	Peak (kW)	Annual (MWh)		Peak (kW)		Annual (MWh)		Peak (kW)		Annual (MWh)		Peak (kW)		Annual (MWh)		Peak (kW)		Annual (MWh)		Peak (kW)		Annual (MWh)		Peak (kW)		Annual (MWh)		Peak (kW)	
C	CM	1083	432	1217	11%	432	0%	1012	-7%	432	0%	994	-9%	427	-1%	982	-10%	424	-2%	1013	-7%	419	-3%	1038	-4%	418	-3%	956	-13%	385	-12%
	GC	1755	725	2015	13%	725	0%	1652	-6%	726	0%	1621	-8%	718	-1%	1602	-10%	713	-2%	1636	-7%	702	-3%	1682	-4%	702	-3%	1545	-14%	647	-12%
	GR	615	253	701	12%	253	0%	572	-8%	251	-1%	558	-10%	247	-2%	550	-12%	245	-3%	573	-7%	245	-3%	582	-6%	243	-4%	522	-18%	219	-16%
	LE	163	66	182	10%	66	0%	153	-7%	66	0%	149	-10%	65	-1%	147	-11%	65	-2%	152	-7%	64	-3%	154	-6%	64	-4%	138	-19%	57	-17%
	MA	848	345	966	12%	345	0%	790	-7%	344	0%	776	-9%	340	-2%	767	-11%	337	-2%	792	-7%	334	-3%	809	-5%	333	-4%	738	-15%	304	-13%
	ME	699	285	793	12%	285	0%	641	-9%	281	-2%	622	-12%	276	-3%	611	-14%	273	-5%	651	-7%	276	-3%	660	-6%	273	-4%	587	-19%	244	-17%
E	BI	300	121	338	11%	121	0%	291	-3%	125	3%	291	-3%	125	3%	291	-3%	125	3%	280	-7%	118	-3%	286	-5%	117	-4%	259	-16%	106	-14%
	BS	537	219	606	11%	219	0%	523	-3%	225	3%	523	-3%	225	3%	523	-3%	225	3%	500	-7%	212	-3%	511	-5%	211	-4%	464	-16%	192	-14%
	CE	1325	539	1514	12%	539	0%	1282	-3%	550	2%	1282	-3%	550	2%	1282	-3%	550	2%	1238	-7%	522	-3%	1276	-4%	524	-3%	1187	-12%	487	-11%
	CH	2913	1141	3187	9%	1141	0%	2844	-2%	1153	1%	2844	-2%	1153	1%	2844	-2%	1153	1%	2713	-7%	1105	-3%	2834	-3%	1118	-2%	2691	-8%	1061	-8%
	PH	2147	843	2351	9%	844	0%	2100	-2%	853	1%	2100	-2%	853	1%	2100	-2%	853	1%	2000	-7%	817	-3%	2078	-3%	823	-2%	1954	-10%	774	-9%
	PO	142	56	155	9%	56	0%	138	-3%	59	4%	138	-3%	59	4%	138	-3%	59	4%	132	-7%	55	-3%	135	-5%	54	-3%	124	-14%	50	-13%
	STT	52	19	60	13%	19	0%	49	-6%	19	2%	49	-6%	19	2%	49	-6%	19	2%	49	-7%	19	-3%	52	0%	19	0%	52	0%	19	0%
N	AAB	322	141	351	8%	141	0%	322	0%	141	0%	322	0%	141	0%	322	0%	141	0%	299	-8%	137	-3%	287	-12%	130	-9%	221	-45%	103	-37%
	AAC	283	124	308	8%	124	0%	283	0%	124	0%	283	0%	124	0%	283	0%	124	0%	263	-8%	120	-3%	252	-12%	114	-9%	194	-46%	91	-37%
	AAD	232	103	254	9%	103	0%	232	0%	103	0%	232	0%	103	0%	232	0%	103	0%	216	-8%	99	-3%	208	-11%	95	-8%	165	-41%	77	-33%
	AI	1651	648	1758	6%	648	0%	1650	0%	647	0%	1650	0%	647	0%	1650	0%	647	0%	1535	-8%	627	-3%	1598	-3%	631	-3%	1503	-10%	594	-9%
	BM	3228	1296	3493	8%	1296	0%	3207	-1%	1293	0%	3207	-1%	1293	0%	3207	-1%	1293	0%	2998	-8%	1254	-3%	3114	-4%	1262	-3%	2912	-11%	1182	-10%
	BP	654	275	740	12%	275	0%	653	0%	275	0%	653	0%	275	0%	653	0%	275	0%	611	-7%	267	-3%	624	-5%	265	-4%	566	-16%	242	-14%
	SG	606	261	712	15%	261	0%	606	0%	261	0%	606	0%	261	0%	606	0%	261	0%	568	-7%	253	-3%	590	-3%	256	-2%	560	-8%	243	-7%
	SV	2523	978	2563	2%	929	-5%	2523	0%	978	0%	2523	0%	978	0%	2523	0%	978	0%	2349	-7%	947	-3%	2484	-2%	966	-1%	2417	-4%	940	-4%
S	LC	2002	821	2190	9%	821	0%	2001	0%	821	0%	2001	0%	821	0%	2001	0%	821	0%	1884	-6%	798	-3%	2002	0%	821	0%	2002	0%	821	0%
	PA01	248	94	266	7%	94	0%	247	0%	93	0%	247	0%	93	0%	247	0%	93	0%	234	-6%	91	-3%	243	-2%	92	-2%	233	-6%	88	-6%
	PB01	55	20	58	5%	20	0%	55	0%	20	0%	55	0%	20	0%	55	0%	20	0%	52	-6%	20	-3%	54	-2%	20	-2%	52	-7%	19	-7%
UNIL	BCH	1029	443	1131	9%	443	0%	1029	0%	443	0%	1029	0%	443	0%	1029	0%	443	0%	962	-7%	430	-3%	956	-8%	420	-6%	823	-25%	365	-21%
	BSP	1245	556	1400	11%	556	0%	1244	0%	556	0%	1244	0%	556	0%	1244	0%	556	0%	1158	-8%	539	-3%	1143	-9%	523	-6%	956	-30%	445	-25%
W	BC	809	364	932	13%	364	0%	809	0%	364	0%	809	0%	364	0%	809	0%	364	0%	753	-7%	352	-3%	752	-8%	344	-6%	646	-25%	300	-21%
	CO	897	381	1023	12%	381	0%	896	0%	380	0%	896	0%	380	0%	896	0%	380	0%	838	-7%	369	-3%	859	-4%	368	-3%	789	-14%	340	-12%
	ELA	220	93	249	12%	93	0%	220	0%	93	0%	220	0%	93	0%	220	0%	93	0%	205	-7%	90	-3%	209	-5%	90	-4%	188	-17%	81	-15%
	ELB	271	116	305	11%	116	0%	271	0%	116	0%	271	0%	116	0%	271	0%	116	0%	252	-7%	112	-3%	255	-6%	111	-5%	226	-20%	99	-17%
	ELD	395	166	441	10%	166	0%	395	0%	166	0%	395	0%	166	0%	395	0%	166	0%	369	-7%	161	-3%	374	-6%	159	-4%	335	-18%	143	-16%
	ELE	269	111	298	10%	111	0%	269	0%	111	0%	269	0%	111	0%	269	0%	111	0%	252	-7%	108	-3%	257	-5%	107	-4%	235	-15%	98	-13%
	ELG	314	133	355	12%	133	0%	314	0%	133	0%	314	0%	133	0%	314	0%	133	0%	293	-7%	129	-3%	299	-5%	128	-4%	272	-16%	117	-14%
	ELH	194	80	215	10%	80	0%	194	0%	80	0%	194	0%	80	0%	194	0%	80	0%	182	-7%	78	-3%	187	-4%	78	-3%	174	-12%	73	-10%
	ELL	99	41	108	9%	41	0%	99	0%	41	0%	99	0%	41	0%	99	0%	41	0%	92	-7%	40	-3%	93	-6%	39	-5%	83	-19%	35	-17%
	INF+J	693	291	781	11%	291	0%	693	0%	291	0%	693	0%	291	0%	693	0%	291	0%	647	-7%	282	-3%	662	-5%	282	-3%	606	-14%	259	-13%
	INM	507	204	545	7%	204	0%	507	0%	204	0%	507	0%	204	0%	507	0%	204	0%	474	-7%	198	-3%	481	-5%	196	-4%	433	-17%	177	-15%
	INN	265	113	300	11%	113	0%	265	0%	113	0%	265	0%	113	0%	265	0%	113	0%	247	-7%	110	-3%	250	-6%	108	-5%	221	-20%	97	-17%
	INR	264	113	298	11%	113	0%	264	0%	113	0%	264	0%	113	0%	264	0%	113	0%	246	-7%	109	-3%	249	-6%	108	-5%	220	-20%	97	-17%
	MXC	337	144	378	11%	144	0%	337	0%	144	0%	337	0%	144	0%	337	0%	144	0%	313	-8%	140	-3%	312	-8%	136	-6%	266	-26%	118	-22%
	MXD	210	89	234	10%	89	0%	210	0%	89	0%	210	0%	89	0%	210	0%	89	0%	195	-8%	86	-3%	194	-8%	84	-6%	164	-28%	72	-24%
	MXE	269	111	297	9%	111	0%	269	0%	111	0%	269	0%	111	0%	269	0%	111	0%	252	-7%	107	-3%	256	-5%	107	-4%	232	-16%	97	-14%
	MXF	156	67	175	11%	67	0%	156	0%	67	0%	156	0%	67	0%	156	0%	67	0%	145	-8%	65	-3%	144	-9%	63	-6%	121	-29%	54	-25%
	MXG	288	124	324	11%	124	0%	288	0%	124	0%	288	0%	124	0%	288	0%	124	0%	267	-8%	120	-3%	267	-8%	118	-6%	230	-25%	102	-21%
	MXH	376	155	414	9%	155	0%	376	0%	155	0%	376	0%	155	0%	376	0%	155	0%	352	-7%	150	-3%	355	-6%	148	-5%	315	-19%	132	-17%
	PPB	202	88	226	11%	88	0%	202	0%	88	0%	202	0%	88	0%	202	0%	88	0%	188	-8%	85	-3%	187	-8%	83	-6%	158	-28%	72	-23%
	PPH	526	226	593	11%	226	0%	526	0%	226	0%	526	0%	226	0%	526	0%	226	0%	490	-7%	219	-3%	495	-6%	216	-5%	438	-20%	193	-17%
	PSEA	138	60	153	10%	60	0%	138	0%	60	0%	138	0%	60	0%	138	0%	60	0%	129	-8%	58	-3%	127	-9%	56	-6%	108	-28%	48	-24%
	PSEB	176	77	197	10%	77	0%	176	0%	77	0%	176	0%	77	0%	176	0%	77	0%	164	-8%	75	-3%	162	-9%	73	-6%	137	-29%	62	-24%
	PSEC	257	111	288	11%	111	0%	257	0%	111	0%	257	0%	111	0%	257	0%	111	0%	239	-7%	107	-3%	241	-7%	106	-5%	212	-21%	94	-18%
	TCV	460	193	514	11%	193	0%	460	0%	193	0%	460	0%	193	0%	460	0%	193	0%	430	-7%	188	-3%	437	-5%	186	-4%	396	-16%	169	-14%

Appendix C

Appendix on part 3

C.1 Hourly profile of typical days

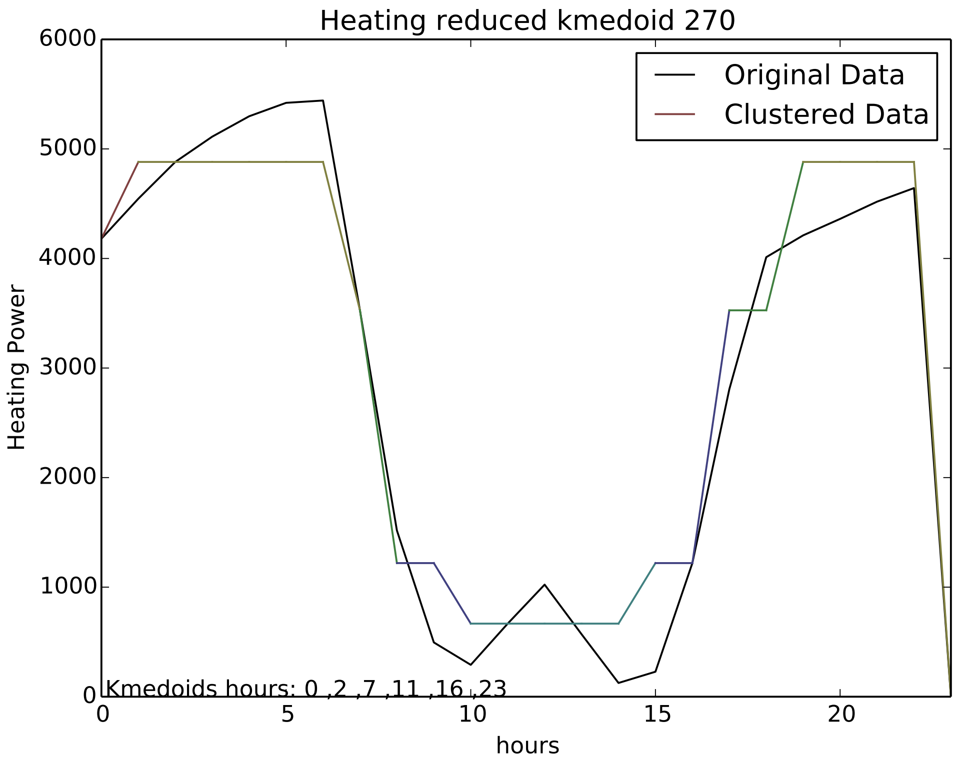

Figure C.1: Original and clustered heating profile of consumption on the 26^{th} **of september** - own illustration

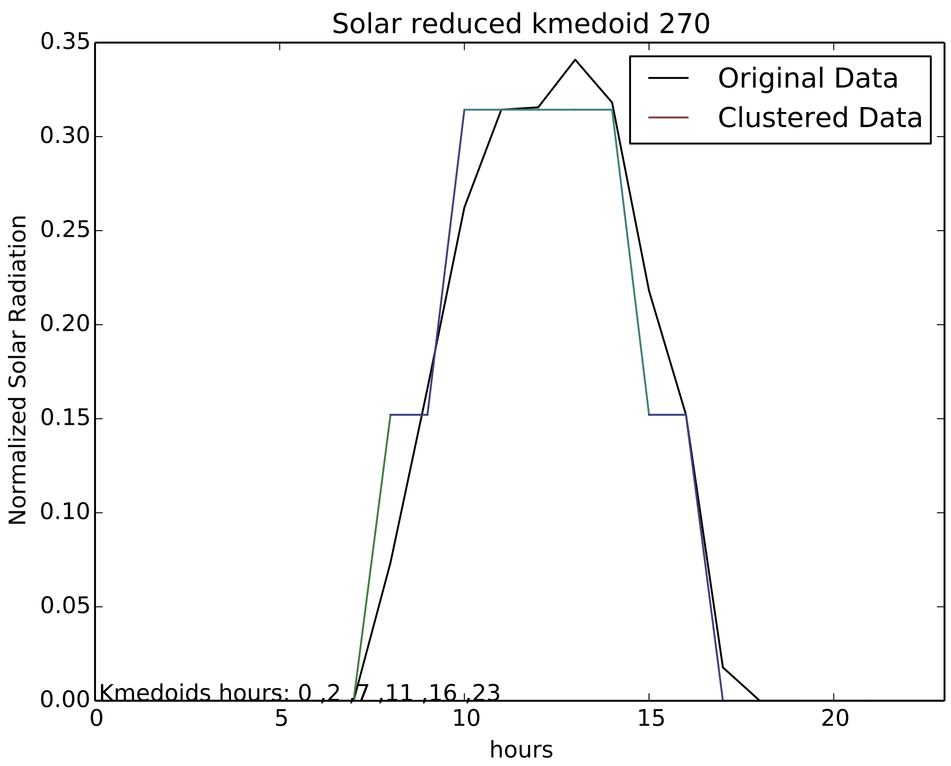

Figure C.2: Original and clustered solar profile of consumption on the 26^{th} **of september -** own illustration